

REVIEW ARTICLE

A Brief Atlas of Insulin

Esra Ayan¹ and Hasan DeMirci^{1,2,3,*}

¹Department of Molecular Biology and Genetics, Koc University, 34450, Istanbul, Turkey; ²Koc University Isbank Center for Infectious Diseases (KUISCID), Istanbul, Turkey; ³Stanford PULSE Institute, SLAC National Laboratory, 94025, Menlo Park, CA, USA

ARTICLE HISTORY

Received: December 10, 2021
Revised: January 30, 2022
Accepted: February 10, 2022

DOI:
10.2174/1573399819666220610150342

Abstract: Insulin is an essential factor for mammalian organisms: a regulator of glucose metabolism and other key signaling pathways. Insulin is also a multifunctional hormone whose absence can cause many diseases. Recombinant insulin is widely used in the treatment of diabetes. Understanding insulin, biosimilars, and biobetters from a holistic perspective will help pharmacologically user-friendly molecules design and develop personalized medicine-oriented therapeutic strategies for diabetes. Additionally, it helps to understand the underlying mechanism of other insulin-dependent metabolic disorders. The purpose of this atlas is to review insulin from a biotechnological, basic science, and clinical perspective, explain nearly all insulin-related disorders and their underlying molecular mechanisms, explore exogenous/recombinant production strategies of patented and research-level insulin/analogs, and highlight their mechanism of action from a structural perspective. Combined with computational analysis, comparisons of insulin and analogs also provide novel information about the structural dynamics of insulin.

Keywords: Insulin, Diabetes, Insulin analogs, Insulin structures, Recombinant insulin, Insulin dynamics.

1. INTRODUCTION

Recombinant insulin is a critical life-saving molecule for the treatment of insulin-dependent diabetes mellitus (DM). Diabetic pathobiology is characterized by insulin therapy. Disorders that are candidates for insulin therapy are typically categorized as juvenile-onset type 1 diabetes (T1D) and adult-onset type 2 diabetes (T2D). Usage of insulin is more common in T2D compared to T1D [1]. Recombinant insulin was first produced in the 1970s and commercialized in the 1980s. This is a milestone in insulin history [2, 3]. Recombinant biosynthesis provides a more robust approach in terms of massive production. An unlimited amount of insulin can be obtained compared to the conventionally obtained native insulin methods, which only provide a limited amount. Along with the recombinant DNA (rDNA) technology, cost-effective insulin analogs have continued to improve the pharmacological aspect of insulin production [4]. Insulin therapies lead to the production of sustained and rapid-acting analogs that represent the state-of-the-art therapy for millions of insulin-dependent diabetic patients [5]. Furthermore, therapeutic approaches and pharmacokinetic advances in normalizing blood glucose levels to date continue with reports of polypharmacy to ensure the regulation of optimized glucose and body weight management [6-8]. In

addition, advances in materials science paved the way to control insulin release through real-time continuous blood glucose monitoring and a closed-loop system for the regulation of blood glucose levels [9, 10]. However, even with such remarkable advancements, current treatments provide suboptimal results for most patients.

Failure to develop a complete solution to diabetes caused insulin-oriented studies to remain on the agenda. It has been repeatedly emphasized by studies, systematic reviews, and meta-analyses that diabetes, which has been considered a major health problem since 1922 [10-12], will increase exponentially in the coming years [13, 14]. Innovative techniques in the fields of structural biology and structural proteomics enabled the high-resolution analysis of insulin and insulin-associated proteins. Each novel structure paves the way to new production approaches, optimization techniques, and clinical trials. Insulin is not only a molecule categorized with diabetes but an important hormone targeted by a wide variety of diseases due to its vital role in the human proteome. Therefore, it will not be sufficient to consider only a single aspect of the multi-faceted insulin molecule.

In this atlas, we aimed to evaluate all insulin-oriented details from a holistic perspective: from the history of insulin to its production techniques, from its structure to the signaling pathways, and from diagnosis therapy to omics approaches. Additionally, the literature is characterized by gaps in the knowledge of the structures and dynamics of insulin analogs. Holistically, we also desired to give the bird's eye information about the differences between the analog struc-

*Address correspondence to this author at the Department of Molecular Biology and Genetics, Koc University, 34450, Istanbul, Turkey; Koc University Isbank Center for Infectious Diseases (KUISCID), Istanbul, Turkey and Stanford PULSE Institute, SLAC National Laboratory, 94025, Menlo Park, CA, USA; E-mail: hdemirci@ku.edu.tr

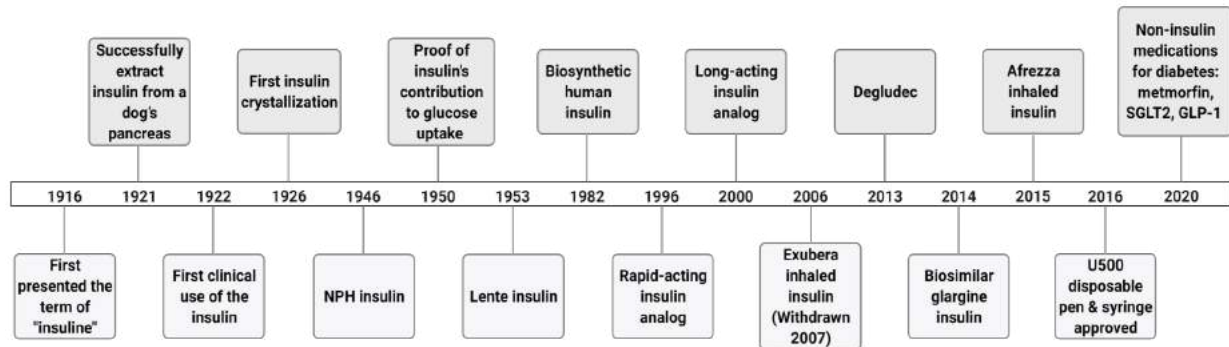


Fig. (1). Discovery, history, and chronological milestones of insulin development.

tures and dynamics. This type of review is one of the gaps in the literature and this is what our "insulin atlas" aims to accomplish.

2. DISCOVERY AND HISTORY OF INSULIN

The discovery of insulin was a milestone in the main treatment for DM. After its discovery, it took another 30 years for recombinant insulin to be optimized as a therapeutic product in clinical use (Fig. 1). Insulin's discovery and DM treatment history is a notable story in Michael Bliss's notes [15]. The name of insulin predates its discovery in 1889. Joseph von Mering and Oskar Minkowski discovered that some model organisms of pancreatectomy are characterized by severe DM [16]. It caused speculation about a substance produced by the pancreas, which is responsible for metabolic regulation, and thought to be responsible for carbohydrate metabolism [15]. In the following years, 1910 and 1916, Sir Edward Albert Sharpey-Schafer introduced pancreatic islets, regarding Langerhans islands, called "insulin" that could control glucose metabolism [16, 17]. However, according to some scientists, the discovery of insulin was by Belgian Jean de Meyer. In 1920, Frederick Grant Banting, an orthopedic surgeon, focused on internal secretions and degenerate islets in dogs. First, Frederick Grant Banting and Charles Best worked together on account of John James Rickard Macleod, an expert in carbohydrate metabolism. Critical *in vivo* trials then began in May 1921 and continued until December [18].

Bantings and Best observed that the extract they studied lowered blood sugar in diabetic dogs. James Bertram Collip, who was interested in pancreas studies at that time, also joined this team. Although their presentation about the extract on December 30 (1921) did not give satisfactory results due to their inexperience and haste, the team's further results were promising since the use of the relevant extract caused the restoration of glycogen mobilization in the liver. In January (1922), Banting and Best tried using a pancreatic extract on Leonard Thompson, who had severe DM [17, 18]. This test failed due to slight decreases in glycemia and glycosuria. In addition, this extract test did not show any positive effect on the patient nor his ketoacidosis and caused a sterile abscess formation. After this treatment, they started a new series of injections and this time, Thompson recovered. His ketonuria and glycosuria almost disappeared, and his blood sugar level turned out to be normal. It symbolized conclusive

evidence that the extract that was thought to have been obtained by James Bertram Collip replaces the impaired function in DM. He successfully developed a robust method of extraction by optimizing the concentrations of acidic alcohol solutions in the beef pancreas. Eighteen months later, Banting and Macleod won the Nobel Prize in Physiology or Medicine, sharing this glory with Best and Collip [15, 18]. Since the discovery of insulin, the focus was brought to biosimilar/biobetter/derivative production methods, including long- and short-acting insulin analogs. Currently, the focus of DM-oriented studies has been insulin-based therapies, and these therapies dominate the market.

3. AN OVERVIEW OF INSULIN

Insulin is a peptide hormone that has an essential regulatory effect. It has an anabolic role in the uptake of glucose into cells and provides carbon energy storage in the body. It is expressed in the β -cells of the pancreas and circulates through the blood. As a result, it is exported to the liver [19]. β -cells receive the glucose through Glucose Transporter 2 (GLUT-2) receptors after being triggered by internal and external stimuli such as glucose, sulfonylureas, and arginine. After the transport of glucose into the cell, glucokinase, acting as glucose sensor, oxidizes the glucose. If the concentration of glucose is below 90 mg/dL, a threshold known as "substimulatory glucose concentration", insulin release does not occur. This causes effluxing of K^+ ions through K_{ATP} channels, which are characterized by the negative potential of the β -cell membrane, followed by the closing of the voltage-gated calcium channels. However, if plasma glucose rises above 90 mg/dL, there is an increase in glucose uptake followed by an increase in metabolism, resulting in an increase in ATP concentration and the closing of K_{ATP} channels. This means triggering membrane depolarization followed by the opening of voltage-gated calcium channels. Therefore, the calcium influx causes an increase in the intracellular calcium ion concentration, resulting in exocytosis of insulin through microvesicles [18, 20, 21] (Fig. 2). On the other hand, once glucose enters β -cells, it triggers various regulators of the insulin promoter, such as pancreatic duodenal homeobox factor-1 (PDX-1), β -cell E box transactivator 2 (E47/b42), and basic leucine zipper protein MafA to stimulate transcription of INS gene [22] and some proto-oncogenes such as c-Abl to inhibit GLUT-2 production [23], causing activation of the feedback mechanism [24] (Fig. 2).

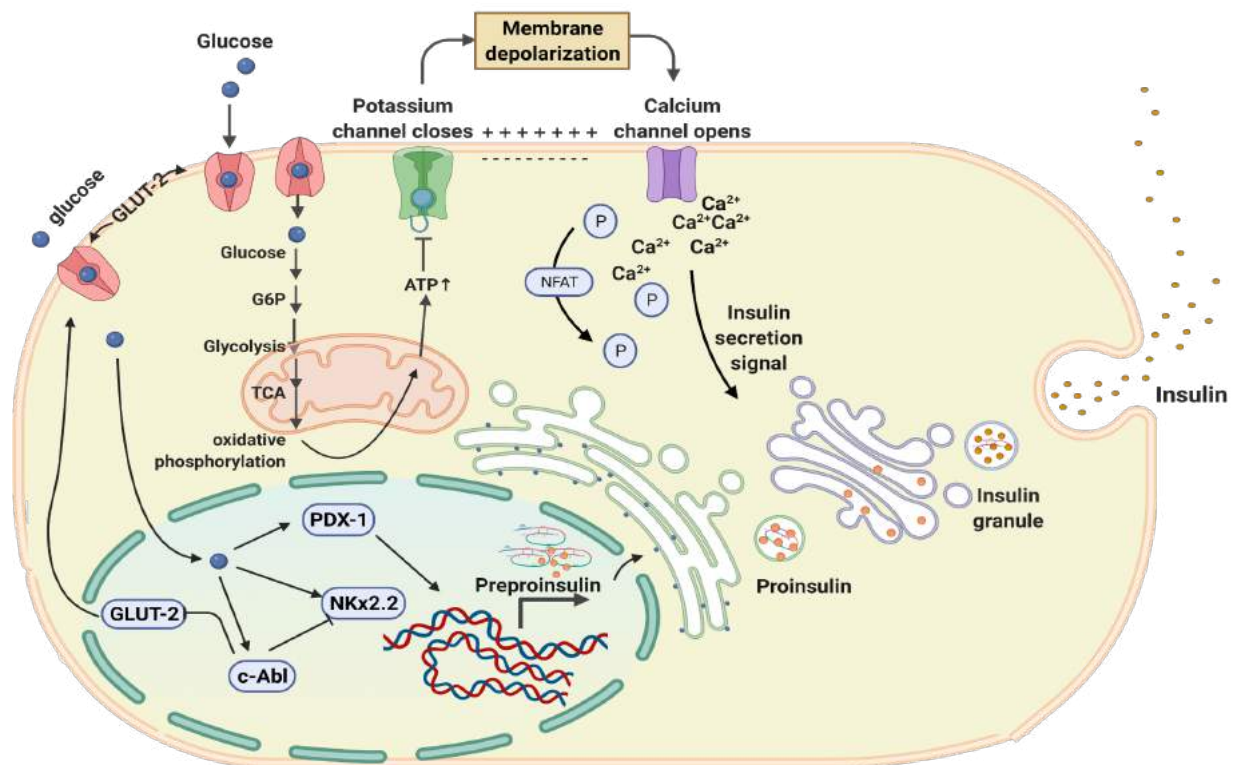


Fig. (2). Endogenous insulin production pathway in β -cells. Demonstration of insulin secretion through both Ca^{2+} -mediated membrane depolarization and promoter-mediated feedback mechanisms. (A higher resolution / colour version of this figure is available in the electronic copy of the article).

The production of insulin synthesized as pre-proinsulin from a 110 amino acid precursor is performed by the transcription and translation of the INS gene on chromosome 11 [25]. Pre-proinsulin has a 24-amino-acid-long N-terminal signal peptide recognized by cytoplasmic Signal Recognition Particles (SRP) to be localized to the Rough Endoplasmic Reticulum (RER) membrane. The processes in the RER are characterized by cleavage of this SRP sequence by the signal peptidase, folding of proinsulin, and formation of three disulfide bonds. These processes need a wide range of Endoplasmic Reticulum (ER) oxidoreductases and chaperones, such as protein-thiol reductase. After the ER-mediated oxidative folding process, proinsulin is transported to the Golgi apparatus by microvesicles for further processing, which includes cleavage to mature insulin and C-peptide and the formation of pale secretory "progranules," containing proinsulin-zinc hexamers. This results in the formation of mature insulin [26]. After C-peptide and insulin are stored together with some cell secretion products and islet amyloid polypeptide (amylin or IAPP) [27], proinsulin is converted to mature insulin using prohormone convertases 2 & 3 and carboxypeptidase E. This results in the secretion of mature granules that form water-insoluble insulin crystals from the β -cell into the bloodstream through microtubules and microfilament dependent transport [18, 26] (Fig. 3). Some studies suggest that although crystallization enhances the ability of soluble proinsulin to mature into insoluble insulin, non-

crystallization of insulin does not adversely affect proinsulin processing [28-31].

After expression, insulin is secreted from the pancreas to the liver through the portal circulation. At the first pass, 50% of insulin is cleared from circulation in the liver hepatocytes to regulate the homeostatic insulin level. In contrast, the rest of the insulin is exported from the liver through the hepatic vein. Then, insulin is distributed to the body through the arterial circulation and promotes vasodilation, a mechanism that causes blood vessels to dilate. Insulin also returns to the liver, where it exerts the metabolic effect, and further clearance occurs with a second pass [19, 32, 33] (Fig. 4).

During circulation, hexamer insulin disperses into an active monomer to enter cells [34]. After the monomer binds to the insulin Receptor Tyrosine Kinase (RTK), it triggers the autophosphorylation of tyrosine residues (Fig. 5). Some of these residues are recognized by the phosphotyrosine binding (PTB) domain of Insulin Receptor Substrates (IRS), phosphorylating many tyrosine residues. The other tyrosine residues are recognized by the Src Homology 2 (SH2) domain, which belongs to the Phosphoinositide 3-Kinase (PI3K) [35, 36]. Accordingly, the catalytic subunit p110 of PI3K is taken into the plasma membrane to phosphorylate the inositol ring-D3 position of phosphatidylinositol-(4,5)-bisphosphate (PIP_2). This triggers the formation and increases the concentration of phosphatidylinositol (3,4,5)-triphosphate (PIP_3)

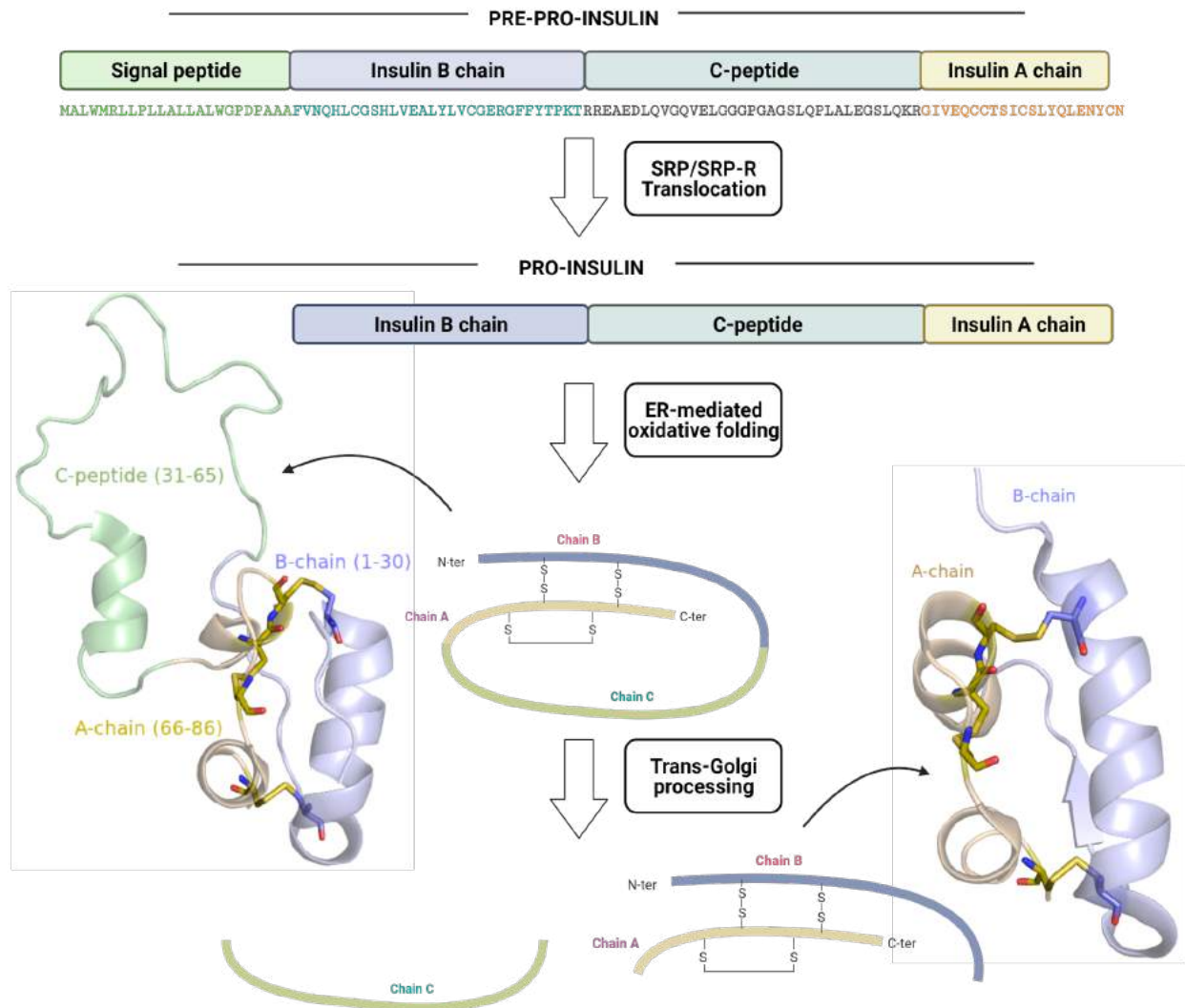


Fig. (3). Representation of the process from pre-proinsulin to mature insulin on a structural and sequence basis. (A higher resolution / colour version of this figure is available in the electronic copy of the article).

(Fig. 5B). Studies have shown that PIP_3 is the second messenger, and inactivation of PIP_3 causes inhibition of critical cellular responses associated with insulin, including glucose transport and stimulation of insulin synthesis. Additionally, a close interaction of PIP_3 with Protein Kinase B (Akt/PKB) in insulin signaling has been demonstrated by studies [37, 38]. Accordingly, PKB interacts with PIP_3 through the Pleckstrin Homology (PH) domain located at its amino terminus (Fig. 5C). Thus, PKB has recruited the plasma membrane where PIP_3 is localized. Here, PKB and PIP_3 interaction does not directly affect PKB but phosphorylate the Ser473 and Thr308 residues, resulting in PKB being active [35, 39]. Thus, PIP_3 regulates PKB, Serine/threonine protein kinase (SGK), and p70 ribosomal protein S6 Kinase (S6K) activation. Therefore, PKB becomes a Phosphoinositide-Dependent Kinase-1 (PDK1) substrate. Accordingly, it is important that SGK and S6K also have PH domains for closely related interaction with PIP_3 [40] (Figs. 5B and 5C).

Additionally, the binding of insulin to the receptor triggers the phosphorylation of proto-oncogene Cbl (Casitas B-lineage Lymphoma) in the c-Cbl-Associated Protein (CAP)-Cbl complex, resulting in the participation of the CAP-Cbl complex in the lipid raft (Fig. 5B). Thus, Cbl interacts with the Crk adaptor protein, which is closely related to the Rho-family guanine nucleotide exchange factor (C3G). This causes the activation of TC10, which belongs to the GTP-binding protein family, to stimulate Glucose transporter type 4 (GLUT4) translocation [35, 41]. Finally, insulin interacts with INSR in a monomeric form. It is a multifunctional and versatile hormone; it regulates glycogen synthesis by triggering glucose uptake [42, 43] and stimulating housekeeping mechanisms such as lipogenesis [44], glycolysis [45], apoptosis [46], and protein synthesis [47, 48] (Fig. 5). Furthermore, it plays a vital role in many intra- and intercellular endocrine system reactions by regulating various homeostatic signaling pathways [35, 49-51].

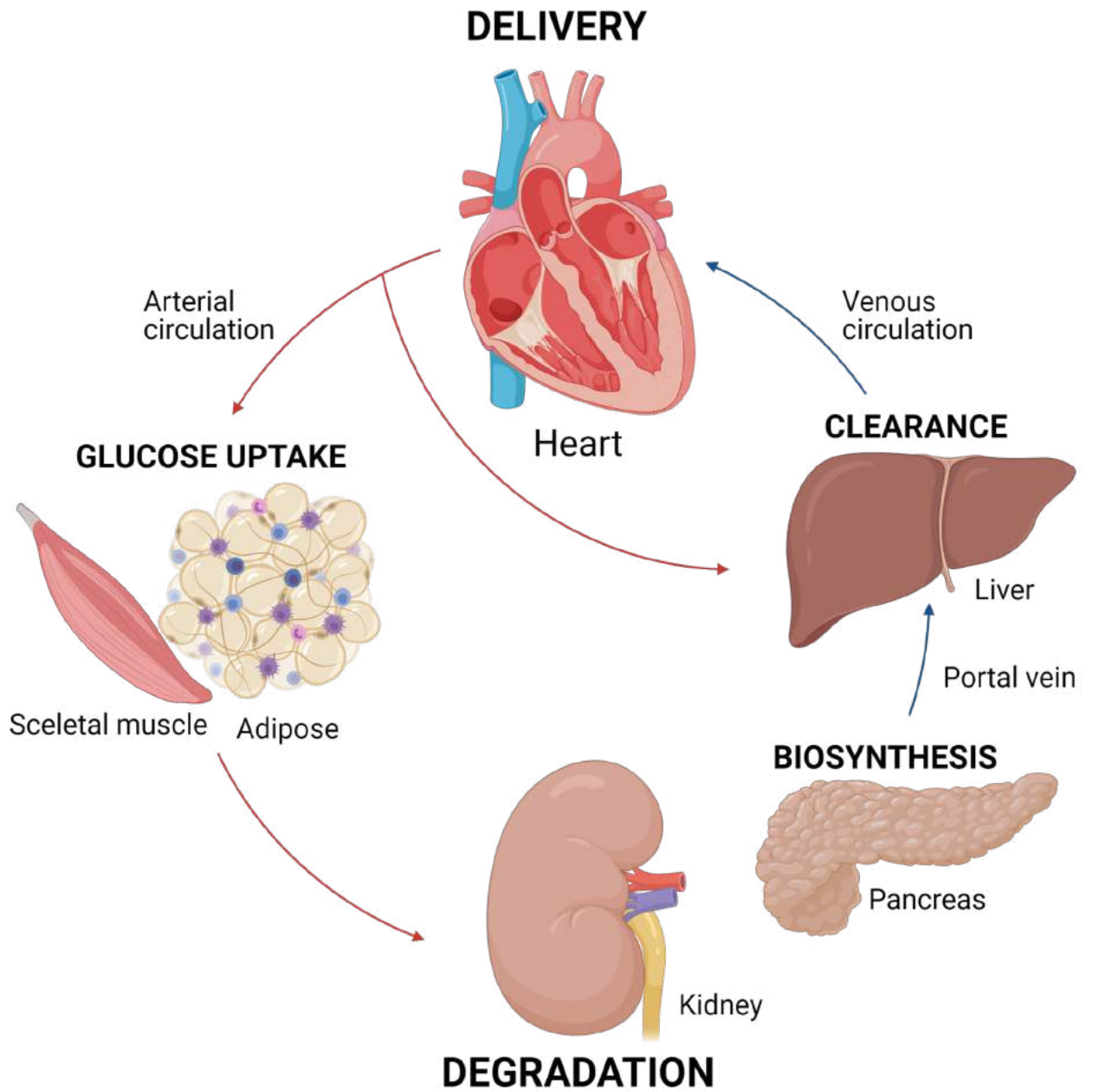


Fig. (4). Representation of circulation, clearance and degradation of insulin. (Inspired by Tokarz *et al.* (2018)). (A higher resolution / colour version of this figure is available in the electronic copy of the article).

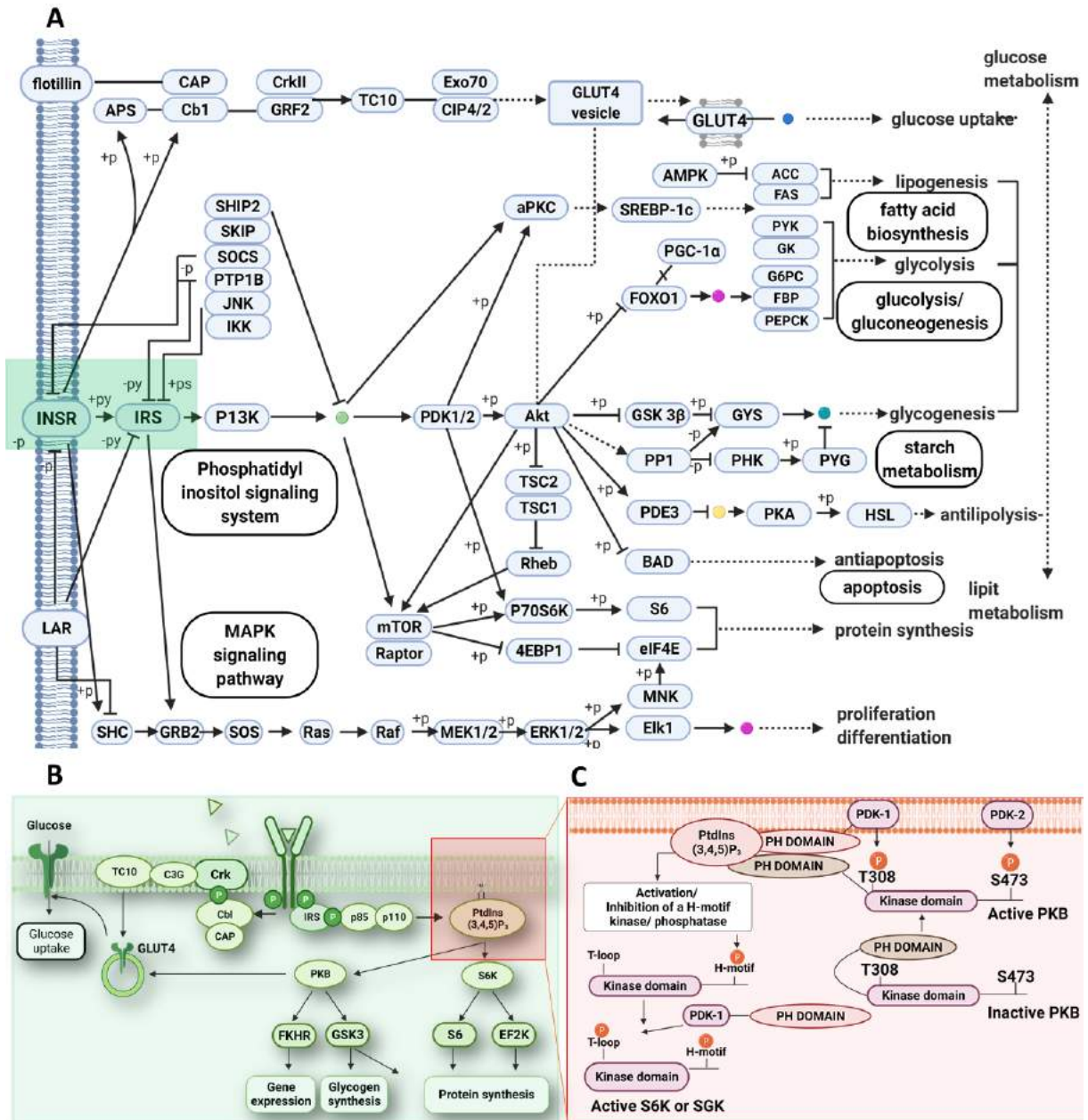


Fig. (5). Representation of insulin-mediated signaling pathways. **(A)** Overall demonstration of insulin signalling pathway. The interaction of insulin and insulin receptor (IR) triggers phosphorylation of insulin receptor substrates (IRS) through insulin receptor tyrosine kinase (INSR), resulting in the interaction of the regulatory subunit of phosphoinositide 3-kinase (PI3K) and IRS. PI3K activation triggers 3-phosphoinositide-dependent protein kinase 1 (PDK1) and Akt (a serine kinase); this triggers glycogen synthase kinase 3 (GSK-3) inactivation, leading to glycogen synthesis through glycogen synthase (GYS) activation. Akt activation also triggers translocation of GLUT4 vesicles to the plasma membrane, thereby triggering glucose uptake into the cell. Akt activation also promotes mTOR-mediated protein synthesis through p70S6K and eIF4. GLUT4 translocation can also occur through CAP/Cbl/TC10 signaling by phosphorylating *via* Cbl INSR. Thus, other signal transduction pathways, especially GRB2, which is part of the RAS, SOS, MEK, and RAF cascade, interact with the IRS. SHC, which is another substrate of INSR, associates with GRB2 through tyrosine phosphorylation, thus enabling the RAS/MAPK pathway to be activated independently of IRS-1. **Green sphere:** Fosfatidilinositol 3,4,5-Trifosfat (PIP3); **blue sphere:** glucose; **magenta sphere:** DNA; **cyan sphere:** glycogen; **yellow sphere:** cAMP. **Arrows, →:** molecular interaction/relation; **⊠:** unknown reaction/indirect connection; **-:** molecular inhibition; **⊗:** missing interaction. **+p:** phosphorylation; **-p:** dephosphorylation. **(B)** A close look at the relationship between insulin and major metabolic responses in cells. Representation of glucose uptake through GLUT4 translocation after a series of signal transduction. **(C)** PtdIns(3,4,5)P3 mediates activation of PKB, S6K, and SGK through their T-cycles, and is upregulated by insulin and other agonists in contrast to PDK1 indirect activity. (A higher resolution / colour version of this figure is available in the electronic copy of the article).

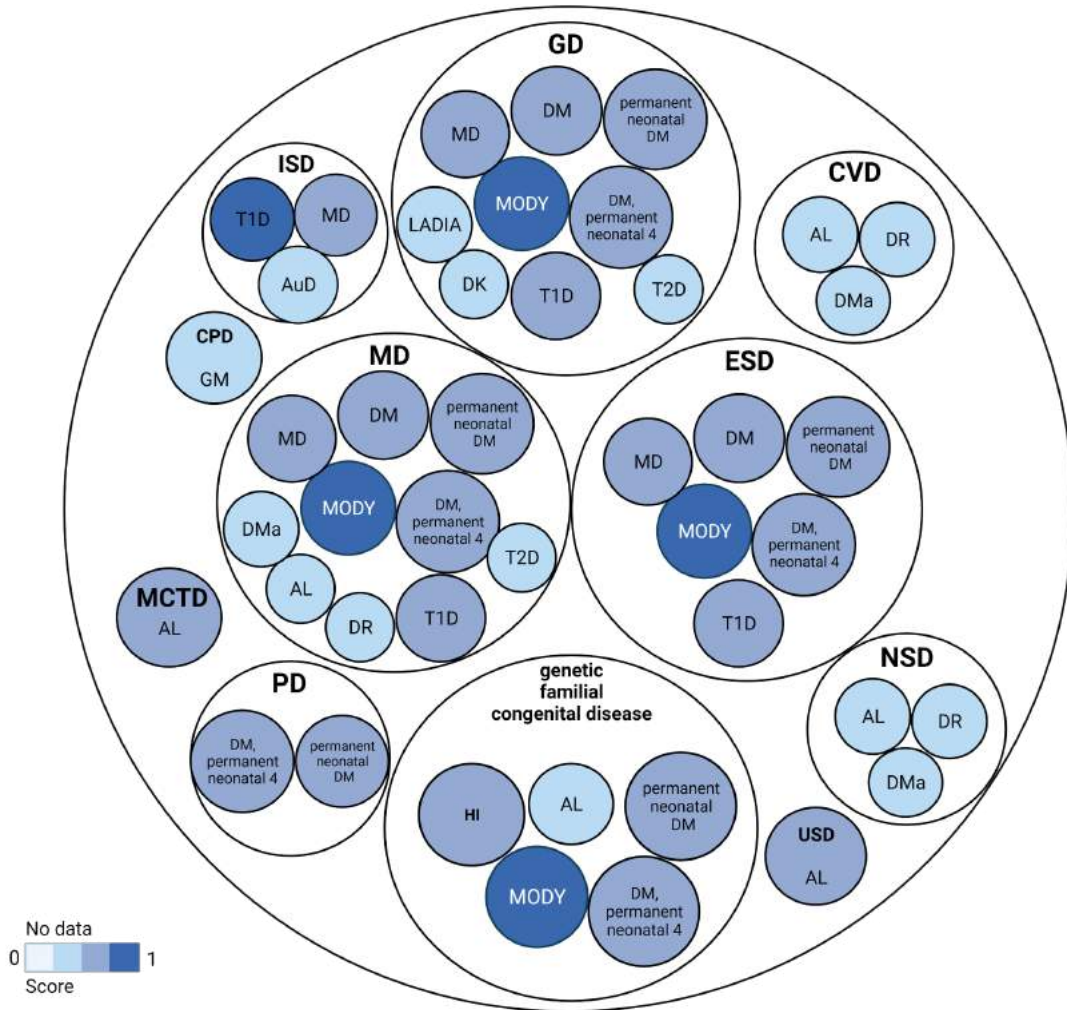


Fig. (6). Bubbles diagram based on association score (As) representing main insulin-related diseases/ phenotypes related to *INS* gene. GD: Gastrointestinal Disease, MD: Monogenic Diabetes (As: 0.528), DM: Diabetes Mellitus (As: 0.406), Permanent Neonatal DM (As: 0.506), DM, permanent neonatal 4 (As: 0.715), MODY: Maturity Onset Diabetes of the Young (As: 0.722), LADIA: Latent Autoimmune Diabetes In Adults (As: 0.265), DK: Diabetic Ketoacidosis (As: 343), T1D: Type-I Diabetes (0.684), T2D: Type-II Diabetes (0.324); MD: Metabolic Disease, DMa: Diabetic Maculopathy (As: 0.376), AL: AL amyloidosis (As: 0.462), DR: Diabetic Retinopathy (As: 0.400); ESD: Endocrine System Disease; CVD: Cardiovascular Disease; NSD: Nervous System Disease; USD: Urinary System Disease; Genetic familial congenital disease; HI: Hyperinsulinemia (As: 0.665), PD: Pregnancy or Perinatal Disease; MCTD: Mixed Connective tissue Disease; CPD: Cell Proliferation Disorder; GM: Glioblastoma Multiforme (As: 0.290); ISD: Immune System Disease, AuD: Autoimmune Disease (As: 0.291). (A higher resolution / colour version of this figure is available in the electronic copy of the article).

4. PATHOLOGY

Due to the function of insulin and its interaction with essential proteins, various insulin-related diseases have been observed and classified. Currently, 1099 diseases associated with the Insulin (*INS*) gene are available on the *Open Targets Platform* [52]. Although generally characterized as "pancreatic diseases," insulin-related disorders span a large spectrum and range from "genetic disorders" to "infectious diseases" (Fig. 6).

5. INSULIN AND PANCREATIC DISEASE

Any disease affecting the pancreas, including pancreatic insufficiency, pancreatitis, neoplastic carcinoma, neuroendo-

crine neoplasms, cystadenomas, and lymphomas, is referred to as a pancreatic disease, and diabetes is the most prominent category among pancreatic diseases [53].

DM is an endocrine pancreatic disease and is classified into a wide variety of diseases from "rare genetic diabetes mellitus" to "glucose metabolism disease". However, it is characterized by two most common forms: T1D and T2D (Fig. 7). T1D is an autoimmune disease created by the destruction of insulin-producing β -cells, in which insulin cannot be produced, thus causing insulin deficiency (Fig. 7A). Typically characterized by childhood and adolescence, T1D leads to severe hyperglycemia and diabetic ketoacidosis and may cause death without insulin therapy. Thousands of studies for the treatment of T1D have occurred in the literature,

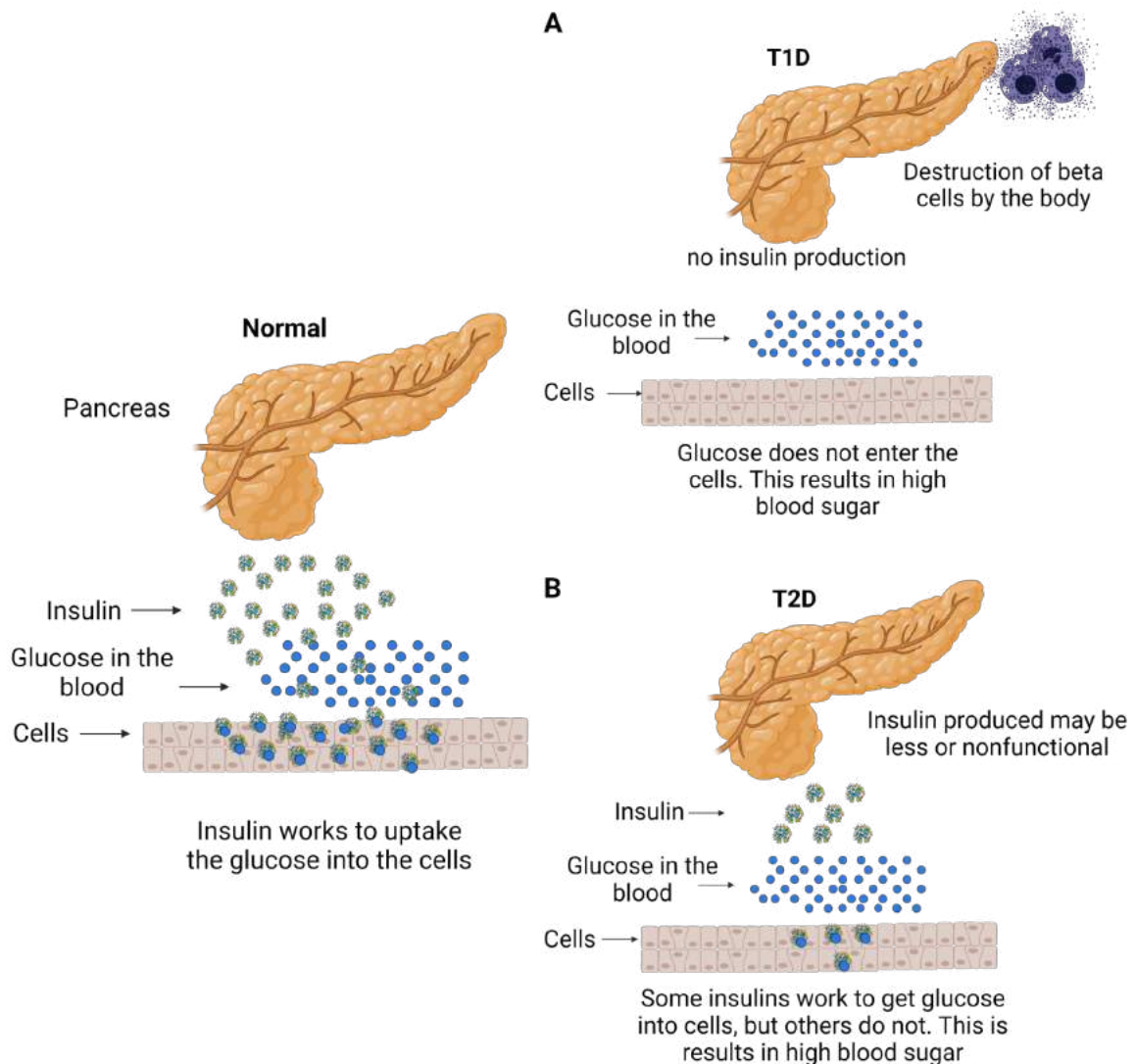


Fig. (7). Demonstration of T1D (**A**) and T2D pathophysiology compared to normal physiology (**B**). (A higher resolution / colour version of this figure is available in the electronic copy of the article).

and research is still in progress as well as recent studies in T1D treatment are promising. Studies conducted in 2020 discovered that slowly progressive T1D correlates with islet antibody loss and a different β -cell phenotype [54]. In another study, it was discovered that autoreactive T-cells infiltrate the islets of Langerhans by destroying insulin-secreting β -cells and early symptoms can characterize it, thus being preferred as an early-stage marker in clinical studies [55].

T2D is a progressive metabolic disease that accounts for greater than 90% of the global diabetes epidemic (Fig. 7B). It is not insulin-dependent besides being an insulin-sensitive disease. It is characterized by insulin resistance and hyperinsulinemia and is closely related to glucose intolerance and hyperglycemia. The overwhelming majority of studies on T2D are in progress, both clinically and exploratory approaches. Potential mechanisms of *Agriophyllum oligosac-*

charide plants in T2D were investigated in an in vivo study conducted in 2020. Accordingly, the "ancient medicine" herb activates insulin by triggering the INS-R/IRS2/PI3K/AKT/Glut4/PPAR-signaling pathway in T2D patients, proliferating hepatocytes, and decreasing blood glucose levels [56]. In a 2020 study, the remarkable effect of sleeve gastrectomy was investigated with a negligible risk of complications and a simple operational system in the control of glycometabolism. Accordingly, the downregulation of the SNHG5 gene and the expressional change of the TGR5 gene have alleviated the colorectal damage caused by high glucose. Furthermore, the mechanism under the positive effect of sleeve gastrectomy in T2D was indicated [57]. Eventually, insulin plays a vital role not only in diabetic diseases but also in a wide variety of pancreatic diseases such as hyperinsulinism [58], pancreatic neuroendocrine tumor [59], and malignant pancreatic neoplasm [60].

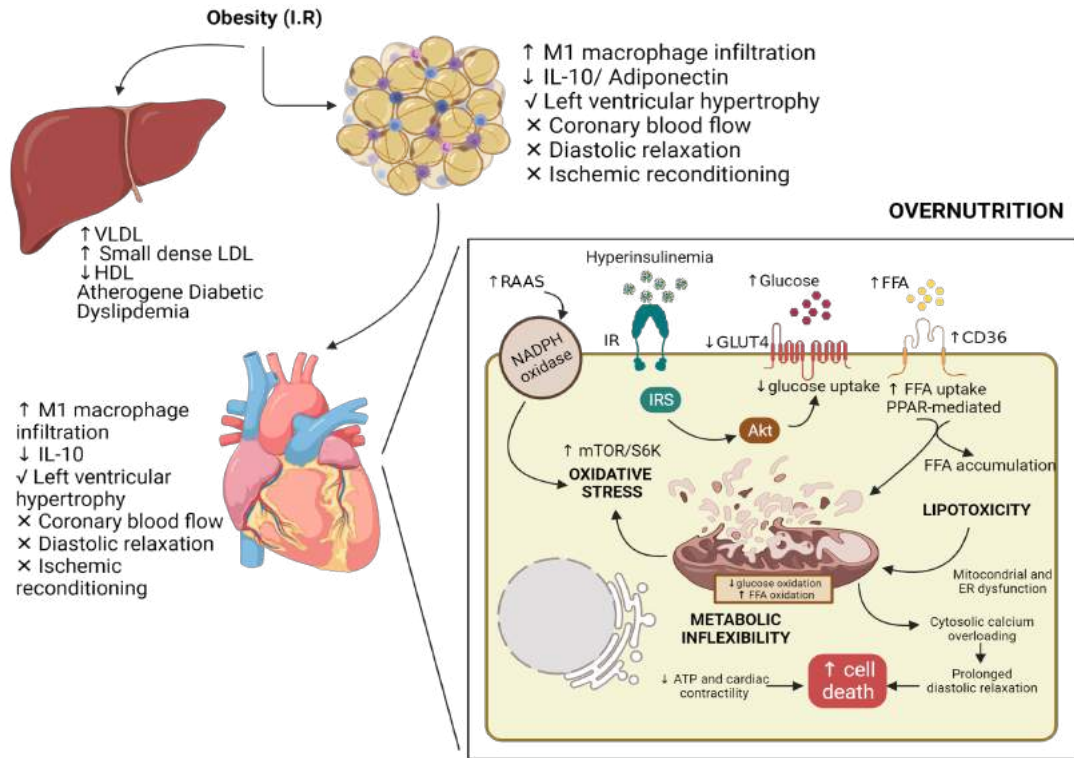


Fig. (8). Demonstration of CVD-insulin-related pathophysiological and molecular mechanisms. In the case of obesity-related insulin resistance, metabolic dysregulation centered on low glucose oxidation and high lipid oxidation leads to abnormal Ca²⁺ utilization, resulting in low ATP production leading to cardiomyocyte death. (A higher resolution / colour version of this figure is available in the electronic copy of the article).

6. INSULIN AND CARDIOVASCULAR DISEASE

Any diseases related to the cardiovascular system are classified under cardiovascular diseases (CVD) [61-63]. In general, pathological conditions associated with CVD begin to appear at an exceedingly early age [64]. Obesity is associated with insulin resistance and is directly involved in the origin of CVD (Fig. 8) [64-66]. Insulin triggers the use of metabolic substrates in the heart as well as in other tissues. In cardiomyocytes, although insulin provides the intake of glucose and fatty acids, it prevents the use of fatty acids as an energy source [67]. This causes insulin resistance, and the pancreas tries to increase insulin secretion, which leads to a phenomenon called hyperinsulinemia [67]. Furthermore, glucose concentration, insulin resistance, and hyperinsulinemia contribute to the development of atherosclerosis and trigger mechanisms such as inflammation, dyslipidemia, and hypertension [68, 69]. Therefore, studies prove that the toxic effects of high glucose concentrations due to insulin resistance are strongly associated with CVD, even in people without diabetes [66, 70-72] (Fig. 8). In a systematic review conducted in 2020, it was shown with ultrasonographic evidence that carotid disease increases the possibility of diabetic retinopathy (DR), highlighting a direct relationship between carotid disease and DR [73]. Variable glucose grades due to impaired insulin levels play a key role in the etiology of CVD. Accordingly, it was demonstrated that serum insulin level plays a remarkable role in CVD pathophysiology, showing a strong relationship with the carotid plaque [74]. In

addition, a study of cats with asymptomatic hypertrophic cardiomyopathy (aHCM) demonstrated that inflammation, insulin, and insulin-like growth factor-1 (IGF-1) had significant effects on aHCM and paved the way for clinical trials [75]. Additionally, recent studies have proven that insulin plays a critical role in CVDs, particularly acute myocardial infarction [76], thrombotic disease [77], and heart failure [78, 79]. This suggests that insulin triggers signaling pathways closely related to CVD.

7. INSULIN AND IMMUNE SYSTEM DISEASE

The innate and adaptive immune system is a coordinated and critical system that maintains the organism's homeostasis against internal and external pathogenic agents [80, 81]. Additionally, if metabolic dysfunction occurs in the organism, immune system components can be activated and cause pathology. Therefore, there is a close relationship between immune dysfunction and metabolic diseases. (Fig. 9) [82]. In a study, macrophages play a critical role in triggering chronic inflammation in obesity, which is associated with insulin resistance [83, 84]. With the increase of fatty acids released from the adipose of the obese organism, the M1-polarized macrophages associated with inflammation are translocated into adipose tissue (Fig. 9A). M1-macrophages, which lead to the activation of c-Jun N-terminal kinase (JNK) or inhibition of nuclear factor-κB (IκB) kinase (IKK) pathways, cause insulin resistance as they trigger inflammatory stress in the cell. Accordingly, inflammation is suppressed by the

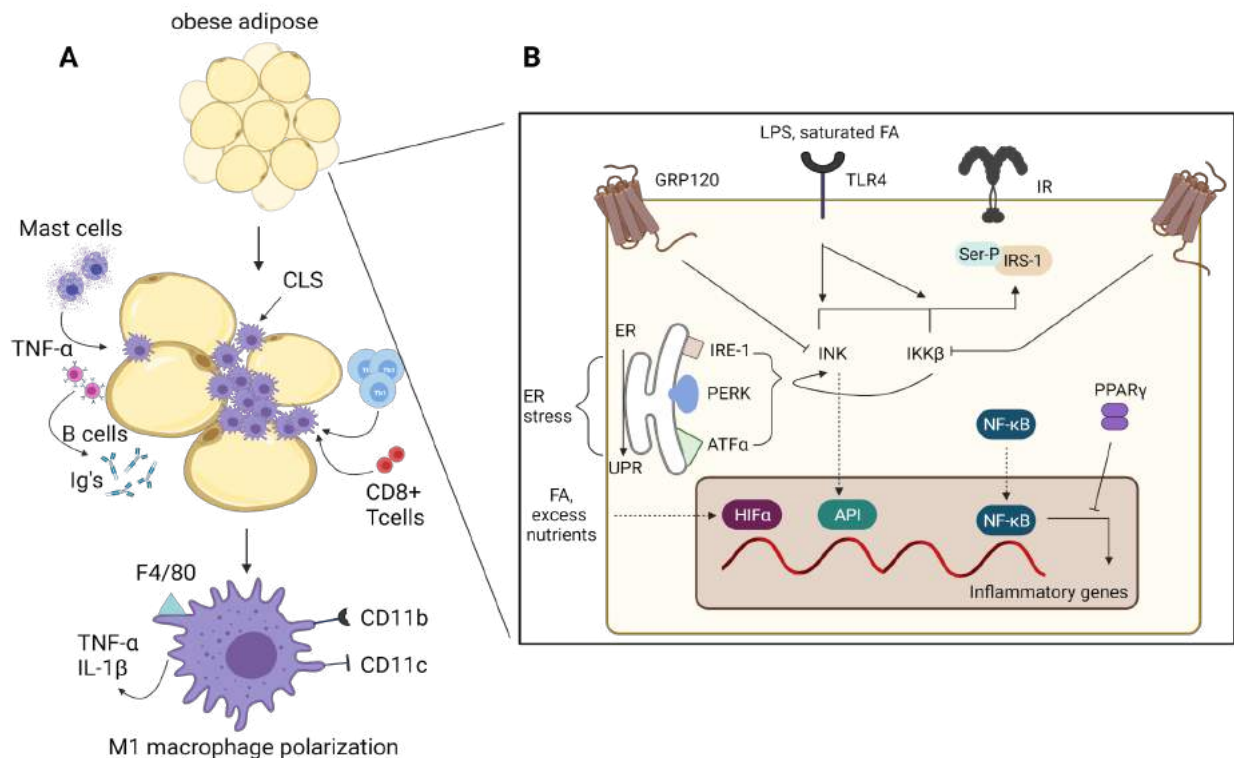


Fig. (9). Demonstration of immune system-insulin-related pathophysiological and molecular mechanisms. **(A)** In obese adipose tissue, the TH1-type cytokines interferon (IFN)- γ trigger a phenomenon called "M1 macrophage position". However, this condition is characterized by T-helper type 2 (TH2) cells and M2 macrophage polarization in normal adipose tissue. Thus, immunoglobulins (Igs), B-cells and mast cells, which are characterized by insulin resistance, increase in obese adipose tissue. CD8(+) T-cells increase in correlation with increased pro-inflammatory gene expression. In contrast to normal tissue, macrophages in obese adipose tissue are not homogeneously separated and form an accumulation called crown-like structures (CLS). M1 macrophages are pro-inflammatory that secrete cytokines such as IL-1 β and TNF- α and, unlike M2 macrophages, they also increase the expression of CD11c marker. **(B)** Activator and inhibitory mechanisms that trigger the inflammatory system in the case of insulin resistance. Arrows indicate inflammatory pathways that increase insulin resistance. The weakening of insulin action is related to the phosphorylation of insulin receptor substrate protein-1 (IRS-1) of the activator mechanism. The positive interaction between IKK β and nuclear factor- κ B (NF- κ B) enables NF- κ B to bind to DNA, thereby activating inflammatory mediators. The positive association between JNK1 and API is also important in the regulation of these mediators. The increase in ovarian nutrition and fatty acid (FA) triggers the Endoplasmic Reticulum (ER) stress and thus the unfolded protein response (UPR), which is characterized by three main pathways (IRE-1, PERK and ATF α). Activation of omega-3 fatty acid receptors (GRP120) and PPAR γ , which are promoters of insulin sensitivity, is characterized by the interference of NF- κ B and API signaling pathways. (A higher resolution / colour version of this figure is available in the electronic copy of the article).

activation of peroxisome proliferator-activated receptor (PPAR) signals associated with M2-macrophages. However, when these are inhibited, the inflammation becomes chronic. This molecular regulation is closely related to the function of macrophages, lymphocytes, and mast cells, causing inflammation to increase gradually (Fig. 9B). Therefore, the increase in fat mass in the tissues is characterized by insulin resistance, thereby triggering inflammation of adipose tissue [85-87].

A recent study showed that intestinal worms causing immunosuppressive and asymptomatic chronic infections prevent streptozotocin-induced diabetes through their trehalose. This shows therapeutic effects on streptozotocin-induced diabetes by increasing the Ruminococcus spp and activating cytotoxic (CD8⁺) Treg cells [88]. As a result of a series of experiments conducted while considering the relationship of CD8⁺T cells to Major Histocompatibility Com-

plex I (MHC-I), it was shown that these cells gained an effector function during the clinical diagnosis period by presenting an antigen-experienced phenotype. Accordingly, evidence has been provided that these cells cause T1D [89]. In addition, it has been proven in the latest studies that insulin plays a role in various immunoreactive diseases, such as Shwachman-Diamond syndrome [90], type II hypersensitivity reaction disease [91], anemia [92], and celiac disease [93]. All these suggest that insulin triggers signaling pathways closely related to immune system diseases.

8. INSULIN AND CANCER

Insulin, with its well-known mitogenic effects on cells, is considered a growth factor [94]. It is known how crucial growth factors are to the development of cancer. By considering these situations, the effects of insulin on cancer cells are apparent. Insulin shows its effect by its interactions with

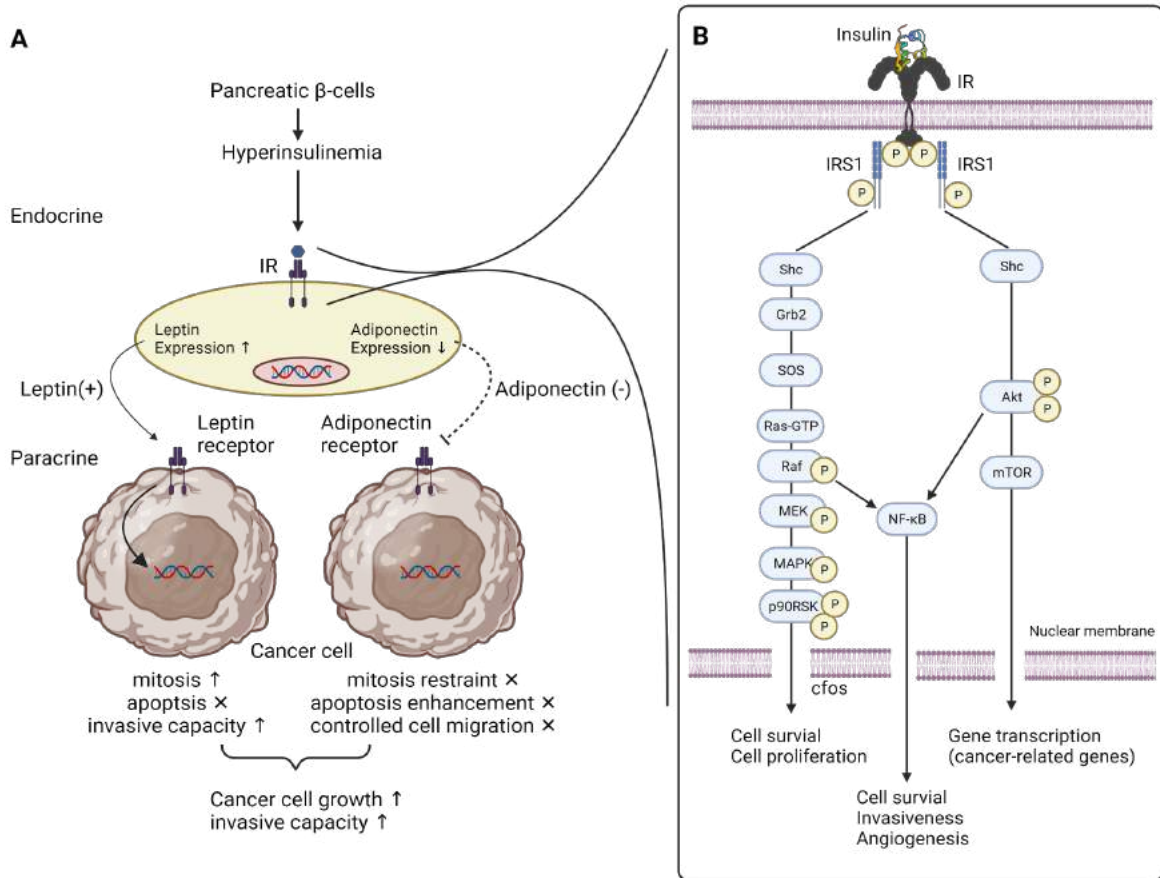


Fig. (10). Demonstration of cancer-insulin-related pathophysiological and molecular mechanisms. **(A)** Cancer cell growth characterized by paracrine stimulation is triggered by leptin invasion, adiponectin inhibition, and hyperinsulinemia. **(B)** Positive effect of PI3K/Akt/mTOR and The Ras/MAPK signaling pathway in cancer cell proliferation and anti-apoptosis through NF- κ B nuclear translocation. (A higher resolution / colour version of this figure is available in the electronic copy of the article).

the receptors on the cell surface that are composed of Insulin Receptor (IR) and Insulin-like growth factor receptor (IGFR) [95, 96]. It has been observed many times that IGFR and IR have a key role in cancer development [97]. Moreover, studies have shown that the relationship between higher circulating IGF families is positively correlated with the increased risk for various cancer types containing colorectal, ovarian cancer, prostate, and breast cancers (Fig. 10) [98]. Thus, it can be said that some types of cancer cells are more sensitive to growth by insulin when compared to normal cells. Therefore, understanding insulin and interactions with receptors from a holistic perspective can accelerate cancer treatment studies.

9. INSULIN AND NERVOUS SYSTEM DISEASE

Any neoplastic or non-neoplastic disorder, including the brain, spinal cord, or peripheral nerves, is classified as a nervous system disease [99]. Although there is no evidence that neurons or the central nervous system (CNS) are insulin-dependent, this system is insulin-responsive and has a vital role in glucose homeostasis (Fig. 11) [100]. Insulin and insulin-like growth factor type-1 (IGF-1) function as modulators that have an essential role in the central nervous system's

metabolic function and neuronal growth, and their receptors are abundantly expressed in the CNS. Insulin and IGF-1 play vital roles in neurite growth, neuronal migration, and synapse formation due to synthesizing related proteins and neuronal development, survival, and differentiation [101-104]. Although information about the presence of insulin in the brain and its immunoreactive effects is insufficient, studies have shown that insulin can transport across the blood-brain barrier into the cerebrospinal fluid [105]. Accordingly, studies have proven that the brain can use both local and peripheral insulin for various functional requirements, including cognitive functions [106, 107]. Therefore, possible dysfunctional disorders that may occur in the molecular mechanism of insulin will directly affect CNS neurons [108]. Numerous studies related to diabetes and nervous system diseases, especially Alzheimer's Disease (AD) [108], support this hypothesis (Fig. 12). Accordingly, it is shown that the strong relationship between neuronal insulin resistance and A β -oligomers, driven by IRS inhibition and TNF- α activation, results in impaired synaptic plasticity, synaptic dysfunction, and synapse loss [109-115]. Collectively, recent studies have shown that insulin is closely related to nervous system-related diseases, including nicotine dependence [116], stroke

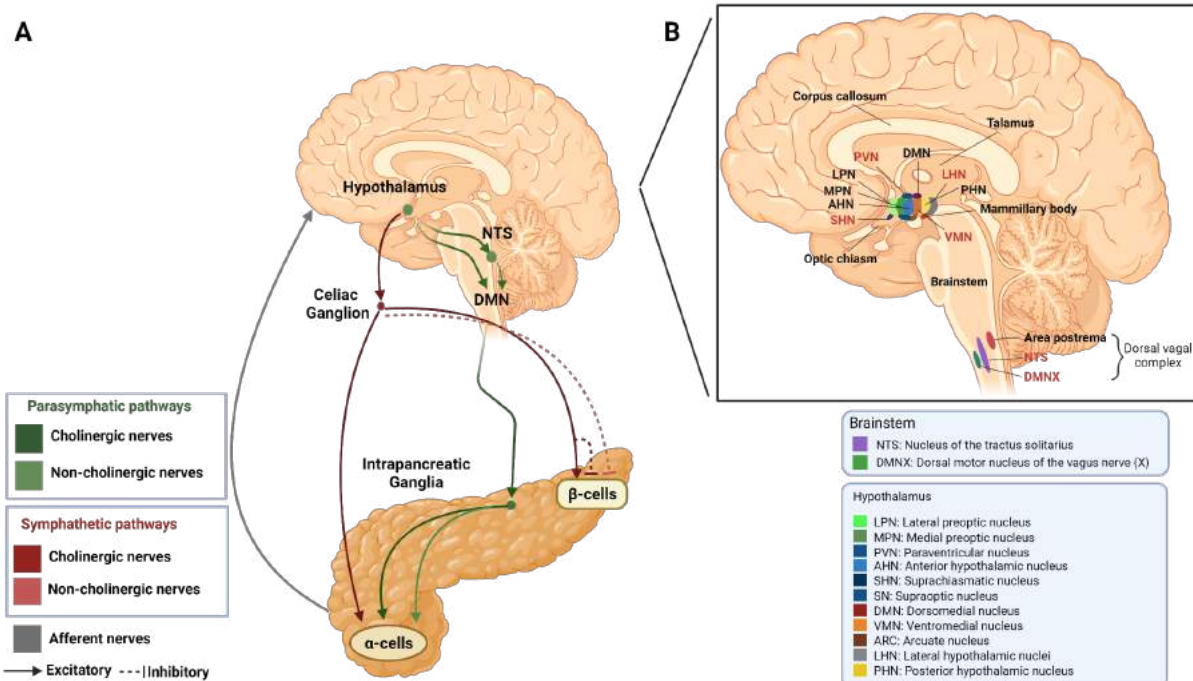


Fig. (11). Schematic representation of the connection between the brain and the pancreas, and sagittal representation of a human brain in terms of energy/glucose homeostasis. **(A)** The relationship of pancreatic α - and β -cells with postganglionic sympathetic and parasympathetic nerves are shown in green and red, respectively. Connections to the brain are shown in gray. **(B)** Representation of glucose homeostasis in relation to key hypothalamic nuclei. (A higher resolution / colour version of this figure is available in the electronic copy of the article).

[117, 118], unipolar depression [119], acromegaly [120, 121], epilepsy [122], social anxiety disorder [123, 124], amyotrophic lateral sclerosis [125], peripheral nerve injury [126], and proximal spinal muscular atrophy [127].

10. INSULIN AND GENETIC DISORDERS

Diseases caused by ancestral genetic variations before or rarely at birth are classified as genetic, familial, or congenital diseases [128]. The close relationship between insulin and key signaling pathways represents an exceptionally large signal network from a metabolic perspective. Besides, recent studies have proven that insulin has been related to a wide variety of diseases such as familial hyperinsulinism (Fig. 13), pancreatic neuroendocrine tumor [59], congenital muscular dystrophy [129], multiple endocrine neoplasia type 1 (ectopic insulinoma) [130], MEHMO Syndrome [131], Complete Androgen Insensitivity Syndrome [132], cryptorchidism [133], 46, XX gonadal dysgenesis [134, 135].

11. INSULIN AND MUSCULOSKELETAL DISEASE

Diseases involving various musculoskeletal disorders, including connective tissue, have been represented as musculoskeletal or connective tissue diseases [136]. Studies have proven that insulin dysfunction/resistance is associated with muscle metabolic defects (Fig. 14) [137, 138], and various musculoskeletal diseases such as panniculitis [139, 140], hypertrophic cardiomyopathy [141], osteoporosis [142, 143], Sanfilippo syndrome type B [144], pseudohypoparathyroidism [145], and cholangiocarcinoma [146].

Collectively, insulin is closely related to various diseases including urinary system diseases [147-150], cell proliferation disorders [151-154], gastrointestinal diseases [155], breast diseases [156-160], hematologic system diseases [161], infectious diseases [162, 163], and psychiatric disorders [164, 165].

12. DIAGNOSIS AND CLINICAL TREATMENT: DIABETES

A wide variety of pathogenic processes are involved in the development of DM directly associated with insulin. Many different anomalies, from the destruction of pancreatic β -cells to insulin resistance, constitute critical points in the development of diabetes. The dysfunction caused by insulin insufficiency in target tissues forms the basis of abnormalities in protein, fat, and carbohydrate metabolism in diabetes. In DM, which correlates closely with hyperglycemia, hyperglycemia's prominent symptoms are characterized by weight loss, polyphagia, polydipsia, polyuria, and blurred vision. Additionally, susceptibility to certain infections and growth disturbances is also part of chronic hyperglycemia. Ultimately, uncontrolled diabetes will lead to life-threatening non-ketotic hyperosmolar syndrome or hyperglycemia with ketoacidosis [166]. Therefore, early diagnosis and screening are vital for people at risk and those with early-onset disease. In this context, the diagnostic limit for diabetes is mainly the fasting plasma glucose level and the glucose-containing hemoglobin level. These levels allow the patient to be diagnosed with diabetes or prediabetes [167].

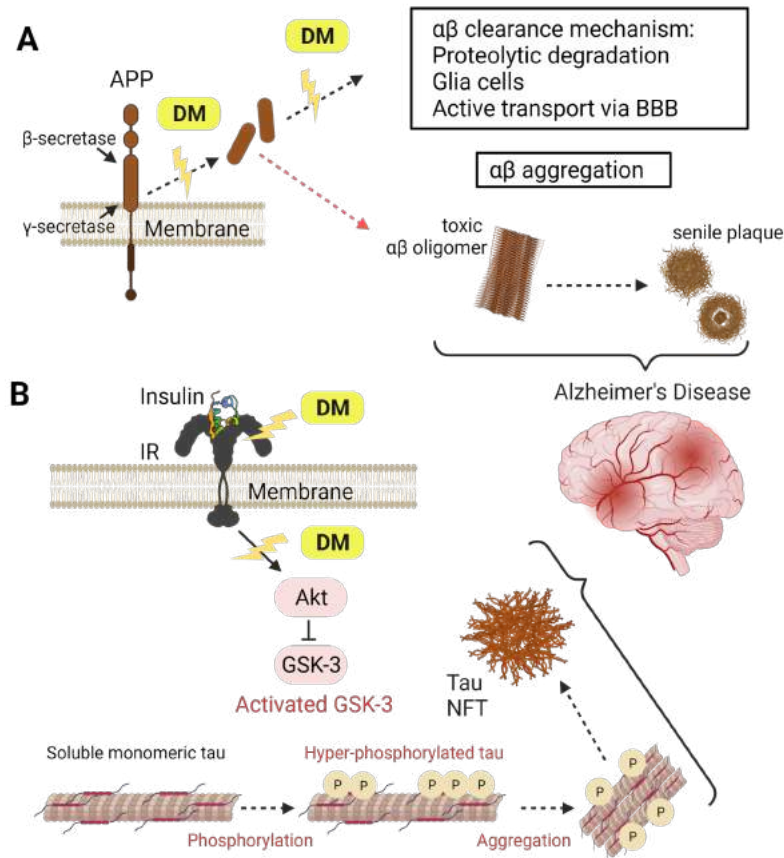


Fig. (12). Demonstration of the effect of diabetes on Alzheimer's amyloid and tau pathology with multiple mechanisms. (A) Insulin resistance caused by DM includes both senile plaque formation and amyloid pathology of the brain and (B) it triggers the activation of GSK-3 leading to hyperphosphorylated tau aggregation characterized by NFTs. DM diabetes mellitus, BBB blood-brain barrier, APP amyloid precursor protein, P phosphorylation, NFT neurofibrillary tangle, GSK-3 glycogen synthase kinase-3. (A higher resolution / colour version of this figure is available in the electronic copy of the article).

The first clinically established therapeutic approach type II diabetes, directly related to insulin deficiency and resistance, progresses in a way characterized by diet, exercise, and weight loss activities. The goal of this process is to reach the optimal A1C level. Although frequently preferred, the second step is to initiate metformin treatment in the absence of contraindications. This treatment was initiated in tandem with a lifestyle intervention following the diagnosis of diabetes. While basal oral treatment, including metformin, is a common treatment, insulin therapy is preferred for relatively severe cases of the disease. Insulin treatment requires consideration of the differences in micro and macrovascular complications and mortality of insulin regimens. If insulin is used during treatment, the use of insulin is facilitated for patients by adopting a basal insulin approach instead of prandial. For example, NPH or detemir is optimal before bedtime; on the other hand, glargine or degludec is optimal for starting regimens in the morning or at bedtime. In treatments involving insulin, exercise and regimen patterns are adjusted with an extra review. If the patient shows symptoms at the bolus insulin level instead of basal insulin, administering short (regular) or fast-acting insulin to patients is a reasonable treatment approach for moderate cases. In such a

case, oral agents other than metformin are not used to reduce the cost compared to basal insulin therapy. Another critical point is that patients using prandial insulin do not use mixed insulin. All things considered, insulin complications should always be followed up, their triggers identified, and patients should be educated accordingly [168,169].

13. CHRONOLOGICAL MILESTONES TO GUIDE THE HISTORY OF INSULIN

The discovery of insulin in 1921 has caused an increase in what we know about insulin cumulatively each passing day (Fig. 1) [170]. Not only is insulin knowledge widened, but also the diseases that are caused by the dysfunction of this versatile hormone are examined. As a result, therapeutic studies and biotechnological applications were conducted [171]. The studies on insulin itself, its function, its receptor on cells, and some pathways it triggered were performed between 1950 and 1985 [171]. Then, studies were performed on insulin's intact expression sequences and its receptor with cloning for the first time between 1985 and 1991 [171]. As insulin's function and structure began to be enlightened, its relationship with the disease gradually emerged. A closely related relationship between diabetes and insulin was

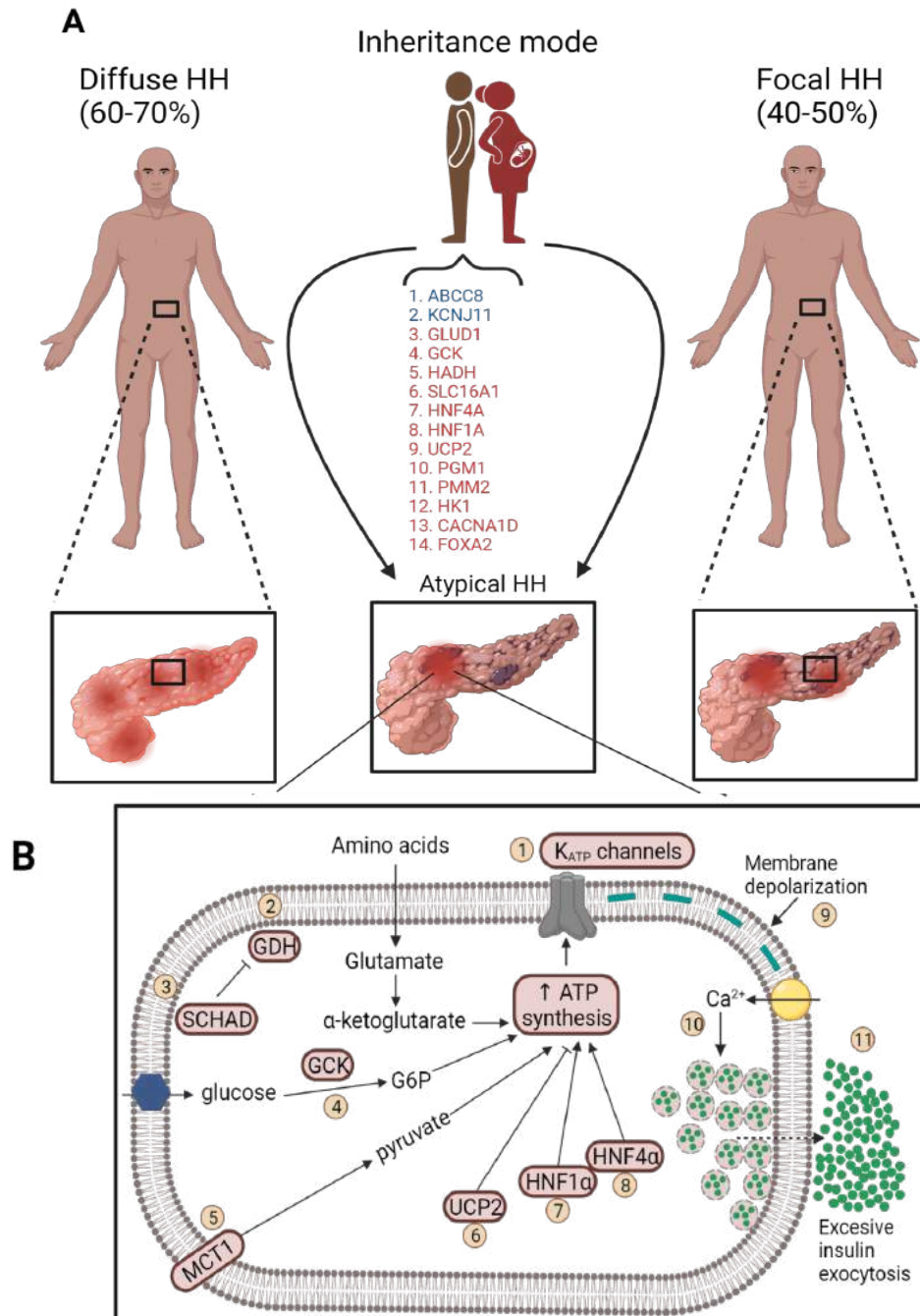


Fig. (13). Schematic presentation of the genetic mechanisms and histological subtypes of Congenital hyperinsulinism (CHI). **(A)** Diffuse subtype HH is characterized by hyperplasia and hyperchromatic β -cell enlargement. The Focal subtype HH is characterized by certain large and small focal lesions. Inheritance mode characterized by Atypical HH is known to be associated with both biallelic recessive and dominant mutations. **(B)** Genetic defects of CHI-associated genes play a critical role in dysregulated insulin secretion. The main of these defects involve pancreatic K_{ATP} channels (ABCC8 and KCNJ11). In addition, enzymatic defects (GLUD1, UCP2, HK1, SCHAD, GCK, etc.) and defects in transcription factors (HNF4A, HNF1A, etc.) are also associated with CHI. β -cell insulin secretion is dependent on a wide variety of metabolic signals, from genes to proteins, and defects in these pathways result in dysregulated membrane depolarization and calcium release caused by channels, resulting in HH. ATP, adenosine triphosphate; Ca^{2+} , calcium; G6P, glucose 6-phosphate; GDH, glutamate dehydrogenase; HNF1 α , hepatocyte nuclear factor 1 α ; HNF4 α , hepatocyte nuclear factor 4 α ; short-chain 3-hydroxyacyl CoA dehydrogenase (SCHAD), UCP2, mitochondrial uncoupling protein 2; monocarboxylate transporter subtype 1 (MCT-1); Uncoupling protein 2 (UCP2); HH, hyperinsulinaemic hypoglycaemia. (A higher resolution / colour version of this figure is available in the electronic copy of the article).

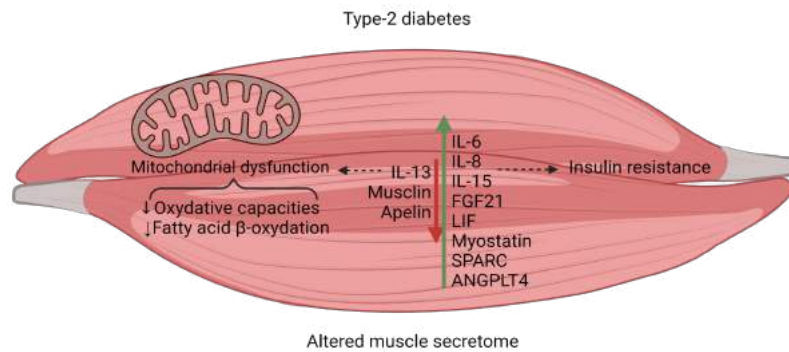


Fig. (14). Demonstration of T2D-related muscle metabolic defects and the effect of myokines on the mechanism of the altered muscle secretome. Muscle metabolic defects and altered muscle secretome are strongly associated with T2D diabetes. Secretion of myokines, RNAs, mtDNA, and metabolites, and sedentary behaviors also play a role in altering this mechanism. An altered secretome is also characterized by skeletal muscle mitochondrial function and triggers the development of insulin resistance. IL-6, Interleukin 6; IL-8, Interleukin 8; IL-15, Interleukin 15; FGF21, Fibroblast growth factor 21; LIF, Leukemia inhibitory factor; SPARC, Secreted Protein Acidic And Cysteine Rich; ANGPTL4, Angiopoietin-like 4. (A higher resolution / colour version of this figure is available in the electronic copy of the article).

revealed in a study conducted on dogs in 1921 [171]. The study found that insulin controls diabetes. Since then, therapeutic approaches to diabetes have always been based on the treatment of insulin or insulin analogs [170,171].

In the direction of finding insulin analogs, scientists have started to play with insulin since 1936 [172]. For this purpose, protamine was added to insulin for the first time in 1936, allowing insulin to remain in circulation for a long time [173]. It was released by Novo Nordisk under the name "Neutral Protamine Hagedorn" (NPH) [173]. In addition, around the 1950s, intermediate-acting Lente insulin was produced, which is now obsolete [174]. The discovery of the insulin receptor after 1971 was followed by the introduction of the use of U100 insulin [171]. In the years when U40 and U80 were used routinely, the U100 went down in history as a great convenience [171]. After the invention of the wearable insulin pump in 1976, recombinant human insulin production was realized with the first transportable insulin pump in 1978, and it was approved in 1982 [171]. Two years after the metformin approval, which was in 1996, fast-acting insulin lispro was introduced by Eli Lilly and his company for the first time [171]. Then, stimulating insulin secretion in the presence of glucose was another ground-breaking event in which a repaglinide drug was developed by Novo Nordisk [171]. Two years later, Sanofi Aventis in the US introduced long-acting insulin Lantus (glargine) as a basal insulin analog [171].

As the insulin-based drugs and their derivatives were released, an examination was needed for the usage of other drugs with insulin. These examinations were performed in detail between 2005 and 2008 [171]. First, Exubera [175] inhaled insulin, which was withdrawn in 2007 [176], then long-acting Degludec insulin was produced in 2013 [177]. Today, various insulin modifications are still being tested and many patients are still active in this area. Although there are countless milestone studies on insulin, the most dynamic and disruptive field today is undoubtedly omics and structural-based protein discovery and analog inventions.

14. THE MULTI-OMICS APPROACH TO INSULIN

Since the discovery of insulin, the most critical issue associated with many diseases, especially diabetes, is 'insulin

resistance.' Understanding the molecular differences and the underlying mechanism of insulin resistance is important to take right strategic steps regarding the disease process, inhibit the progression of pathogenesis, and plan good therapeutics accordingly. In this context, the emergence of new "omics" approaches will provide invaluable opportunities to realize the prospective strategies mentioned in this phenomenon [178].

15. INSULIN AND GENOMICS & EPIGENOMICS

As known, the underlying mechanism of many insulin-related diseases, especially T2D, correlates strongly with the interaction between genetics and the environment. In this context, some new insulin-related genes, including Transcription factor 7-like 2 (TCFL2) [179] and Peroxisome Proliferator Activated Receptor Gamma (PPARG) [180], were confirmed and identified with genomics-based studies, analyses, and prospective approaches conducted in the early 2000s. Of these, TCFL2 was determined to have a critical cell-autonomous role in controlling β -cell mass and function [181]. These studies were further advanced by next-generation sequencing and complex genomics analyses; following which a dozen new insulin-related genes were discovered, including the Solute Carrier Family 30 Member 8 (*SLC30A8*), CDK5 Regulatory Subunit Associated Protein 1 Like 1 (*CDKAL1*), and Insulin Like Growth Factor 2 MRNA Binding Protein 2 (*IGF2BP2*) genes [182-184]. While Zinc transporter 8 (ZnT8), a product of *SLC30A8*, provides the regulation of the pathways involved in the regulation of granulated Zinc intake required for insulin secretion; *SLC30A8* haploinsufficiency has been proven by GWAS studies, combined with a meta-analysis, to lead to insulin-related diseases [185, 186]. For example, Ayers *et al.*, in their first genomics-based study on cryptorchidism, found a direct relationship between insulin-like peptide 3 (*INSL3*) and recessive variants of its receptor, relaxin family peptide receptor 2 (*RXFP2*), with this disease and showed that it was associated with testicular descent in humans [187]. In the last years, studies have proven that the GWAS approach has been widely adopted in studies that analyze diseases, including their relationships with insulin, such as Simpson-Golabi-Behmel syndrome [188], cardiometabolic disease [189], and

cryptorchidism [190]. These have given large-scale genomics results. Additionally, combining GWAS studies with expression quantitative locus (eQTL) [191] and DNA methylation [192, 193] provides a more integrative analysis approach to clearly determine the causal effects of genetic variants of these diseases from a molecular perspective. More than 150 T2D variants have been identified in large-scale GWAS studies. This suggests the need for genomic-based approaches to understanding insulin-related pathways [194].

Epigenetics, which reveals the importance of the environment in the phenotype, refers to the expressional changes in the gene without changes in the nucleotide sequence. Doubtless, epigenetic changes are inherited phenomena that can dynamically modulate the genome and reshape the phenotype. Several epigenetic mechanisms, including histone and chromatin modification [195-197] DNA methylation modifications [198, 199], and non-coding RNAs [200-203], show critical effects on the islets and β -cell adaptation [204, 205]. Epigenomics studies conducted in this direction have shown that DNA methylation has great importance in T2D pathophysiology. According to these studies, the promoter of PPARG Coactivator 1 Alpha (PPARGC1A) [206], pancreatic and duodenal homeobox 1 (PDX1) [207,208], and similar 254 genes, which play a role in the regulation of insulin released from human islets, is hypermethylated in T2D compared to healthy subjects [209]. This result is inversely correlated with expression results and β -cell survival, indicating that insulin mRNA is downregulated in T2D patients as a result of the methylation of these promoters [210]. In a further study using the whole-genome bisulfite sequencing (WGBS) approach, they identified 25,820 methylation sites in the genome, 80% of which are CpGs, including genes important for the functions of β -cells, such as PDX1 [211]. In epigenomics studies, blood-based DNA methylation biomarkers can become among the commonly used methods to evaluate β -cell survival [212].

16. INSULIN AND TRANSCRIPTOMICS & EPI-TRANSCRIPTOMICS

Transcriptomics is another field of omics that can provide invaluable information from a molecular perspective that includes insulin-related details. Especially oligonucleotide microarray tools used in islets studies performed on patients and healthy subjects. They are among the most useful tools primarily preferred in transcriptomics studies [178]. mRNA levels of many insulin-associated genes, such as Insulin Receptor (INSR), Insulin Receptor Substrate 2 (IRS2), AKT Serine/Threonine Kinase 2 (AKT2), and Hepatocyte Nuclear Factor 4 Alpha (HNF4a) [213], and GWAS identified genes, such as Insulin Like Growth Factor Binding Protein 2 (IGFBP2) [214], were downregulated in patients compared to controls that had been proven by transcriptomic based studies. Our knowledge about the expressional regulation of diseases has increased exponentially with transcriptome-based studies. In a study conducted on the subject, 83 islets were analyzed using genomics approaches, including *tour de force* transcriptomic analysis [215]. This study is the most comprehensive study performed in human islets, revealing many variants associated with β -cells, mainly 5'-Nucleotidase Ecto (NT5E), p21 protein (Cdc42/Rac)-activated kinase 7 (PAK7), Transmembrane emp24 domain-containing

protein (TMED), and Tetraspanin-33 (TSPAN33) [216]. Although this technique has limitations [217], this handicap has been overcome with fluorescence-activated cell sorting (FACS) strategies [218]. In another study on the subject, a systematic analysis of prospective islet progenitors with epigenetic and transcriptomic profiling techniques was presented, and clinical replacement therapies were criticized in this direction [219]. Another method is single-cell RNA sequencing (scRNA-seq) [219-221]. Using this technique, transcriptome-based genetic programs of each cell type in islets were examined and affected genes, such as FXYD Domain Containing Ion Transport Regulator 2 (FXYD2) and Glycerol-3-Phosphate Dehydrogenase 2 (GPD2), were revealed in sick cells [222]. Accordingly, in an *in vivo* study, it was shown that the ablation of FXYD2 from β -cell caused an increase in β -cells and hyperinsulinemia [222, 224, 225].

Transcription, the most crucial step of the central dogma, requires comprehensive regulation to ensure optimal gene expression. Damages that may occur during the genomic and epigenetic editing of mRNA copied from the genomic DNA locus may cause many diseases [223]. Necessary chemical modifications of mRNA (messenger RNA), tRNA (transfer RNA), and rRNAs (ribosomal RNA) in translational steps are required for proper translation efficiency [223-225]. One of these, mRNA methylation (m6A), is a very dynamic phenomenon, and this has been demonstrated by the clear identification of α -ketoglutarate-dependent dioxygenase AlkB family of proteins (ALKBH5) [226] and obesity-related proteins (FTO) [227]. Interestingly, studies show that obesity is closely related to insulin. In other words, m6A controls mRNA translation, translocation, splicing, and its decay, thereby modulating a variety of cellular functions involving the adaptation of β -cells associated with insulin resistance [228].

17. INSULIN AND PROTEOMICS

All kinds of proteomic studies on human insulin, especially its measurement, are critical for all sorts of insulin-related conditions such as diabetes, toxicology, hypoglycemia, and sports antidoping [229]. Studies in which insulin and insulin analogs are detected and addressed are closely related not only to the treatment of diabetes and hypoglycemia but also to antidoping and toxicology [230-234]. Undoubtedly, these studies' critical value is their contribution to immunological tests, including the detection of insulin and insulin analogs. However, these tests cannot show the desired success in determining insulin analogs [235]. Regarding the differences in the unique sequence and mass, the only technique that analogs can be measured with is proteomics-based approaches, such as mass spectrometry [236]. These proteomics-based methods, in which endogenous insulin and all kinds of analogs can be detected, are basic science results and are preferred for versatile biological applications [237]. Today we know that a strategic experimental move has thousands of proteomic outputs and provides critical information, thanks to proteomics approaches that include the quantitative analysis of the entire proteome. For example, proteomic analysis of islets obtained from only eight mouse strains could yield diabetes-related metabolic profiles of the islets proteome of the genetic background and provide evidence of the vital link between dopamine and insulin secretion [238].

Thanks to lipid droplet analysis with proteomic approaches, which have multi-process steps, more in-depth information was obtained about the storage and processing of lipids in cells, and the presence of proteins belonging to the mitochondrial category was observed at a high rate in cases of diabetes. Therefore, these results indicate the metabolic importance of β -cell mitochondria in insulin secretion [239].

Additionally, proteomic techniques are not limited to discovery and invention-based studies. Still, they are an approach that provides excellent convenience to researchers in clinical studies and accelerates studies in this direction. In this context, a high-throughput proteomics study showed that proteins such as growth hormone receptors, insulin-like growth factor-binding protein 2, and aminoacylase-1 are closely related to diabetes according to the plasma proteome results obtained from diabetics, and new candidate proteins were determined [240]. In another similar high-throughput proteomics study, high efficiency results were obtained by determining the amount of insulin in plasma while simultaneously detecting all kinds of additional insulin isoforms and isoform sequences [241]. Proteomics approaches are also used as the choice of a fast and robust validation of previous expressional studies [242]. In a discovery-based study with proteomics techniques, a strong association of GLUT4 storage vesicles (GSVs) with low-density lipoprotein receptor-related protein 1 (LRP1) was determined, and secretion of this receptor required for GLUT4 storage vesicle function [243]. In conclusion, many insulin-related mechanisms, especially insulin secretion, signaling pathways, and complex functions of β -cells, have been elucidated by proteomics strategies.

18. INSULIN AND METABOLOMICS

Metabolomics is the most common method of omics, as it is used to identify and quantify endogenous small-molecule metabolites (<1,500Da) [244]. A wide variety of metabolites in urine, blood, and tissues can be detected with nuclear magnetic resonance (NMR), gas or liquid chromatography-mass spectroscopy (GC-MS, LS-MS), and similar approaches, which form the backbone of omics methods [245]. Thanks to these techniques, whose sensitivity is characterized by minimal metabolic changes, biomarker detection is routinely performed in clinical [245-247] and *in vivo* studies [248, 249]. A study conducted in this direction was discussed to find useful biomarkers that employ the metabolomic profile obtained from diabetic kidney disease (DKD) and its progression [250]. Other studies have shown that the changing metabolomic states of obese individuals reflect metabolic disorders and shed light on the disease's underlying mechanism [251, 252]. In another study related to this, plasma metabolic profiles were examined to further elucidate the mechanisms underlying obesity associated with insulin resistance in children. It was determined that acylcarnitines, aromatic amino acids, and BCAAs could be prospective biomarkers [253]. In a study investigating the effect of nutrients on insulin secretion, a detailed metabolomic analysis was performed on a β -cell line using GC-MS to reveal the critical role of a coordinated signaling cascade dependent on glucose metabolism [254, 255]. In another study on T2D, the metabolomics and gut microbiome integrated mechanism of Naoxintong Capsule (NXT), a formulation of traditional

Chinese medicine, was investigated and its effect on diabetic rats was revealed [249].

19. INSULIN AND GLYCOMICS

Following the overwhelming presence of approaches such as genomics and proteomics in studies, it has become clear that it is necessary to use various omics techniques, considering posttranslational modifications (PTM), to see the big picture [256]. When protein databases are sifted through, it will be easily seen that glycosylation (N-glycosylation) constitutes 70% of the PTMs occurring in proteins [257, 258]. The layer formed by the glycoproteins surrounding the cell is the first point of contact with the extracellular matrix. It is here that oligosaccharides play a crucial role in providing epitopes to protein receptors, cell-matrix, and cell-cell interactions [259-261]. Considering the critical importance of N-glycans in protein folding and conformational maturation [262-264], disruptions, such as dysfunction of glycoproteins and disorders in their secretion, will cause the onset of many diseases [265]. One of such is insulin resistance, which is undoubtedly associated with glycosylation. Insulin resistance includes numerous metabolic syndromes such as cardiovascular disease, diabetes, obesity, hypertension, and dyslipidemia [266, 267]. Although the underlying mechanisms are not clear, studies show that dysfunctional mechanisms in the hexosamine biosynthetic pathway (HBP) lead to insulin resistance in peripheral tissues [268, 269].

Interestingly, the effect of the combined injection of insulin and glucosamine in rats was proved to be more effective than the result of insulin alone [269,270], indicating a strong correlation of insulin with HBP. A direct relationship between N- and O-glycans and insulin has been shown in studies conducted up to this time. For example, it has been observed that changes in the activity of enzymes associated with glycosylation cause changes in fucose and sialic acid contents in patients with insulin resistance [271-274]. Likewise, while insulin deficiency shows an inverse correlation with plasma sialic acid amount, chronic hyperinsulinemia shows an inverse correlation with plasma sialic acid, indicating a strong relationship between insulin and glycosylation [275]. Studies on weaning rats show that the regulation of galactosyltransferase and α -1,2-fucosyltransferase is directly related to insulin levels. This and numerous other glycomics-based studies strongly suggest that complex glycans are associated with insulin resistance [276].

In addition, current hot topics about insulin-related subjects in the context of recent knowledge and the available literature is here; in a study observing the effect of glucose loading on serotonin transporter (SERT) availability from the brainstem in humans, the presence of SERT was reported to be negatively associated with BMI after glucose loading in humans. Accordingly, it has been stated that SERT may play a role in eating behavior with the direct effect of insulin [277]. Another study using various bioinformatic assays demonstrated that genes expressed by thiopurine methyltransferase (TPMT) in patients with colon cancer function as extracellular matrix (ECM) structural component, insulin-like growth factor binding, cell adhesion molecule binding, and growth factor binding. As a result, it has been discussed

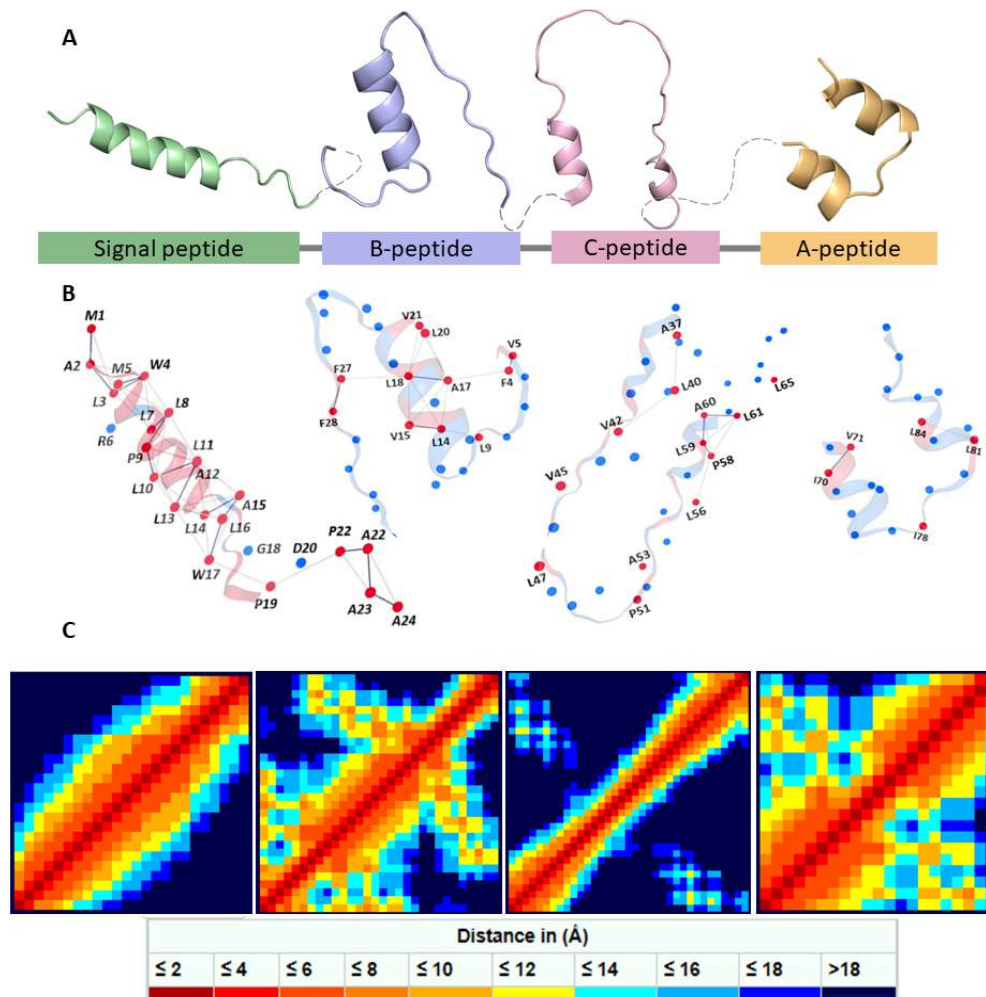


Fig. (15). Demonstration of preproinsulin domains using AlphaFold and Network Analysis of Protein Structures (NAPS) server. (A) Structural and schematic representation of the human preproinsulin (Uniprot ID: P01308) precursor using AlphaFold server. (B) 3D network analysis of human preproinsulin precursor for hydrophobic residues using the NAPS server. Hydrophobic residues are colored in red. (C) Residual distance matrix analysis of human preproinsulin domains using NAPS server. (A higher resolution / colour version of this figure is available in the electronic copy of the article).

that the mRNA level of TPMT may be a new prognostic biomarker for patients with colon cancer [278]. In a study showing promising effects of bile acids in drug encapsulation for oral administration, cloned pancreatic β -cell lines were encapsulated using bile acid-Eudragit NM30D® capsules. The relationships between the stability of the capsules and the cellular biological activities were observed to show improved cell viability, insulin, inflammatory profile and bioenergetic as well as thermal and chemical stability when compared to the control [279].

20. INSULIN STRUCTURES

The human insulin is structurally composed of four parts: a signal peptide, B-chain, C-peptide, and A-chain (Figs. 15 and 16). β -cells in the islets of Langerhans in the pancreas, through the *INS* gene expression, synthesize the precursor insulin known as preproinsulin, which is 110 amino acids long. While the A-chain and B-chain are highly conserved

sequences between vertebrates [280], the C-peptide has a highly variable amino acid length and composition sequence [281]. C-peptide was thought to be an inert byproduct in insulin synthesis and process, acting as a bridge between A and B chains [282]. However, studies have shown that C-peptide is a peptide hormone that positively affects microvascular, kidney, and nervous system functions in diabetic model organisms [283-287]. Studies have proposed that showing the pentapeptide moiety (EGSLQ) in the C-terminal of the C-peptide may have the potential to represent a dynamic, active site for C-peptide itself. Furthermore, this pentapeptide, which includes the Glu1 and Gln6 residues, is thought to function evolutionarily as a hormone-like peptide [288-290].

The preproinsulin pre-part consists of a 24 amino acid long signal peptide that targets this secretory protein to the RER [291]. In RER, this signal peptide is removed by peptidase.

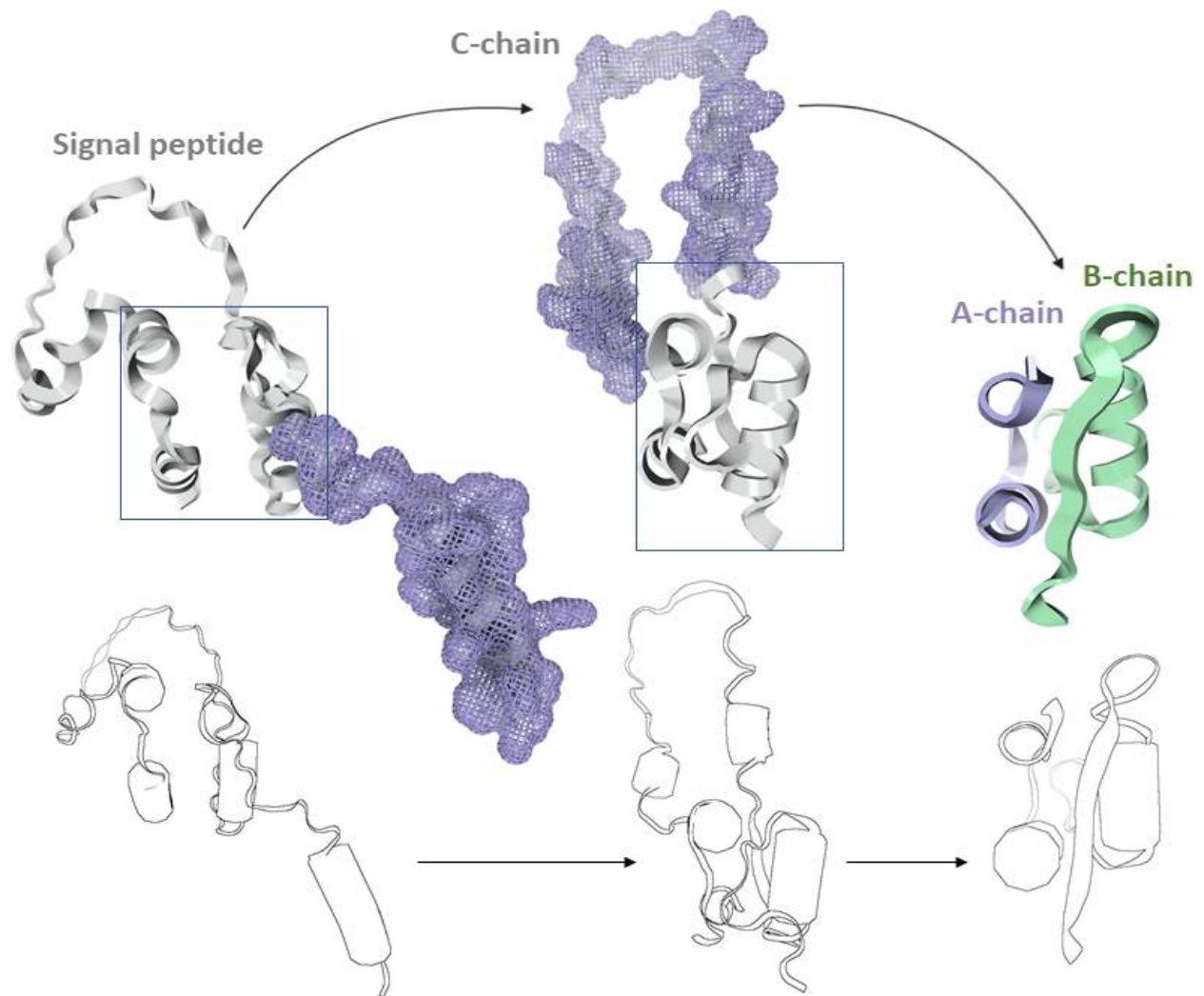


Fig. (16). Demonstration of preproinsulin 3D conformation predicted with AlphaFold and visualized with Protein Imager. Symbolic representation of 3D preproinsulin structure predicted by AlphaFold server, towards mature conformation. Mature insulin is obtained by removing the twenty-four amino acid signal sequence and the C-peptide sequence (represented with colored double mesh in slate). (A higher resolution / colour version of this figure is available in the electronic copy of the article).

The remaining polypeptide is known as proinsulin, and oxidative folding occurs in RER and insulin folds to form disulfide bonds [292]. At this point, misfolding due to mutational genetic predisposition, or the biosynthetic load of the ER, leads to the emergence of phenotypes closely related to diabetes [291-293]. Insulin is inactive in this state, and to take its biologically active form, the 31 amino acid (57-87) part, called C-peptide, must be removed from the polypeptide [294-296]. This process occurs in the Golgi body. In Golgi, 31 amino acids are removed by Prohormone convertase I&II and Carboxypeptidase E [297-299]. After trans-Golgi processing, the remaining two short peptides are connected by disulfide bonds to form mature insulin [300]. Mature insulin consists of two peptides; a 21 amino acid long A chain corresponding to residues between 90-110 and a 30 amino acid long B chain corresponding to residues between 25 and 54. Three disulfide bridges stabilize these peptides [301, 302]. The A-peptide consists of two short helices connected by a

turn, while the B-peptide consists of a strand and a helix connected by a turn. In the B peptide, the N- and C-terminal ends show conformational flexibility [303]. Thus, the first eight residues of the B peptide can arrange either in a helical structure to form a relaxed (R) conformation or a taut (T) conformation or an open (O) conformation with an extended structure (Fig. 17) [303-306]. Another variant of the R form is that the first two residues of the B-peptide form a frayed relaxed conformation in the extended structure, along with the other two conformations [303, 304]. As known, insulin in secretory granules is stored as hexameric microcrystals to prevent aggregation and degradation [307]. Monomer conformations of hexamers can be found in various conformations such as R6, T6, or T3R3 in the states concerned; these three types of hexamers differ both in their surface properties and in their hexamer conformation (Fig. 18) [307, 308]. Although they are different, they can co-exist equally in solution, and if phenol compounds such as phenol

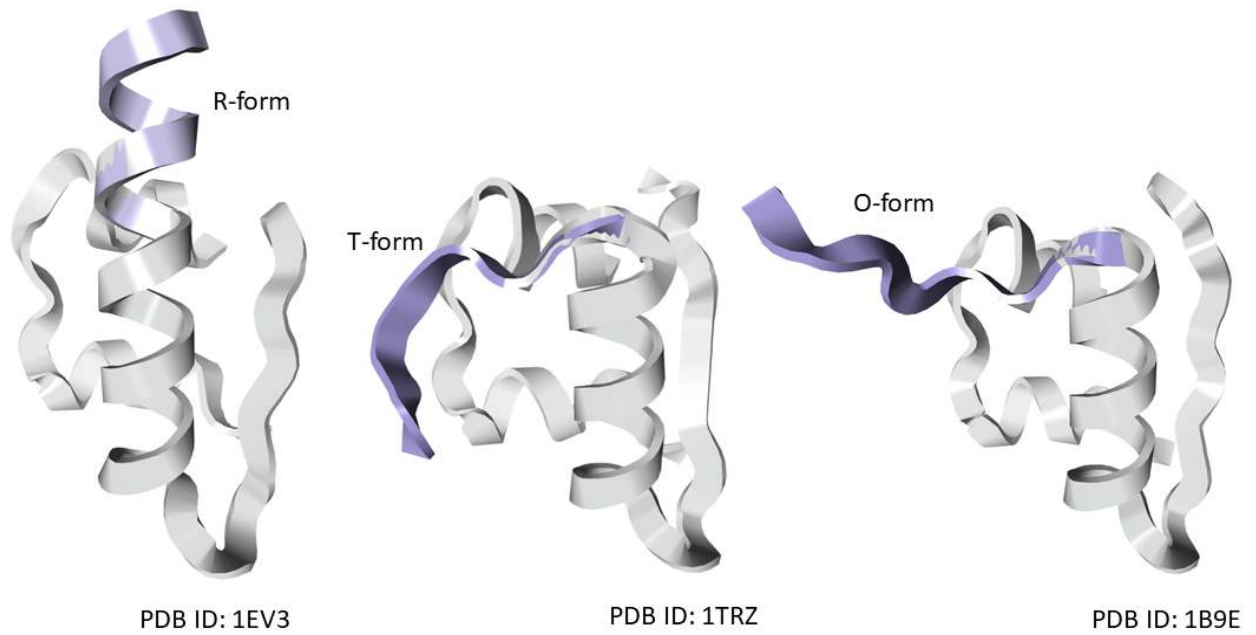


Fig. (17). Conformational forms of insulin. The B-peptide of insulin has three different forms known as the relaxed (R), tense (T) and open (O) form. (A higher resolution / colour version of this figure is available in the electronic copy of the article).

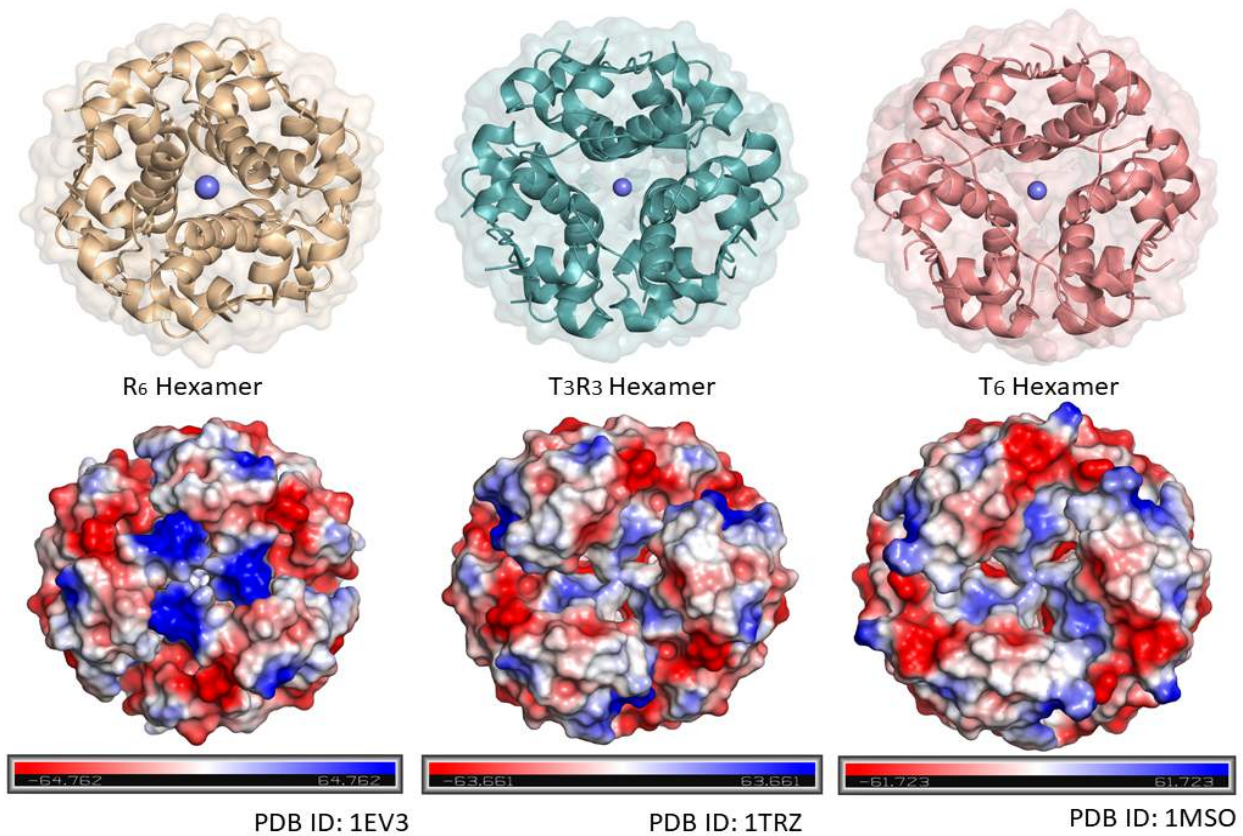


Fig. (18). Representation of the surface mode and the electrostatic surface mode of hexamer insulin comparisons in the R6, T6, or T3R3 forms. Hexamer insulins have different conformations such as R6, T6, or T3R3. Surface properties are different from each other. (A higher resolution / colour version of this figure is available in the electronic copy of the article).

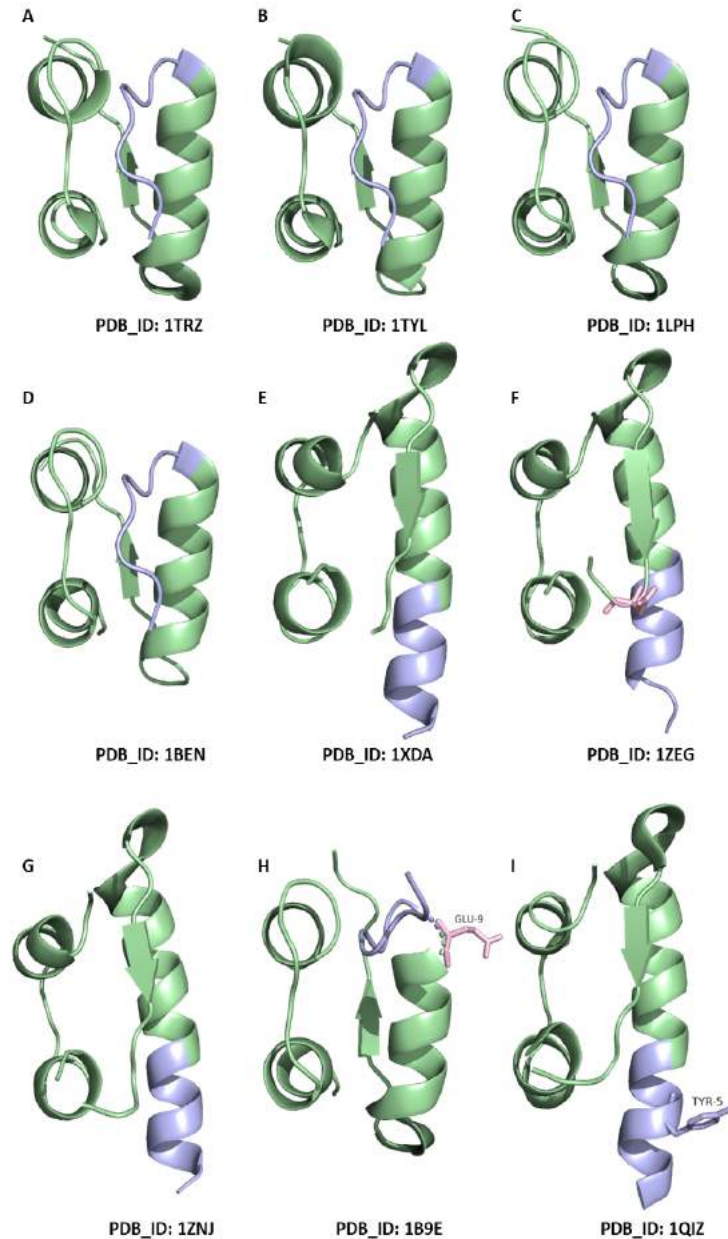


Fig. (19). X-ray diffraction-oriented insulin structures in Protein Data Bank-I. (A higher resolution / colour version of this figure is available in the electronic copy of the article).

or m-cresol are bound to the hexamer, they facilitate hexameric formation such as R6 or T3R3; this is important in forming specific conformations in insulin formulations [309, 310]. After being synthesized as a hexamer and given to the blood, it dissociates into dimers and monomers by diluting the blood before binding to its receptor (Fig. 2) [311-315]. Sometimes the dimer forms and the monomers are always small enough to diffuse through the adherent junctions of the microvasculature surrounding the tissues [313, 314]. Hexameric inactivity and monomeric activity are characterized by the dissociation rate of the injected insulin in the body [30, 316, 317].

21. X-RAY DIFFRACTION (CHRONOLOGICALLY)

In 1994, the T3R3 insulin hexamer structure was determined. T3R3 refers to alpha-helical and extended conformations of the B-chain's first 8 residues. According to this study, it was clearly evaluated the asymmetric unit of TR dimer, localization, and coordination of the zinc ions and their putative off-axial zinc-binding sites [305] (Protein Data Bank (PDB_ID: 1TRZ) (Fig. 19A). In the same year, 4'-hydroxyacetanilide (Tylenol) and hexameric insulin complexes were studied. This nontoxic phenolic derivative was shown to induce the T→R transition, forming a T3R3 hexamer conformation. The results of this study revealed the

differences between therapeutic preparations and human insulin [312] (PDB_ID: 1TYL, 1TYM) (Fig. 19B). In 1995, the fast-acting LysB28ProB29-human insulin was crystallized as a T3Rf3 hexamer. This structure revealed that B-chains cause local conformational changes in the C-terminus. It was stated that dimer stabilization was achieved by eliminating the two hydrophobic interactions and the loss of dimer interactions led to the weakening of hexamerization. This highlights the importance of the rapid-time effect of the hexameric structure in therapeutic formulations [313] (PDB_ID: 1LPH) (Fig. 19C). In 1996, the complex of T3R3f insulin hexamer with 4-hydroxybenzamide was demonstrated. Whereas one phenol /m-cresol/resorcinol /4'-hydroxyacetanilide or methylparaben molecule is bound by each Rf-state monomer, two 4-hydroxybenzamide molecules are connected by each Rf-state monomer. The presence of two molecules causes a wide hydrogen-bonding network between T- and Rf-state trimmers. This network, organized by water molecules, gives stability to the hexamer formation [314] (PDB_ID: 1BEN) (Fig. 19D). In 1997, the fatty acid acylated insulin structure was introduced. Substitution of B29 Lys with insulin prolongs the effect of the hormone by reversibly binding to circulating albumin [315] (PDB_ID: 1XDA) (Fig. 19E). In 1998, the mutant insulin B28 Pro → Asp was introduced as a monomeric, fast-acting hormone. It was shown that this insulin could be stimulated to produce zinc hexamers *via* small phenolic derivatives such as phenol and m-cresol. This mutant insulin causes increased structural flexibility in the B chain through the loss of intermolecular van der Waals interactions. This demonstrates the importance of understanding the monomeric properties of the mutant insulin from the perspective of the monomer-monomer interface [316] (PDB_ID: 1ZEG, 1ZEH) (Fig. 19F). In the same year, two crystalline forms of natural insulin structure were identified and refined at room temperature (PDB_ID: 1ZNI, unpublished) (Fig. 19G). In a 1999 study, Yao *et al.* showed that the insulin O state is different from the natural R and T forms. They demonstrated this with the B9 mutation (Ser-Glu) in human insulin. According to this study, the O state can be characterized by the natural form of insulin with a lower aggregation structure and is possibly related to insulin fibril formation [317] (Fig. 19H). In the same year, B5 His → Tyr mutant insulin was synthesized to see if tyrosine induces the R-state of the insulin structure and if its side chain could mimic the phenol binding effect of the hexamer. This study showed that in the presence of resorcinol and phenol, B5 Tyr hexamers adopt an R6 conformation by destabilizing the T-state. This observation highlights the role of B5 His in regulating crystal packing interactions and in identifying the hexamer conformation [318] (PDB_ID: 1QIZ, 1QJ0) (Fig. 19I). In 2000, the structure of three R(6) hexameric insulins complexed with resorcinol or m-cresol was determined. In this study, the relationship between T→R conformational transitions was determined by deprotonation of the GluB13 side chains in R(6), T(3)R(f)(3), and T(6) hexamers [303] (PDB_ID: 1EV3, 1EV6, 1EVR) (Fig. 20A). In the same year, a new T(3)R(3) Zn-human insulin complex variant was identified by the synchrotron X-ray powder diffraction method. It had been suggested that this approach could be used to explain the structural differences of proteins associated with single-crystal studies [319] (PDB_ID: 1FU2, 1FUB) (Fig. 20B). In

2001, T(3) Rf(3) hexamer insulin was shown to undergo a phase transition when cryo-cooled. Based on this work, it was suggested that this transition is not related to temperature but that conditions, such as shrinking of the crystal itself, shrinking of the cryoprotectant drop, or shrinking of the thin layer of paraffin oil, are associated with pressure [320] (PDB_ID: 1G7A, 1G7B) (Fig. 20C). In the same year, the structure of the destriptide (B28-B30) insulin (DTRI) analog was determined by crystallizing with zinc ions at near-neutral pH. Because of the insulin B-chain C-terminus flexibility, in the native insulin dissociation process, the DTRI hexamer may be taken as a transition state. This can be considered as an advantage that can be achieved in a possible insulin hexamer degradation process due to the DTRI structure [321] (PDB_ID: 1HTV) (Fig. 20D). Lee *et al.* demonstrated a three-dimensional DQ8-immunodominant peptide structure to explain the effect of the major histocompatibility complex HLA-DQ2 and HLA-DQ8 glycoproteins in non-obese diabetic (NOD) mice and humans. This study showed that diabetes may be caused by the same antigen-presenting event in NOD mice and humans. Some residues of the DQ8 structure associated with the P9 pocket are closely related to type 1 diabetes [322] (PDB_ID: 1JK8). In 2002, dab(A8)-insulin was introduced to show the correlation between stability and activity. Unfavorable helical C-cap, which refers to Thr(A8), was substituted with more favorable Arg (A8) and His (A8) amino acids. They also explore alternative mechanisms for A8 activity that suggest multiple substitutions. This study showed that Dab (A8) -insulin is preferable for hypothesis-driven protein design [323] (PDB_ID: 1J73, 1JCA) (Fig. 20E). In 2003, the T(6) hexameric structure of human insulin was demonstrated from a single air-dried crystal at room and cryogenic (100K) temperatures. In this study, some information about the space groups of insulin at two temperatures, their shapes, and the locations of zinc ions has been obtained. Furthermore, one of the different features compared to other structures is the absence of hydrogen bonding contacts between the Glu-B13 residue pairs. Such lack of contact causes disruption of the hydration structure in the hexamer, leading to the disorientation of the Glu-B13 side chains. These results showed that it is important that the hydrated structure is involved in stabilizing the structure of the B13 residues by regulating the charge repulsion between six different B13 glutamates [324] (PDB_ID: 1OS3, 1OS4) (Fig. 20F). In the same year, an inactive chiral analog of T(3)R(3) zinc hexamer insulin structure was identified. This contains nonstandard substitution allo-Ile(A2). It is therefore called allo-Ile (A2)-insulin. Whereas there is a high similarity between both native insulin and this variant, insulin, differences are observed near the variant region of the inactive chiral analog. Additionally, the T- and R-state conformation showed a response to chiral perturbation, suggesting their intrinsic plasticity. These variants retain their native-like protein structure, but this analog has a lower receptor binding activity [325] (PDB_ID: 1Q4V) (Fig. 20G). In the same year, T(6) human insulin was determined at 120K at a 1.0 Å resolution. In the cryofreezing condition, they observed that the B chain's first four residues undergo a conformational shift compared to the room-temperature condition. They also claimed that the disorder observed at room temperature was eliminated when frozen [326] (PDB_ID: 1MSO) (Fig. 20H). In 2004, it was determined that the photo-cross-linking

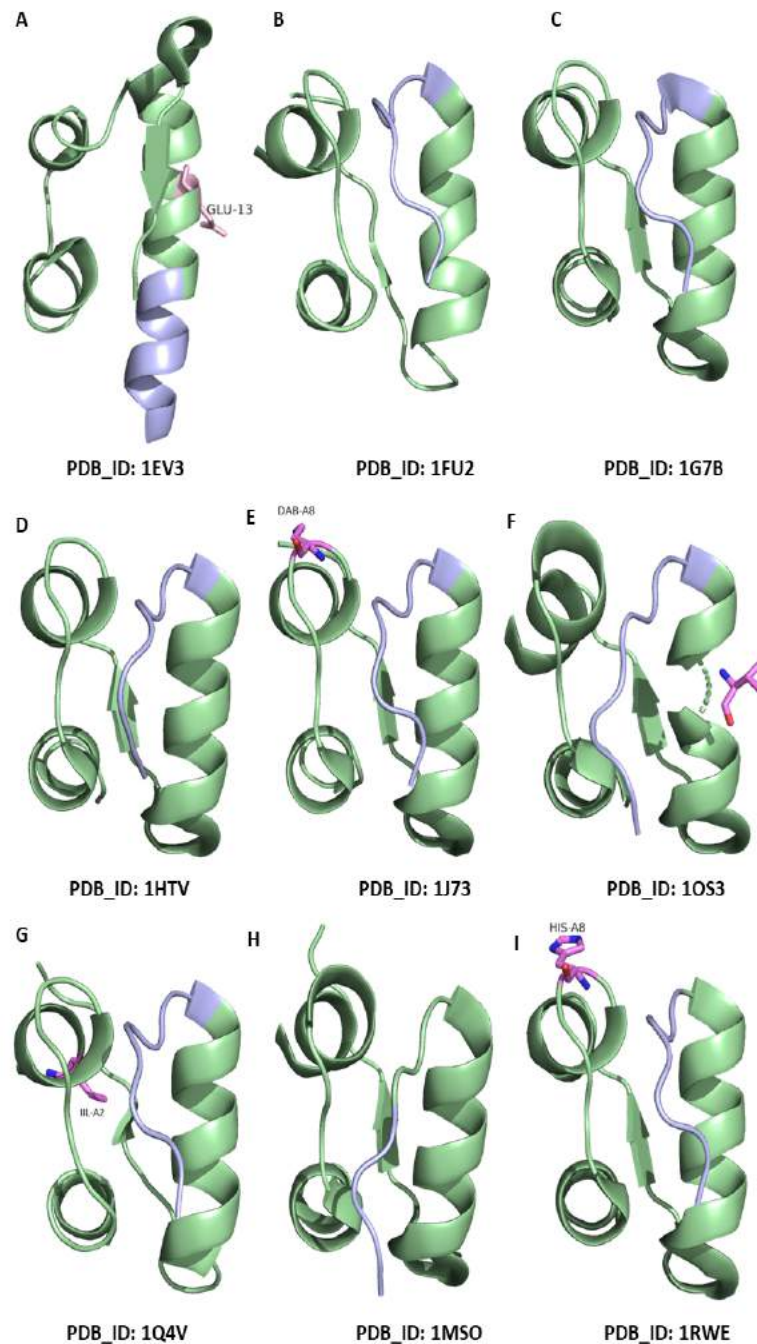


Fig. (20). X-ray diffraction-oriented insulin structures in Protein Data Bank-II. (A higher resolution / colour version of this figure is available in the electronic copy of the article).

properties of Thr(A8) \rightarrow His(A8) insulin (containing p-azidophenylalanine) could be investigated, and the receptor-binding activity of insulin could be enhanced. This work suggests optimization capabilities involving increasing the binding interaction in nonconserved side regions of the insulin surface [327] (PDB_ID: 1RWE) (Fig. 20I). In the same year, N-lithocolyl insulin with long-acting human insulin

was introduced. The addition of such hydrophobic groups increases the strong affinity for circulating serum albumin. Thus, it forms soluble macromolecular complexes at the injection sites and allows insulin analogs to be slowly absorbed into the bloodstream [328] (PDB_ID: 1UZ9) (Fig. 21A). In addition, [TyrB25NMePheB26] insulin mutant function and structural features were introduced. This mutant

insulin could solve a biological and structural transition problem from the metabolic, hormonal activity of insulin to the growth factor activity of the IGF-I insulin analog. This structure is well compatible with an R6 hexamer [329] (PDB_ID: 1W8P) (Fig. 21B). In 2005, substitution in this mutant insulin could disrupt receptor binding 500 times compared to other mutant insulins. To elucidate whether the variant side chain directly or indirectly regulates this reduced activity, they investigated the crystal structure of Leu (A3) - insulin through the photo-crosslinking properties of an A3 analog [330] (PDB_ID: 1XW7) (Fig. 21C). Even if visualized using an X-ray technique, the success of sample alignment along the synchrotron beam is limited due to the structure of insulin, i.e., its small size and several problems with mother liquor and optical microscopes. An XRD study in 2006 proposed using the endogenous fluorescence of aromatic amino acids to identify the crystal with a high success rate. Crystallographic data showed that the approach of UV laser-stimulated fluorescence did not cause any detectable structural damage [331] (PDB_ID: 2C8R) (Fig. 21D). In the same year, despentapeptide insulin (DPI; des-B26-B30) was crystallized in the 20% acetic acid pH 2 condition and this structure was analyzed as the space group I222. Accordingly, DPI was not capable of forming β -helical interactions to create physiological dimer matching. This structure remained as a monomeric conformation and produced an alternative lattice dimer [332] (PDB_ID: 2CEU) (Fig. 21E). In the same year, it was studied in complex with the insulin-degrading enzyme (IDE), insulin B chain, amyloid- β peptide (1-40), amylin, and glucagon. Accordingly, it elucidated novel structural details, such as the amino and carboxy-terminal domains of the IDE, their wide contact with each other, and the repositioning of the IDE. Therefore, this study could help design IDE-based drugs to regulate blood sugar concentrations and therefore, cerebral amyloid- β [333] (PDB_ID: 2G54, 2G56). In 2007, two novel crystal forms of human insulin were discovered. In this study, a new hexamer-hexamer interaction was found in the novel insulin compared to previous insulin crystals. Additionally, different binding sites for urea have been found in the crystals. These results provide more insight into the role of urea in protein denaturation [334] (PDB_ID: 2OLY, 2OLZ, 2OM0, 2OM1) (Fig. 21F). In the same year, the same team focused on the neutral protamine Hagedorn (NPH) because the insulin-protamine complex was unknown. They used three different systems to study protamine binding to insulin. They crystallized it with and without urea and co-crystallized the peptide consisting of 12 arginine residues to insulin for the clear electron density of the peptide. Accordingly, the results support the lack of well-defined conformation between insulin and protamine [335] (PDB_ID: 2OMG, 2OMH, 2OMI) (Fig. 21G). In 2008, two zinc human arg (A0) insulin structures were introduced to elucidate the mechanism of the decrease in insulin activity. This study showed that changes in the charged surface and two-helix orientation in the A chain and decreased surface accessibility can cause a decrease in the activity [336] (PDB_ID: 2QIU) (Fig. 21H). In the same year, $1\text{Rb}1^{+}$, $2\text{Mn}2^{+}$, and $4\text{Ni}2^{+}$ human arg insulin were determined to explain the importance of metal ions in the insulin hexamer. These structures were compared to the $2\text{Zn}2^{+}$ structure. In this study, T&R states metal coordination and their metal-induced structural changes were explained [337]

(PDB_ID: 2R34, 2R35, 2R36) (Fig. 21I). In the same year, the structure of the single-chain insulin analog (SCI-57), including a 6-residue linker (GGGPRR), was introduced. In this structure, the thermodynamic stability of SCI-57 is significantly higher. In addition, some of the connections found in the analog are consistent with the native insulin structure. These results also highlighted the intrinsic flexibility of an insulin monomer. This study suggests that such ultrastable SCIs may assist in enhancing the efficacy and safety of insulin replacement therapy in further studies [338] (PDB_ID: 3BXQ) (Fig. 22A). In 2009, Ultralente insulin was studied. This study presented the crystal structures of ultralente insulin and their precursor microcrystals. According to this study, ultralente crystals and their relationship with the protective agent methylparaben are explained. Thus, the long-term action mechanism of this insulin was revealed [339] (PDB_ID: 2VJZ, 2VK0) (Fig. 22B). In the same year, IDE was studied to elucidate its function on insulin clearance. They used Fourier transform ion cyclotron resonance mass spectrometry (FTICR-MS) and electron capture dissociation (ECD) to investigate the composition and cleavage sites of insulin fragments produced by the IDE. This study revealed the relationship between IDE forms, their effects on the partially unfolded insulin molecule, and their affinity [340] (PDB_ID: 2WBY, 2WC0). In the same year, the structure of human insulin was re-evaluated by XRD at a resolution of 1.6 Å at cryogenic temperature (PDB_ID: 3E7Y, 3E7Z;) (Fig. 22C). Likewise, in 2009, the structure of the T6 human nickel insulin derivative was investigated at a resolution of 1.35 Å at cryogenic temperature (PDB_ID: 3EXX;) (Fig. 22D). In the same year, an insulin analog that binds to IR with higher affinity but has a lower affinity to insulin-like growth factor receptor (IGFR) was designed using a non-standard mutagenesis technique. As a result of this data, it has been suggested that such insulin analogs could aid cancer studies in animal models of hyperinsulinemia [341] (PDB_ID: 3FQ9) (Fig. 22E). In 2010, the insulin- insulin receptor (IR) binding process was studied with the help of different insulin analogs, such as B17A insulin (site 2 mutated), Des A1-4 insulin (site 1 deleted), with and without a fluorescent probe attached. This result showed that insulin site 2 binds to the IR faster in the formation of the IR-insulin complex. Accordingly, this data demonstrates the importance of the A1-A4 terminal residues of the insulin A-chain for the slow binding phase [342] (PDB_ID: 2W44) (Fig. 22F). In the same year, an insulin analog truncated at residue 26 of the B-chain (B26) was introduced. This data showed a structural convergence at the B(24)-B(26) position for active hormone analogs. It has been suggested that this novel β -turnover in residues B(24)-B(26) may be critical in the transition of insulin. These results represent structural details of prospective ligands for further rational design studies [343] (PDB_ID: 2WRU, 2WRV, 2WRW, 2WRX, 2WS0, 2WS1, 2WS6, 2WS7) (Fig. 22G). In the same year, the recombinant human insulin-polysialic acid complex was investigated under microgravity and normal conditions. These results confirmed that these crystals are the same as cubic insulin crystals and that the cubic insulin did not contain polysialic acid or fragments thereof. In this study, the structure of the gene-engineered human insulin was compared with different crystals [344] (PDB_ID: 3I3Z, 3I40) (Fig. 22H). In the same year, the crystal structures of human

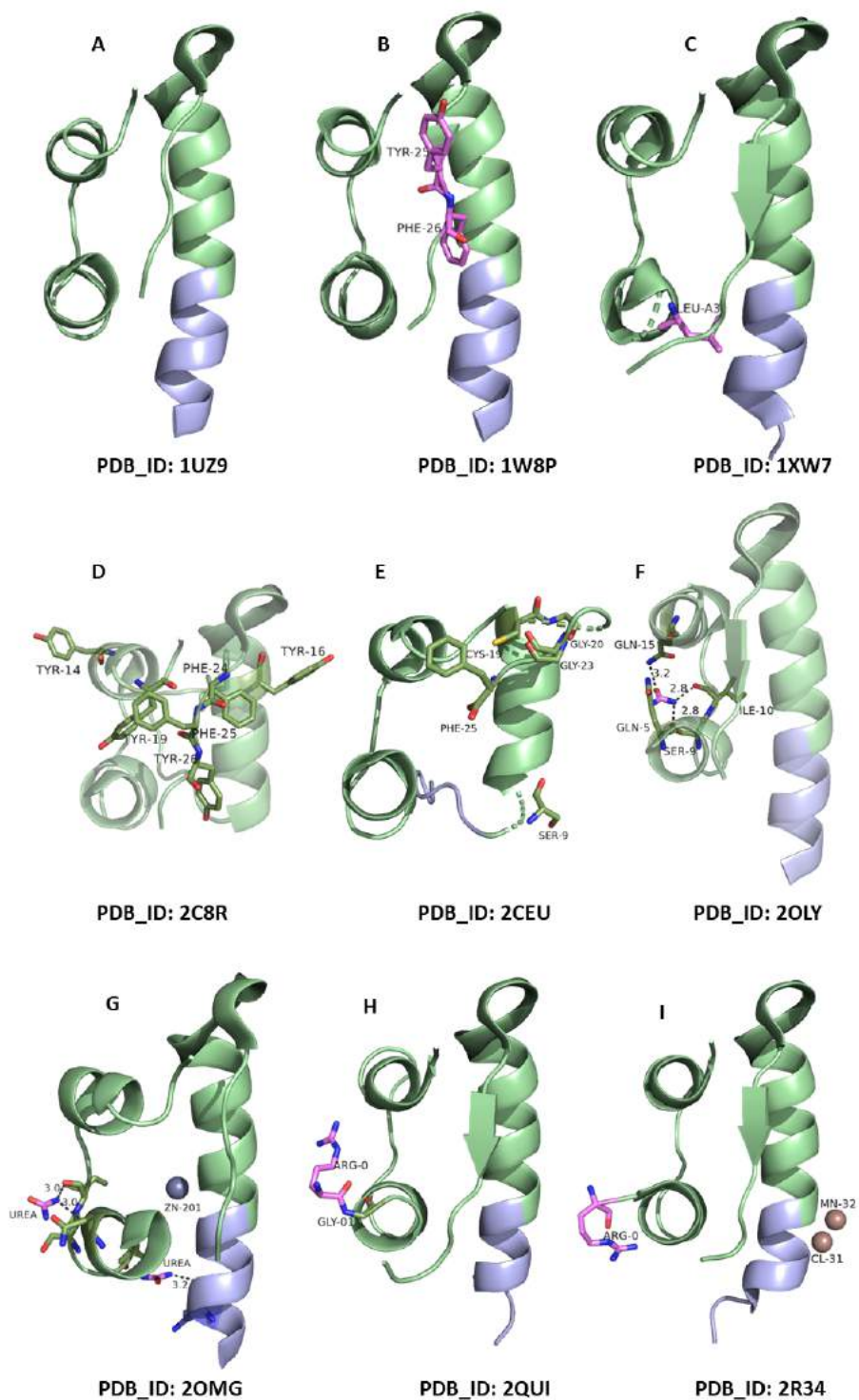


Fig. (21). X-ray diffraction-oriented insulin structures in Protein Data Bank-III. (A higher resolution / colour version of this figure is available in the electronic copy of the article).

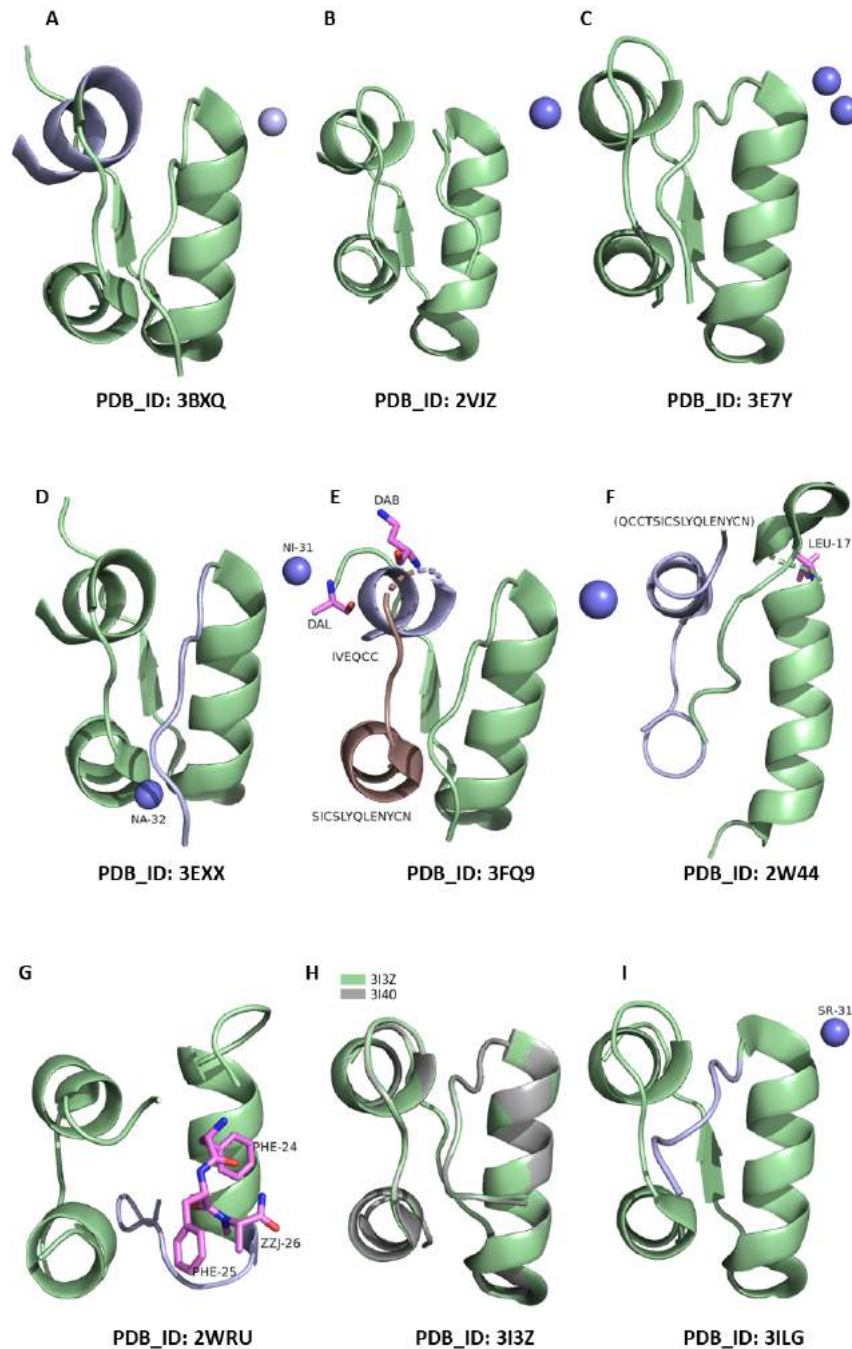


Fig. (22). X-ray diffraction-oriented insulin structures in Protein Data Bank-IV. (A higher resolution / colour version of this figure is available in the electronic copy of the article).

insulin-Ni²⁺, Sr²⁺, and Cu²⁺ complexes were investigated to observe metal-induced 3D changes in human insulin. This data was obtained at 1.8 Å resolution at cryogenic temperature (PDB_ID: 3ILG, 3INC, 3IRO; *unpublished*) (Fig. 22I). In the same year, insulin biosynthesis and activity in neonatal DM were investigated structurally. This study was performed by XRD at room temperature at 2.5 Å resolution (PDB_ID: 3ROV, 3JSD; *unpublished*) (Fig. 23A). In the

same year, it was shown that the pharmacological properties of insulin can be improved by "zinc staples" between hexamers. This structure was different from the previous one as it contained both new zinc ions and classical axial zinc ions at the hexamer-hexamer interfaces. Moreover, the function of the structure is similar to that of the long-acting formulation Lantus, although it has some analogous distinctions. This result suggests that it can provide a pharmacokinetic

strategy to alter the biological properties of the insulin structure [345] (PDB_ID: 3KQ6) (Fig. 23B). In 2011, insulin fibrillation was studied with XRD at 2 Å resolution (PDB_ID: 3P2X, 3P33; *unpublished*) (Fig. 23C). Additionally, the same mechanism was studied to explain insulin fibrillation at 2 Å resolution in 2012 (PDB_ID: 3V19, 3V1G; *unpublished*) (Fig. 23D). In 2011, insulin and its synthetic receptor, known as the cucurbit [7] uryl (Q7) complex, were investigated. It was shown that there is a robust affinity between them compared to the larger protein-receptor complex. In this study, the molecular recognition of insulin has been investigated in detail [346] (PDB_ID: 3Q6E) (Fig. 23E). In the same year, Cu²⁺ human insulin derivative was investigated by XRD analysis at 1.12 Å resolution at cryogenic temperature (PDB_ID: 3TT8; *unpublished*) (Fig. 23F). Additionally, in 2011, insulin analogs modified with B24, B25, or B26 were investigated to identify their structural contribution to the dimer interface. These analogs demonstrated impaired binding affinity to IR, highlighting the importance of the IR-interaction role for amide hydrogens. Together, the study revealed two new analog crystal structures [347] (PDB_ID: 3ZQR, 3ZS2) (Fig. 23G). In the same year, Lys (B29) des (B30) human insulin structure was studied at 1.6 Å resolution at cryogenic temperature (PDB_ID: 3ZU1; *unpublished*) (Fig. 23H). In 2012, a covalently linked insulin dimer was designed to evaluate the relationship between insulin stability, function, and insulin oligomerization. This dimer is the same as a human insulin dimer and can easily form a hexamer structure. Although this engineered dimer did not bind to the IR and did not cause any signal pathways, it was thermodynamically stable, and no amyloid fibril was formed under mechanical stress. This highlights the importance of oligomerization for insulin stability [348] (PDB_ID: 3U4N) (Fig. 23I). In the same year, 1E6-HLA-A*0201-peptide, a type of proinsulin, and its association with CD8(+) T cells were investigated to explain the underlying mechanism of type 1 diabetes. This study suggests that such an association could potentially lead to CD8(+) T cell-mediated autoreactivity and thymic escape [349] (PDB_ID: 3UTQ, 3UTS, 3UTT). In the same year, the manganese derivative of insulin structure was investigated in high resolution in cryogenic structure [350] (PDB_ID: 4FKA) (Fig. 24A). In 2003, the primary binding sites of insulin and its receptor were crystallized to investigate the interaction of this complex in detail. These results can help design therapeutic insulin analogs through this interaction for further studies [351] (PDB_ID: 3W11, 3W12, 3W13). In the same year, 2Zn²⁺ human insulin was studied at 0.92 resolution at cryogenic temperature (PDB_ID: 3W7Y; *unpublished*) (Fig. 24B), while the same molecule was investigated at 1.15 Å resolution at room temperature (PDB_ID: 3W7Z; *unpublished*). In the same year, the dodecamer human insulin structure was studied at 1.4 Å resolution at room temperature (PDB_ID: 3W80; *unpublished*) (Fig. 24C). In the same year, the C-terminus of the B-chain of insulin was crystallized to illuminate the Insulin-IR complex. For this, they characterized a series of B24-modified insulin analogs. This data indicates that the aromatic L-amino acid at the B24 site plays a critical role in binding insulin to its receptor [352] PDB_ID: 3Z13) (Fig. 24D). In the same year, insulin degludec structure, self-assembly, and ligand binding properties were introduced using orthogonal structural methods. The folding

properties of this insulin are similar to human insulin. Accordingly, this study gives us the R(6), R(3),T(3) and T(6) states of information in detail. These results identified the connections between quaternary insulin structures of multi-hexamers, dihexamers, hexamers and their inherent propensity associated with their allosteric state [353] (PDB_ID: 4AJX, 4AJZ, 4AK0, 4AKJ) (Fig. 24E). In the same year, the importance of disulfide bonds was studied to investigate the biological activity of insulin. In this study, they designed insulin with an additional disulfide bond to investigate whether it could increase the structural stability of insulin for pharmaceutical uses. This analog had a higher affinity for IR and increased glucodynamic potency compared with human insulin. It also prevented the formation of insulin fibrils and the R- state of insulin, as well as having the ability to form hexamers. This design is the first analog of human insulin to which an additional interchain disulfide bond has been added [354] (PDB_ID: 4EFX) (Fig. 24F). In the same year, four different normal-acting wild-type human insulins were investigated using a combination of single-crystal protein crystallography (PX), nuclear magnetic resonance (NMR), small-angle X-ray scattering (SAXS), and mass spectrometry (MS) techniques. While all products showed similar oligomeric assembly in DLS and SAXS analysis, they showed a very close association with human insulin in NMR analysis. Together, a meta-analysis of 24 structures revealed close similarity between each other in some variables such as product batch, analytical approach, biological origin, and country origin of that product [355] (PDB_ID: 4EWW, 4EWX, 4EWZ, 4EX0, 4EX1, 4EXX, 4EY1, 4EY9, 4EYD, 4EYN, 4EYP, 4F0N, 4F0O, 4F1A, 4F1B, 4F1C, 4F1D, 4F1F, 4F1G, 4F4T, 4F4V, 4F51, 4F8F, 4FG3) (Fig. 24G). In the same year, ester insulin was introduced for the efficient total synthesis of insulin. This insulin folded faster at physiological pH than proinsulin. Furthermore, this insulin was inactive in lower blood glucose conditions compared to synthetic insulin activity. Accordingly, the biological activity deficiency of ester insulin was discussed in detail in this study [356] (PDB_ID: 4IUZ) (Fig. 24H). In the same year, fast-acting insulin aspart, a human insulin variant B28Asp, was studied by small angle X-ray scattering measurements. Accordingly, this result showed a similar global behavior between aspart and normal human insulin. It has also shown that insulin adopts a T3R3 assembly. This data reveals in detail new structural information about aspart and its T- and R- state conformations [357] (PDB_ID: 4GBC, 4GBI, 4GBK, 4GBL, 4GBN) (Fig. 24I). In 2014, structural and physicochemical analysis of biosimilar insulin glargine formulation was introduced at 1.6 Å resolution at cryo-temperature (PDB_ID: 4IYD, 4IYF; *unpublished*) (Fig. 25A). In the same year, the rational design, synthesis, and characterization of D-ProB8-insulin were introduced to explain the relationship between T-, R-states and the insulin-insulin receptor (IR) complex. These results revealed that a T-like state is more important for folding efficiency than an R-state compatible with an inactive form of insulin. Accordingly, the N-terminal of the B-chain must be distinct from the "conventional" T-state, and the B1-B8 segment flexibility is crucial for an insulin-IR interaction efficiency [358] (PDB_ID: 4CXL, 4CXN, 4CY7) (Fig. 25B). In the same year, the B-chain's C-terminal segment of insulin was studied to explain the relationship between its receptor activation

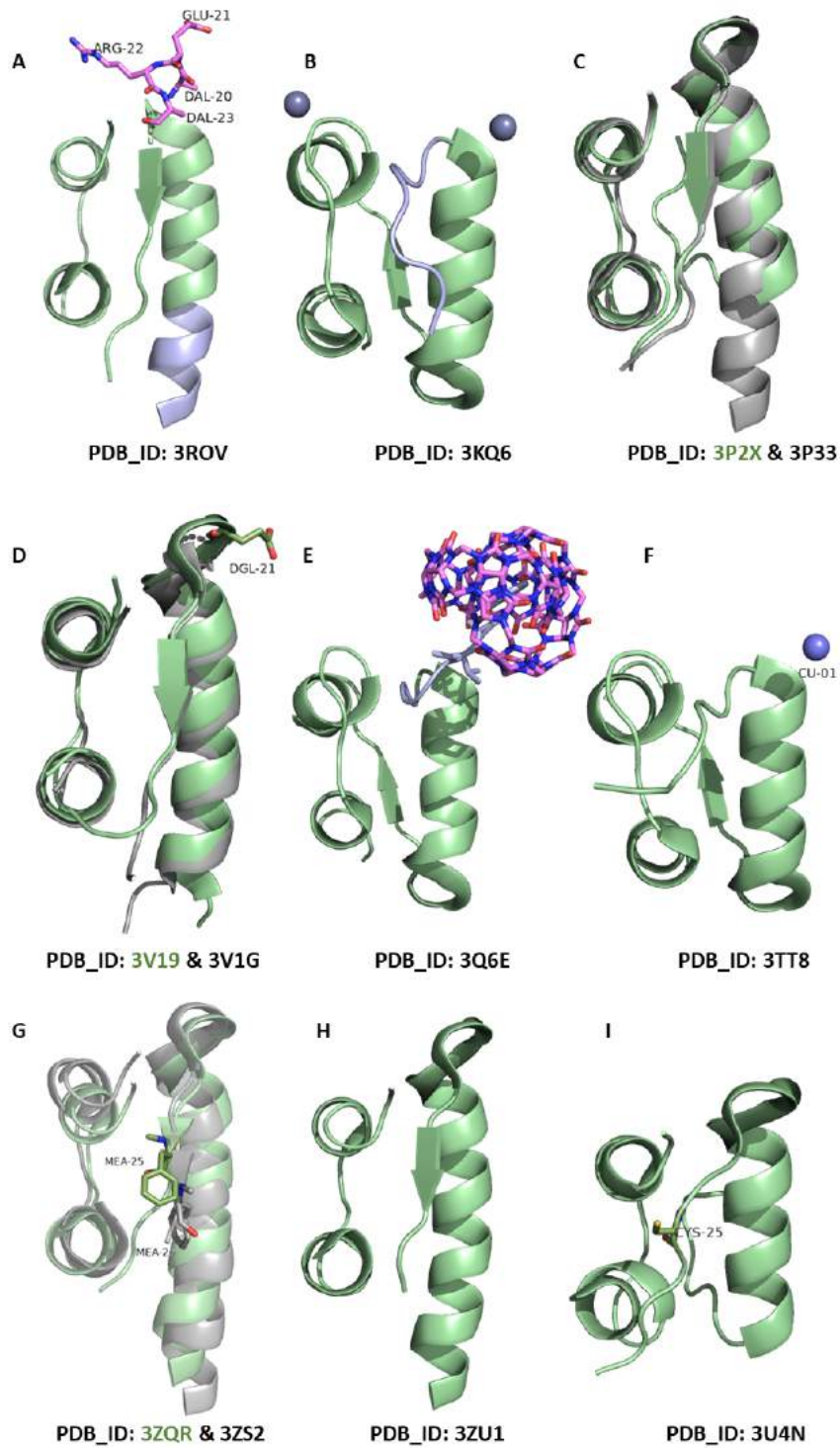


Fig. (23). X-ray diffraction-oriented insulin structures in Protein Data Bank-V. (A higher resolution / colour version of this figure is available in the electronic copy of the article).

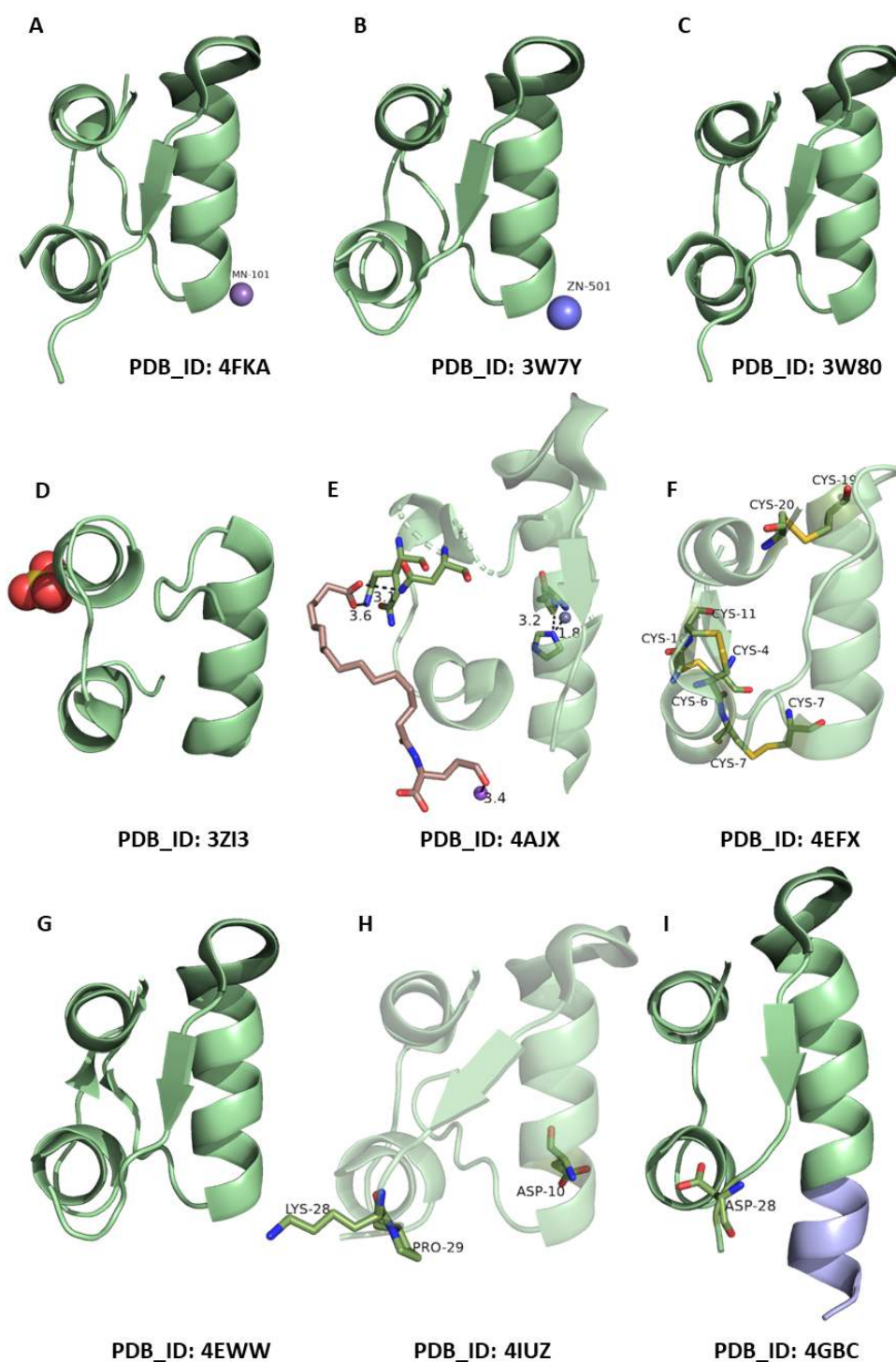


Fig. (24). X-ray diffraction-oriented insulin structures in Protein Data Bank-VI. (A higher resolution / colour version of this figure is available in the electronic copy of the article).

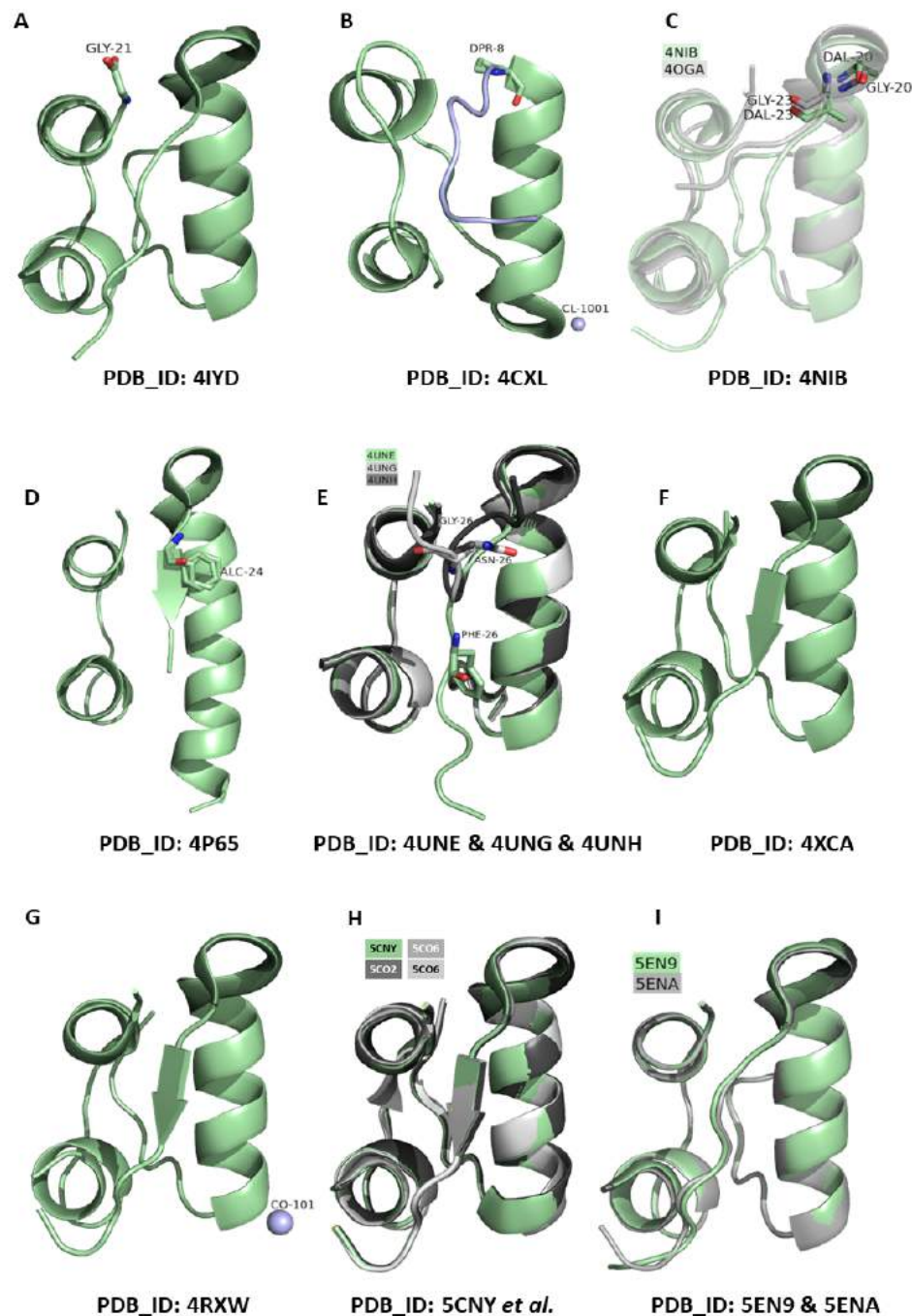


Fig. (25). X-ray diffraction-oriented insulin structures in Protein Data Bank VII. (A higher resolution / colour version of this figure is available in the electronic copy of the article).

and its conformation. They proposed a transition between the receptor-bound and free conformation of insulin, resulting from the combination of function and biosynthesis and its evolutionary structural determinants [359] (PDB_ID: 4NIB, 4OGA) (Fig. 25C). In the same year, Phe24 substitution by cyclohexanylanaline (Cha) of insulin was investigated to explain its importance for DM. These data revealed that B24 residue is required for the binding pocket of the IR because it provides an alternative anchor residue at the hormone-

receptor interface. Accordingly, these results revealed not only the benefit of the residue presence but also the therapeutic utility of the nonstandard Cha analog side chain [360] (PDB_ID: 4P65) (Fig. 25D). In the same year, the importance of the B21-B30 insulin site was investigated to explain the insulin-IR interaction. This study showed that native amino acids altered by the modified amino acids at the Tyr(B)26, Gly(B)26, or Asn(B)26 residues could affect the active form of this hormone. This data suggested that such

analogs could provide the first structural insight into different insulin structural analyses [361] (PDB_ID: 4UNE, 4UNG, 4UNH) (Fig. 25G). In 2015, the insulin- β -cell chaperone sulfatide complex was cocrystallized at 1.5Å resolution at cryogenic temperature (PDB_ID: 4XC4; *unpublished*) (Fig. 25F). In the same year, two T cell receptor Mhc class II molecules containing proinsulin-derived peptides were studied to investigate the relationship between MHC molecules and TCR recognition at 2.5Å resolution at a cryogenic temperature [362] (PDB_ID: 4Y19, 4Y1A). In the same year, the relationship between insulin reactivity and a CD8+T cell clone known to induce T1D was studied to understand the disorder between the MHC class I binding channel and the insulin-derived peptide. This work proposed a new flexible peptide presentation model in the MHC peptide binding channel perspective [363] (PDB_ID: 4WDI, 4Z76, 4Z77, 4Z78). In the same year, the cobalt human insulin derivative was crystallized for investigation at a resolution of 1.73Å at cryo-temperature (PDB_ID: 4RXW; *unpublished*) (Fig. 25G). In the same year, the crystal structure of human zinc insulin was studied at 1.7Å resolution at a cryogenic temperature at pH 5.5 and pH 6.5 (PDB_ID: 5CNY, 5CO2, 5CO6, 5CO9; *unpublished*) (Fig. 25H). In the same year, the dimer formation of human insulin was studied using two-dimensional infrared (2D-IR) spectroscopy. This data revealed the hexameric structure of synthetic human insulin and synthetic ester insulin intermediate in the absence of Zn metal ions and/or phenol derivatives. This result highlights the fractional crystallization of semi-racemic insulin mixtures with two synthetic proteins [364] (PDB_ID: 5EN9, 5ENA) (Fig. 25I). In 2016, the B22-B30 region of insulin was studied to modulate and stabilize the receptor-compatible structure of insulin. The structures and functions of 14 insulin analogs have been extensively characterized. One of the analogs has been shown to be highly active for binding to IR isoforms. These data demonstrated the importance of the B-chain C-terminal of insulin for the metabolic B-isoform of insulin receptor specificity [365] (PDB_ID: 5BOQ, 5BPO, 5BQQ) (Fig. 26A). In the same year, insulin high molecular weight products (HMWPs) were characterized in terms of self-association, tertiary structure, fibrillation properties, and biological activity to explain the covalent insulin dimer state during storage of a marketed pharmaceutical formulation. These data shed light on the description of the characterization of a specific human insulin HMWP type that has been [366] (PDB_ID: 5BTS) (Fig. 26B). In the same year, high-resolution structures of the 1E6 TCR bound to 7 modified peptide ligands were examined to explain the relationship between cross-reactivity of T cell peptides and autoimmunity development. These data showed how pathogen-derived antigens and T cell cross-reactivity can impair self-tolerance to stimulate autoimmune disease [367] (PDB_ID: 5C0D). In the same year, iodination of tyrosine preserved in insulin (Tyr (B26)) was studied to increase the critical properties of a fast-acting analog using molecular-mechanical and hybrid quantum methods. After a series of simulations of the 3-I-Tyr (B26)-insulin structure, the predictions were tested by X-ray crystallography. This result paved the way for the propagation of medicinal chemistry principles on proteins [368] (PDB_ID: 5EMS) (Fig. 26C). In the same year, the cross-reaction of an insulin-reactive T cell with pathogen-derived antigens was studied to understand

the specificity of T cells and whether cross-reactivity profiles could be predicted [369] (PDB_ID: 5HYJ). In the same year, the synthesis of insulin lispro by ester insulin was studied using the fmoc chemistry SPPs-based approach. Accordingly, the optimization of these pilot studies can provide an effective production of insulin lispro using Fmoc chemistry SPPS [370] (PDB_ID: 5UDP) (Fig. 26D). In 2017, two forms of human recombinant insulin structure (Insugen and Intergen) were observed at ultra-high resolution at 100K. In this study, the differences between electron density properties are examined in detail [371] (PDB_ID: 5E7W) (Fig. 26E). In the same year, amino acid mutagenesis was studied by replacing the proline residue at position 28 of the insulin B-chain (ProB28) with (4S)-hydroxyproline to generate more rapidly dissociating insulin. Accordingly, these data pave the way for engineering therapeutic insulin in terms of protein design and medicinal chemistry [372] (PDB_ID: 5HPR, 5HPU, 5HQI, 5HRQ) (Fig. 26F). In the same year, whether endogenous ligands such as serotonin and dopamine stabilize insulin oligomers was investigated by protein crystallography (PC) and molecular dynamics (MD). Accordingly, it was observed that serotonin binds well to insulin hexamer and stabilizes it in the T3R3 structure. This result demonstrated that a T3R3 oligomer is a reasonable conformation for insulin pancreatic storage *via* neurotransmitters, suggesting important implications for clinical insulin formulation [373] (PDB_ID: 5MAM, 5MT3, 5MT9) (Fig. 26G). In the same year, the substitution of the A6-A11 disulfide bond of insulin was studied to investigate its effects on insulin activity. Accordingly, this data sheds light on the allosteric role of the A6-A11 disulfide bond in regulating the transition of insulin to its active conformation [374] (PDB_ID: 5T7R) (Fig. 26H). In the same year, the X-Ray structure of Insulin Glargine was studied at 1.7 resolution at cryogenic temperature (PDB_ID: 5VIZ; *unpublished*) (Fig. 26I). In the same year, the ultrastable single-chain insulin analog was studied to have significant resistance to thermal inactivation. This data showed that the stability of this analog was higher than that of wild-type insulin. Accordingly, such an analog can provide a global therapeutic platform without worries about the cold chain [375] (PDB_ID: 5WDM) (Fig. 27A). In 2018, varied insulin-proline analogs at position B28 and their diverse T- & R- state conformation were studied at 1.17 resolution at cryogenic temperatures (PDB_ID: 5UOZ, 5UQA, 5URT, 5URU, 5USP, 5USS, 5USV, 5UU2, 5UU3, 5UU4; *unpublished*) (Fig. 27B). In the same year, the insulin capture and degradation mechanisms were studied using X-ray crystallography, cryoEM, HDX-MS, and SAXS to investigate both insulin-dependent and apo-dimeric insulin-degrading enzyme (IDE) states. Accordingly, this data not only explains the mechanism by which IDE disrupts amyloidogenic peptides but also suggests new structural insights for progressive IDE-based therapies [376] (PDB_ID: 5WOB). In 2018, the Trp(B)26-insulin analog was studied to elucidate the insulin's dimer interface. In this study, it was suggested that residue substitution of Trp(B)26 and Tyr(B)26 can preserve the natural structure of insulin during the dimerization process. This is an exemplary study on the effects of protein stability-dependent conformation on protein assembly optimization [377] (PDB_ID: 6CK2) (Fig. 27C). In the same year, the synthesis, structure, and properties of a gadolinium-caged cobalt-III (Gd (III)), including the insulin-linked

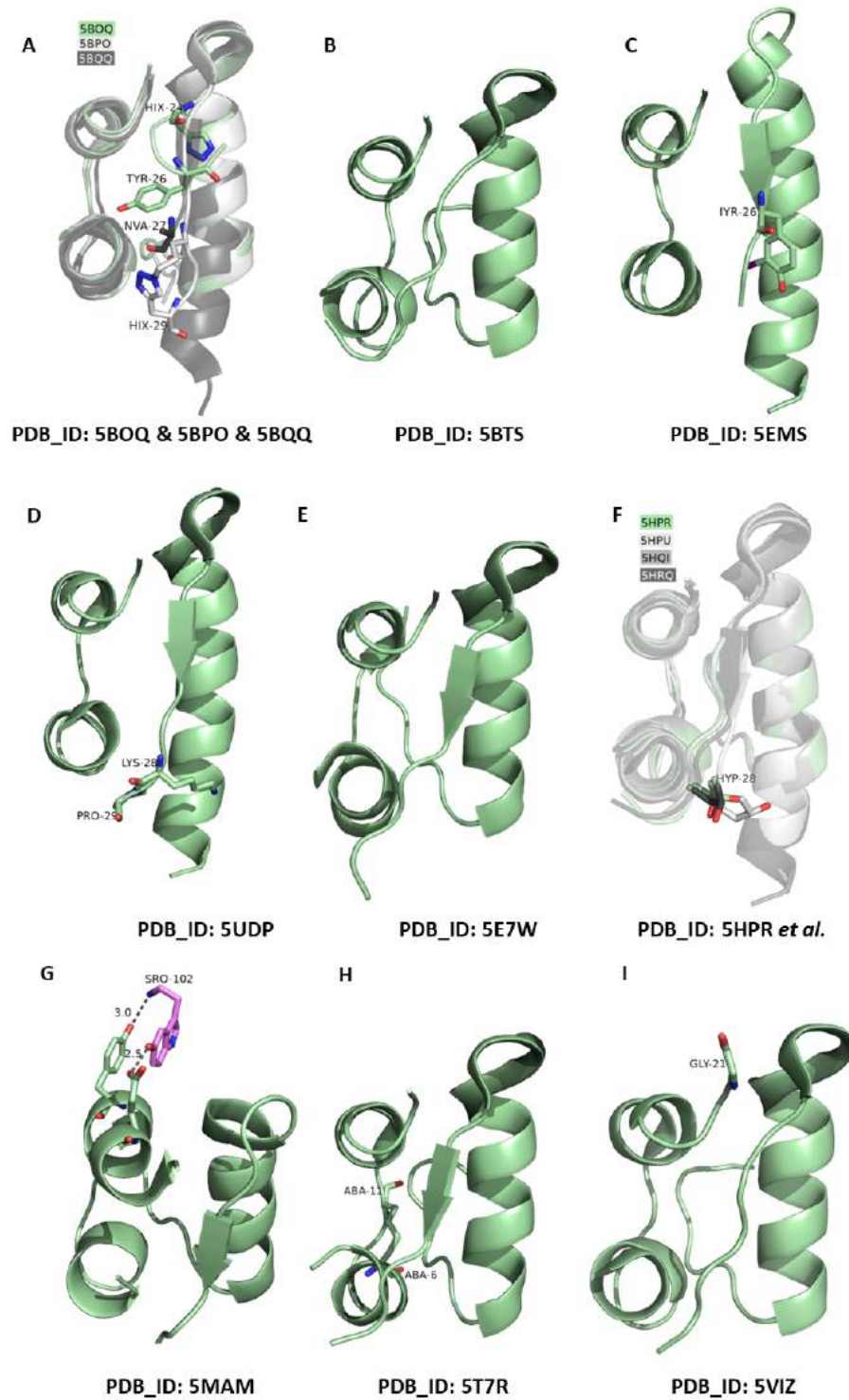


Fig. (26). X-ray diffraction-oriented insulin structures in Protein Data Bank-VIII. (A higher resolution / colour version of this figure is available in the electronic copy of the article).

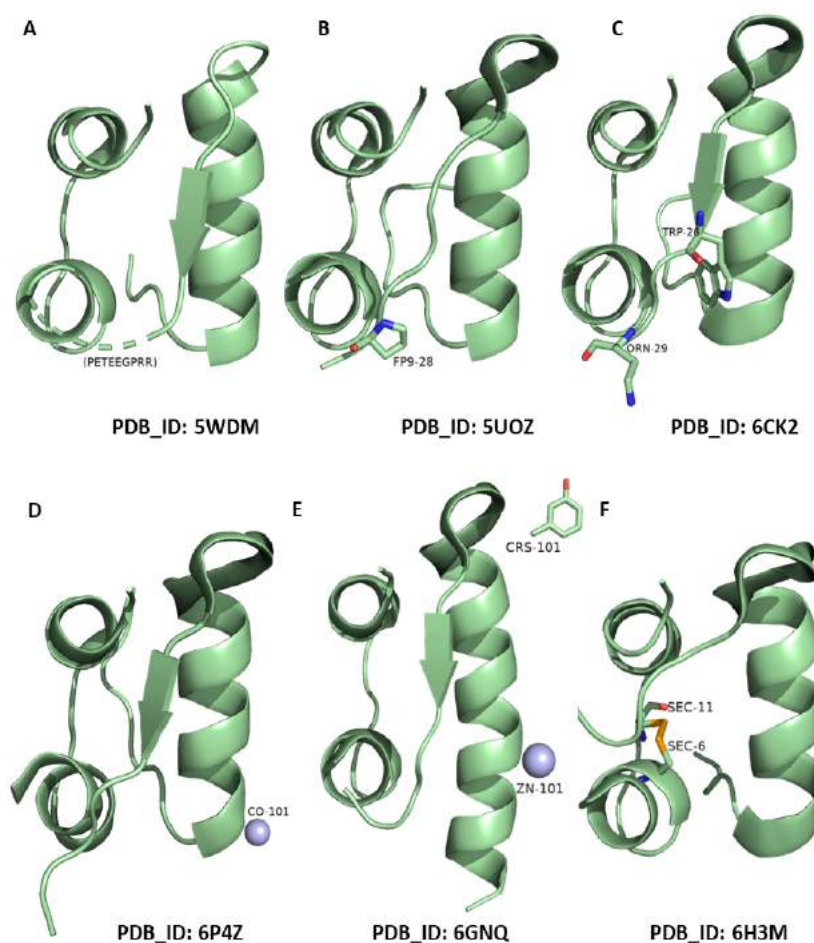


Fig. (27). X-ray diffraction-oriented insulin structures in Protein Data Bank-IX. (A higher resolution / colour version of this figure is available in the electronic copy of the article).

peptide cage, were studied. This study provides much information about the structural dynamics of insulin, including the stability of the hexamer [378] (PDB_ID: 6P4Z) (Fig. 27D). In 2019, human insulin was studied by forming a complex with meta-cresol at 2.2 Å at cryogenic temperature (PDB_ID: 6GNQ; *unpublished*) (Fig. 27E). In the same year, the human seleno-insulin analog was studied to overcome the competition between disulfide aggregation and pairing. In this study, an internal disulfide bridge was replaced with diselenide to increase the stability and foldability of human insulin [379] (PDB_ID: 6H3M) (Fig. 27F). In the same year, zinc-free dimeric human insulin was studied at 1.35 Å resolution in the cryo-synchrotron (PDB_ID: 6S34; *unpublished*) (Fig. 28A). In 2020, Insulin lispro was studied at 1.6 Å at cryogenic temperature (PDB_ID: 6NWV; *unpublished*) (Fig. 28B). In the same year, recombinant human insulin was studied at 1.58 Å at cryogenic temperature (PDB_ID: 6O17; *unpublished*) (Fig. 28C). In the same year, ultra-long oral insulin, glargine-like insulin, was studied to explain its pharmacological and biological properties. This analog is designed to exhibit ultra-long pharmacokinetic properties to

eliminate variability in plasma exposure [380] (PDB_ID: 6S4I, 6S4J) (Fig. 28D). In the same year, a four-disulfide insulin analog, characterized by its high aggregation potency and stability, was studied to prevent the inactivation of insulin by fibrillation/aggregation. They added a 4th disulfide bond between a C-terminal of the A chain and the C-terminal of the B chain. They showed that this analog was similar to native insulin in mice and displayed higher aggregation stability [381] (PDB_ID: 6TYH) (Fig. 28E). In the same year, Mini-Ins, an insulin-like peptide found in cone snail venom, was introduced to overcome self-assembly as dimers/hexamers of insulin and its analogs. This analog has insulin-like *in vivo* bioactivity, *in vitro* insulin signaling, and receptor binding affinity. This study paves the way for therapeutic insulin development [382] (PDB_ID: 6VEP, 6VET) (Fig. 29). In 2021, insulin glulisine was studied by combining the methods of biophysical characterization and X-ray crystallography to understand the function and structure of glulisine. This study revealed information about the pharmacodynamic and pharmacokinetic behavior of glulisine [383] (PDB_ID: 6GV0) (Fig. 28F).

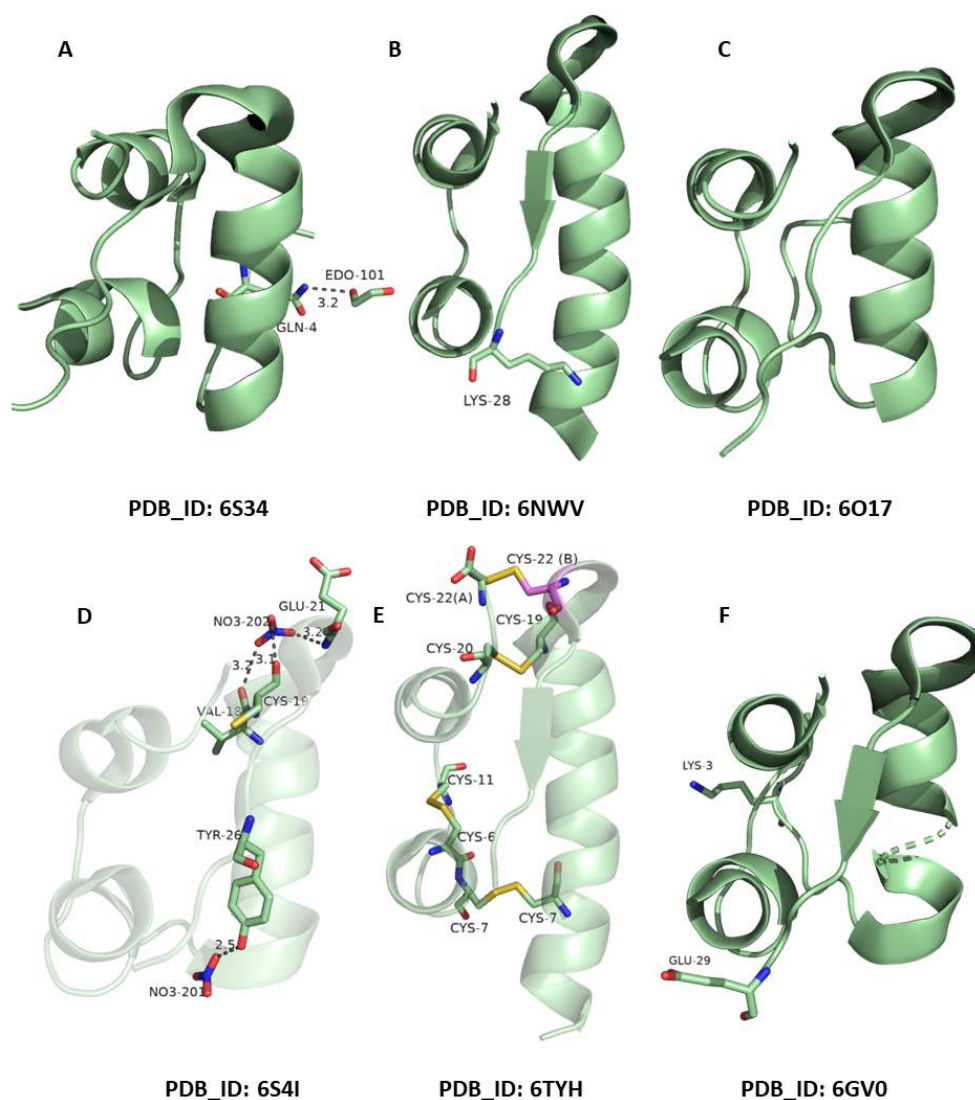


Fig. (28). X-ray diffraction-oriented insulin structures in Protein Data Bank-X. (A higher resolution / colour version of this figure is available in the electronic copy of the article).

22. INSULIN AND INSULIN ANALOGS

In insulin replacement therapy, many types of insulin and insulin-like peptides are available. Typically, insulins are classified according to their action time and maximal effect [384]. Although there are many analogs available on the market, they can be listed according to their action time profile [385]. Typically, these analogs are categorized under three different headings: fast-acting analogs that are lispro, aspart, and glulisine; long-acting analogs that are glargine, detemir, degludec; and premixed analog formulations (25% lispro: 75% neutral protamine lispro; 70% neutral protamine aspart; 30% aspart, 50% lispro; 50% neutral protamine lispro) [386-388].

Recombinant human insulin is a type of short-acting insulin used in the treatment of Type 2 and Type 1 Diabetes. Apart from insulin analogs, this is the same as endogenously

produced insulin, using rDNA techniques [389, 390]. Its marketed name is Humulin R or Novolin R, the action of this insulin begins within 30 minutes, and peak levels occur within 3-4 hours after injection [391]. This insulin is also known as "bolus insulin" because of its similarity with endogenous insulin in terms of its short-acting time [391]. Bolus insulin is often combined with long-acting insulin analogs such as insulin glargine, insulin detemir, and insulin degludec to restore the organism's overnight sugar balance [392, 393]. This insulin has an inhalable version called Exubera, but this has been withdrawn from the market due to some adverse effects such as lung cancer development concerns. After Exubera, Afrezza was introduced. Despite similar concerns, it is still present in the US market [393, 394]. Typically, insulin molecules can self-assemble into the hexameric conformation, but these aggregates tend to dissociate into dimers and monomers over time [395, 396].

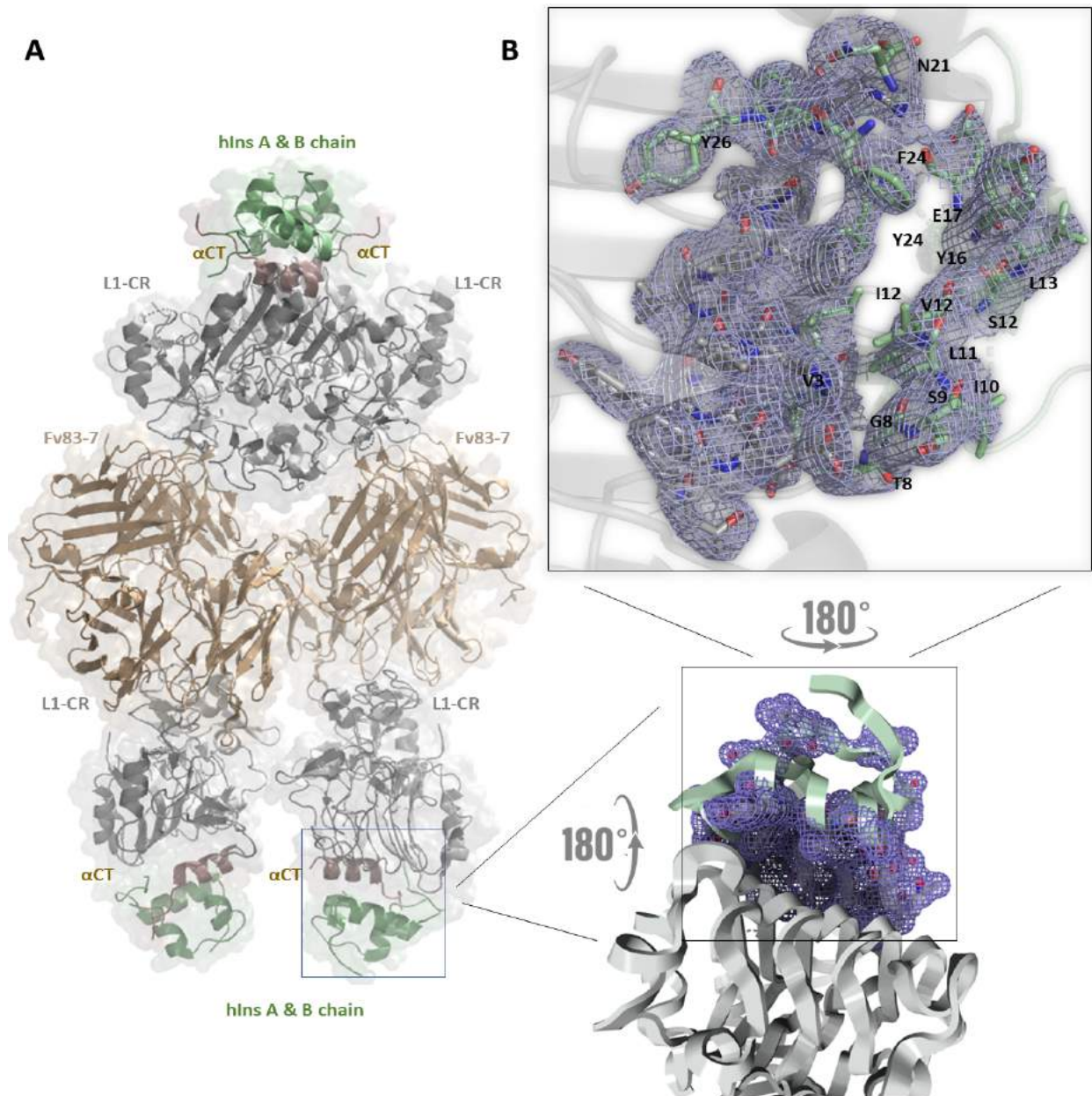


Fig. (29). Representation of the human insulin and microreceptor complex (PDB ID: 6VEP). **(A)** Overview of the microreceptor and insulin complex. Insulin is colored in pale green. **(B)** A closer look at the microreceptor and insulin complex. **(B)** Active residues in insulin & receptor interaction were labeled and demonstrated in mesh mode. Insulin is colored in pale green and the receptor is colored in gray. Receptor's α CT, L1-CR, and Fv83-7 domains are different from each other. hIns A & hIns B: Human Insulin Chain A & Human Insulin Chain B. (A higher resolution / colour version of this figure is available in the electronic copy of the article).

The speed of this tendency is a critical step for insulin to enter the bloodstream through the interstitial fluid. Therefore, in analog formulations, the hexamer dissociation rate of insulin is often altered [27, 397, 398].

In this atlas, we performed Gaussian Network Model (GNM) analysis to compare the dynamics of native insulin and marketing insulin analog structures obtained from the PDB as a bird's eye view. The GNM analysis is a Normal Mode Analysis method from which extensive information

can be obtained about protein's dynamics and the natural states of the relevant proteins [399,400]. Thermal fluctuations obtained with normal modes in GNM analyses and those calculated from X-ray oriented structural analyses are parallel [400]. Accordingly, cross-correlations between residue motions of Humulin structure were analyzed with mean square fluctuations characterized by the flexibility of the residues (Fig. 30). While the intrachain residues' cross-correlation displayed that the first ten residues and 13-20th

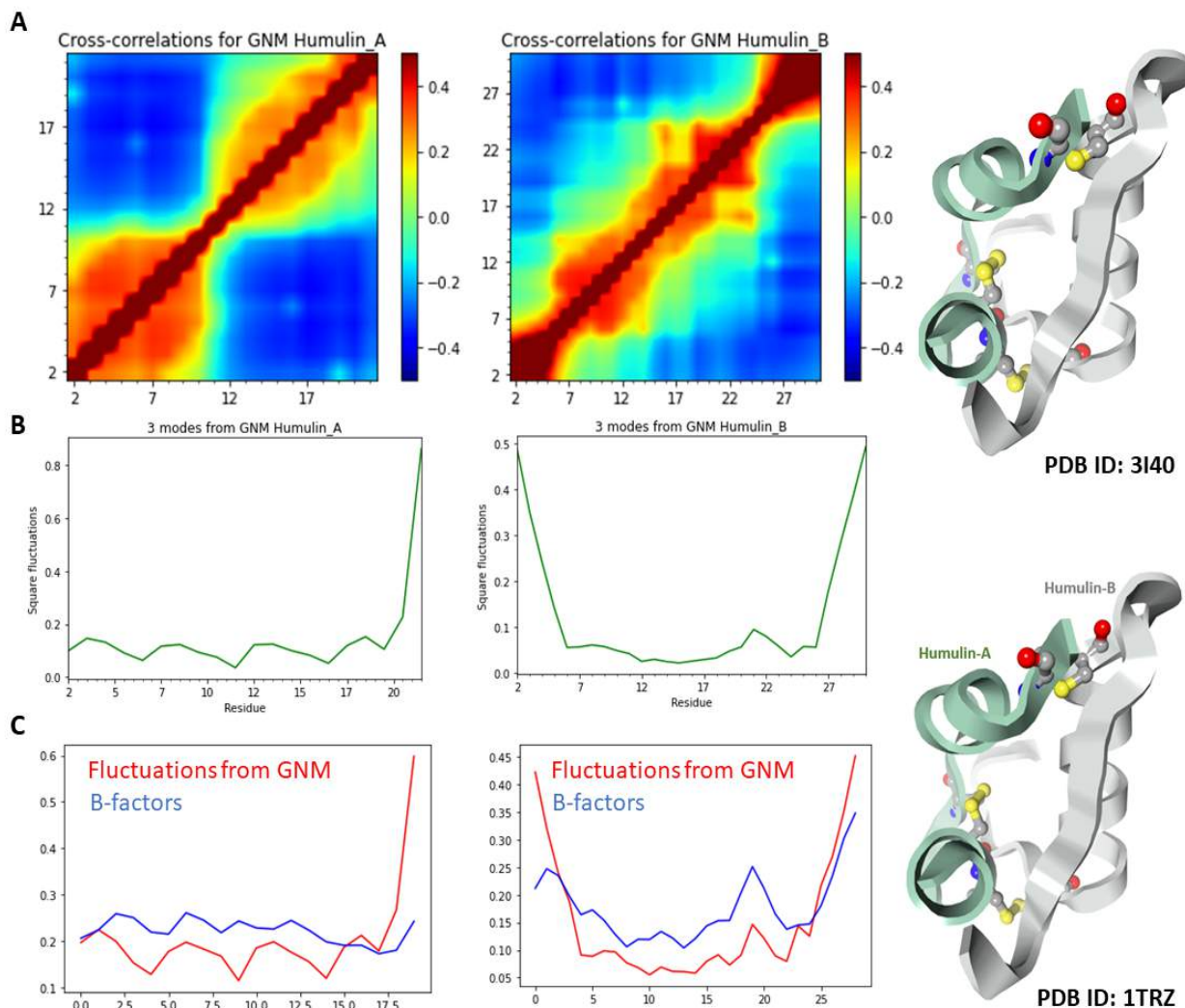


Fig. (30). General analysis of regular insulin (Humulin) in terms of cross-correlation and squared fluctuations from Gaussian Network Model (GNM) analysis. Humulin A and B chains are highly correlated with each other. In the *cross-correlation result from the GNM* analysis, the color range was determined as -0.5 and 0.5 to ensure compatibility between analogs' results (A). According to the squared fluctuations obtained from the weighted 3 *slowest modes*, global motion and residual fluctuations are relatively stable within the first 17 residues for chain A and between 7th-27th residues for chain B (B). While the graphs show the correlation between the theoretical (GNM results; fluctuations from GNM) and the experimental (B-factors), lines show only the residue fluctuations (squared fluctuations even) (C). Human insulin structures (3140 and 1TRZ) are generated using Protein Imager server. (A higher resolution / colour version of this figure is available in the electronic copy of the article).

residues had highly correlated motions in themselves in chain A, a high correlation was observed between 2-6th, 9-16th, 18-24th, and 27-30th residues in themselves in chain B (Fig. 30A). Squared fluctuations of the three modes, theoretical (fluctuation) and experimental (B-factor) results from GNM were inspected closer to further evaluate the intrinsic residue fluctuations of Humulin structure (Figs. 30B and Fig. 30C). The theoretical fluctuations calculated from the three modes are aligned with the B factors in Fig. (30C). Accordingly, the residues at position 17th elucidate the regional flexibility of the C-terminus of insulin chain B (Figs. 30B and 30C). This supports previous studies on the critical aspect of the C-terminus that allows insulin to self-assemble,

bind to its receptor [401-403], and be convenient for analog modifications [404]. We also performed a docking analysis to compare the interaction of regular insulin vs. its analogues with the insulin receptor. Accordingly, the insulin residues in chain A that bind to IR are GIVQTSLEYN, while in chain B, which interacts with IR, are HVEYLFFY. Docking of the insulins' active residues and α CT segment (TFEDYLHNVV FVPRPS) that is vital for insulin binding is shown in (Fig. 31).

23. RAPID-ACTING ANALOG

This type of insulin analog has a shorter duration of activity than regular insulin due to a more rapid onset of its action. Accordingly, three fast-acting insulins are commercially

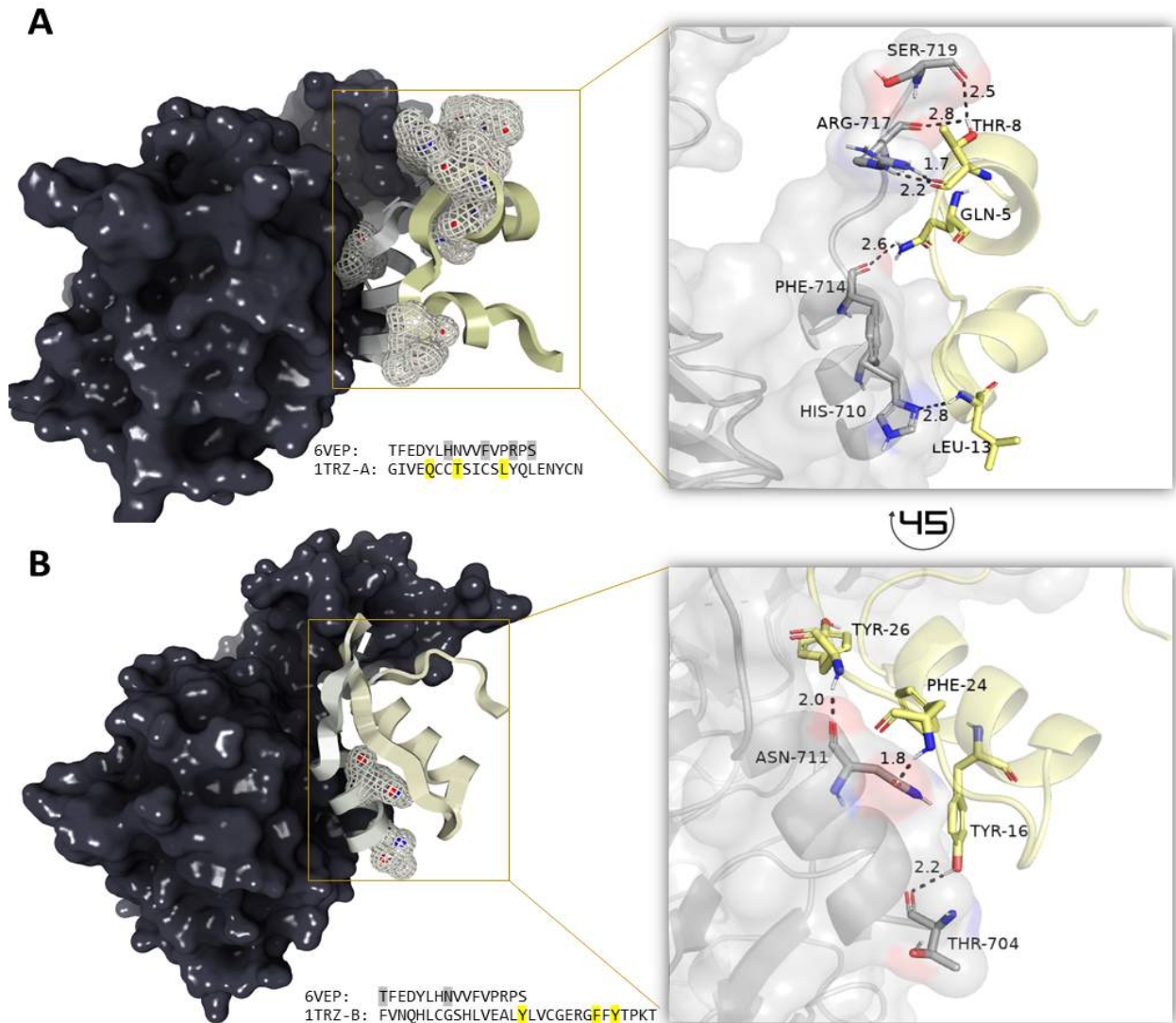


Fig. (31). Regular insulin (Humulin) and insulin receptor interaction. Docking the regular insulin (PDB_ID: 1TRZ) to the Apo-state IR structure (PDB_6VEP) containing α CT domain (colored in gray) that is critical for insulin binding and L1 domain (colored in black). Interaction with insulin-active residues reported in previous studies (Lukman *et al.*, 2015) has succeeded. The insulin chain B (**A**) and chain A (**B**) are excluded for a better view. Interacted residues of α CT domain with the insulin have displayed the mesh mode in the Protein Imager server. (A *higher resolution / colour version of this figure is available in the electronic copy of the article*).

available on the market: insulin lispro, insulin aspart, and insulin glulisine. Although its modifications are relatively minor, involving only a few residue substitutions, these alterations obtain the insulin to be absorbed faster, leading to a reduced tendency to self-associate into hexamers. These minor changes do not disrupt the relationship between insulin and its receptor; thus, the analogs perform the same function as native insulin [405].

24. INSULIN LISPRO

Insulin lispro Humalog (Eli Lilly company) mimics the function of endogenously produced human insulin. Its effect begins within 15 minutes, its peak levels occur 30 to 90 minutes after injection, and the duration of action is approximately 5 hours. It is also known as "bolus insulin" as it pro-

vides high insulin levels in a fleeting time. Additionally, insulin lispro is equivalent to human insulin in terms of molar base. This analog was also produced using a non-pathogenic *Escherichia coli* strain using rDNA techniques and is the first insulin analog to be commercially marketed. The nomenclature LYS-PRO comes from LYS(B28) \rightleftharpoons PRO(B29) inversion, which is different from native insulin residues at position B28, where it is substituted by lysine, and lysine in B29 is modified by proline. Therefore, this change results in 300-fold lower self-assembly than native insulin and results in the dissolution of the dimer and monomer [405]. Further, this modification eliminates some hydrophobic interactions by weakening some polar contacts that contribute to the insulin hexamer stability produced in the presence of zinc, phenol and m-cresol. Finally, this pro-

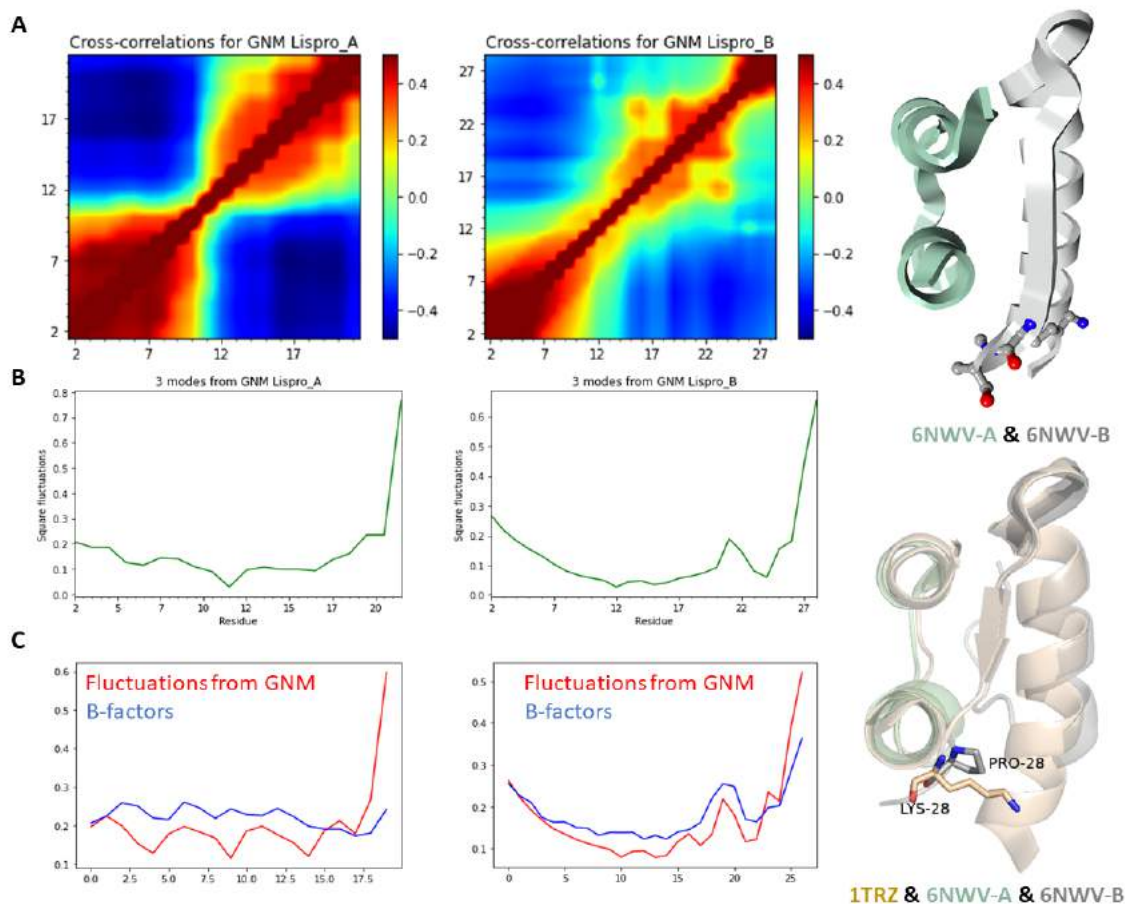


Fig. (32). General analysis of lispro in terms of cross-correlation and squared fluctuations from Gaussian Network Model (GNM) analysis. Lispro A and B chains are highly correlated with each other. In the *cross-correlation result from the GNM analysis*, the color range was determined as -0.5 and 0.5 to ensure compatibility between analogs' results (A). According to the squared fluctuations obtained from the weighted 3 slowest modes, global motion and residual fluctuations are relatively stable (B). While the figures show the correlation between the theoretical (GNM results; fluctuations from GNM) and the experimental (B-factors), lines show only the residue fluctuations (squared fluctuations even) (C). Lispro structures (6NWV) are generated using the Protein Imager server. Superposition of the lispro (6NWV) and human insulin (1TRZ) was generated by PyMOL software (Root-mean-square deviation (RMSD): 0.39). (A higher resolution / colour version of this figure is available in the electronic copy of the article).

cess causes the absorption of insulin more rapidly after the injection than regular insulin. Its absolute bioavailability ranges from 55% to 77% in the presence of doses between 0.1 and 0.2 units/kg. The serum concentration-time curve is 2390 pmol hours/L and 2360 pmol hour/L for HUMALOG U-100 and HUMALOG U-200, respectively. At the same time, the serum insulin concentration is 909 pmol/L and 795 pmol/L for HUMALOG U-100 and HUMALOG U-200, respectively. The median time to maximum concentration for both formulations is 1 hour. The mean volume of insulin lispro distribution, corresponding to a bolus injection dose of 0.1 and 0.2 U/kg, was 1.55 and 0.72 L/kg, respectively. Its half-life after injection is $t_{1/2}$ shorter than regular insulin (1: 1.5 hours) [405].

We performed GNM analysis to compare the dynamics of regular insulin and insulin lispro structures obtained from the PDB as a bird's eye view. Accordingly, cross-

correlations between residue motions of the lispro structure were analyzed with mean square fluctuations characterized by the flexibility of the residues (Fig. 32). Similar to regular insulin, the intrachain residues' cross-correlation displayed that chain A had highly correlated motions with the first ten residues and 13-20th residues. In addition, chain B was observed with higher fluctuations at the 2-10th, 17-24th, and 27-30th positions (Fig. 32A). Three modes, theoretical (fluctuation), and experimental (B-factor) result from GNM, were inspected closer to further evaluate the intrinsic residue fluctuations of the lispro structure (Figs. 32B and 32C). The theoretical fluctuations calculated from the three modes are aligned with the B factors in Fig. (32C). Accordingly, residues' position around the 15th elucidates the regional flexibility of the C-terminus of lispro chain B compared to regular insulin dynamics (Fig. 32C). We also performed a docking analysis to compare the interaction of regular insulin vs. lispro with the insulin receptor. Accordingly, Glu17, Asn21

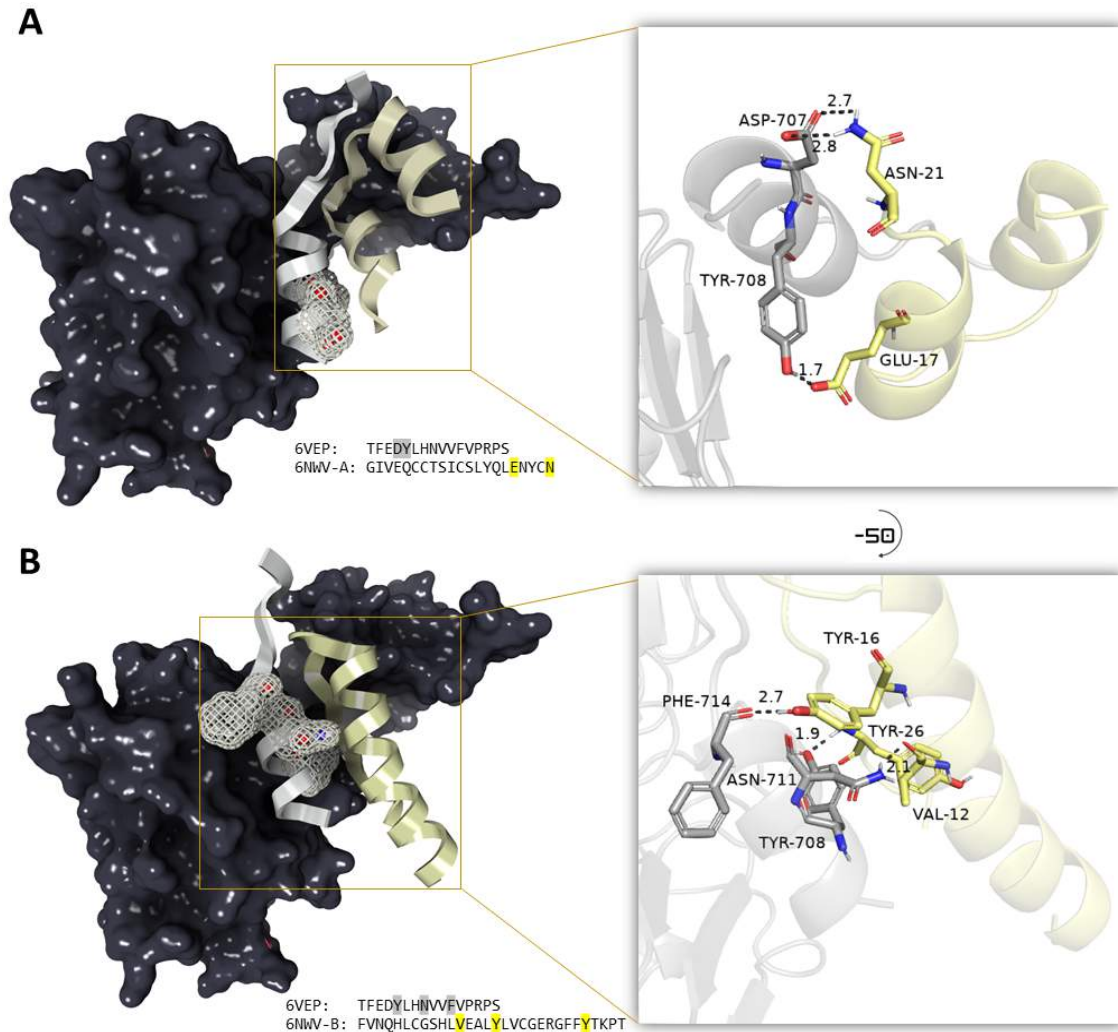


Fig. (33). Insulin lispro and insulin receptor interaction. Docking the lispro (PDB_ID: 6NWV) to the Apo-state IR structure (PDB_6VEP) containing the α CT domain (colored in gray) that is critical for insulin binding and L1 domain (colored in black). Interaction with insulin-active residues reported in previous studies (Lukman *et al.*, 2015) has succeeded. The lispro chain B (A) and/or chain A (B) are excluded for a better view. Interacted residues of α CT domain with the lispro have displayed the mesh mode in the Protein Imager server. (A higher resolution / colour version of this figure is available in the electronic copy of the article).

(Fig. 33A, pale-yellow), and Val12, Tyr16, Tyr26 (Fig. 33B, pale-yellow) residues of lispro insulin have interacted with Asp707, Tyr708 (Fig. 33A, gray), and Tyr708, Asn11, Phe714 (Fig. 33B, gray) residues of the IR- α CT segment; while Gln5, Thr8, Leu13 (Fig., 31A, pale-yellow) and Tyr16, Phe24, Tyr26 (Fig. 31B, pale-yellow) residues of regular insulin have interacted with His710, Phe714, Arg717, Ser719 (Fig. 31A, gray), and Thr704, Asn711 (Fig. 31B, gray) residues of the IR- α CT segment.

25. INSULIN ASPART

Insulin aspart, NovoRapid (Novo Nordisk Company), mimics the function of endogenously produced human insulin and is similar to the lispro action. Its effect begins within 15 minutes, its peak levels occur 30 to 90 minutes after injection, and the duration of action is approximately 5 hours.

It is also known as "bolus insulin" as it provides high insulin levels in a fleeting time. This analog has been produced as a biosynthetic and fast-acting insulin analog using recombinant techniques. This analog works to improve glycemic control in children and adults with diabetes. Compared to native insulin, it has a single residue modification in the position of proline (B28) replaced by aspartic acid. This change causes a higher dissociation effect of aspart than native insulin. It also has a lower binding affinity for plasma proteins, similar to regular insulin. The median time to maximum concentration for regular insulin and the aspart insulin analog is 50/40 minutes versus 120/80 minutes, respectively. Therefore, this analog is also a faster absorption feature than regular insulin after the injection. Typically, a 0.15 U/kg body weight dose for type 1 diabetes is characterized by a maximum concentration (C_{max}) of 82 mU/L. Its half-life after injection is 81 minutes [406-408].

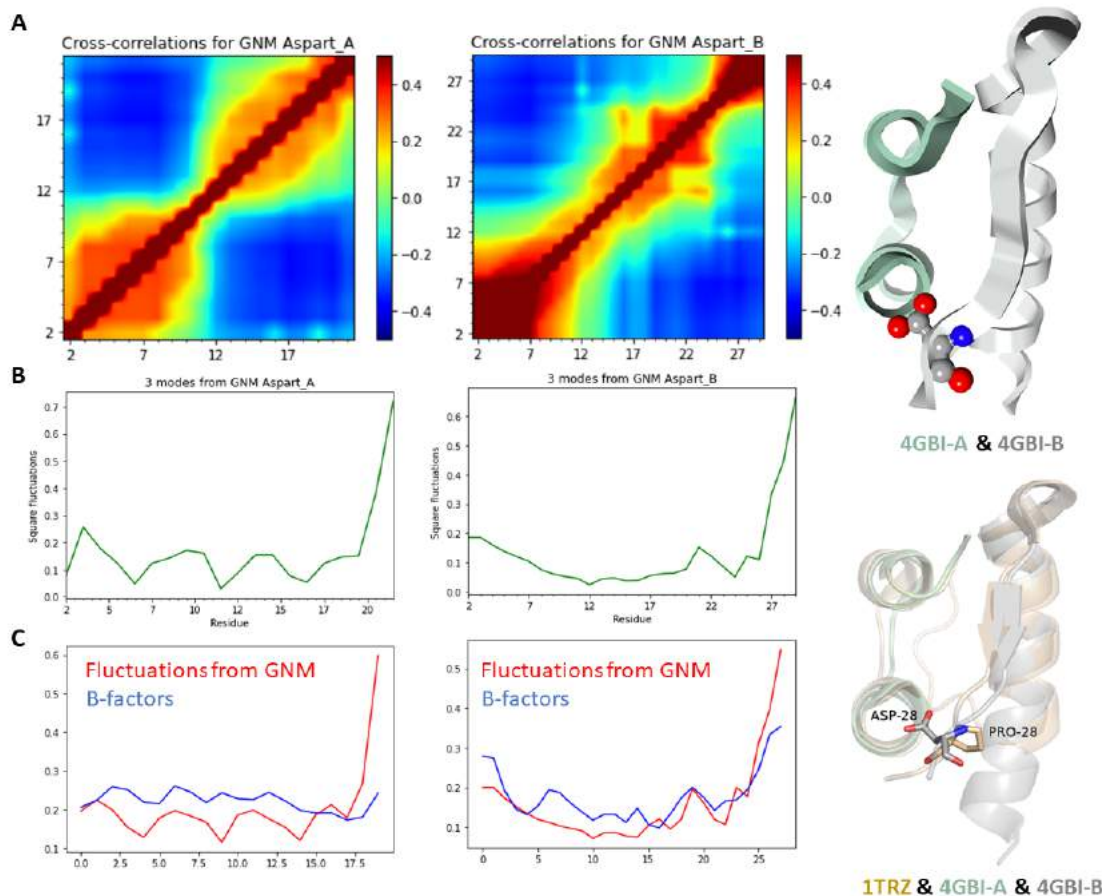


Fig. (34). General analysis of aspart in terms of cross-correlation and squared fluctuations from Gaussian Network Model (GNM) analysis. Aspart A and B chains are highly correlated with each other. In the *cross-correlation result from the GNM* analysis, the color range was determined as -0.5 and 0.5 to ensure compatibility between analogs' results (A). According to the squared fluctuations obtained from the weighted 3 *slowest modes*, global motion and residual fluctuations are relatively stable (B). While the figures show the correlation between the theoretical (GNM results; fluctuations from GNM) and the experimental (B-factors), lines show only the residue fluctuations (squared fluctuations even) (C). Aspart structures (4GBI) are generated using the Protein Imager server. Superposition of the Aspart (4GBI) and human insulin (1TRZ) was generated by PyMOL software (Root-mean-square deviation (RMSD): 0.86). (A higher resolution / colour version of this figure is available in the electronic copy of the article).

We also performed GNM analysis to compare the dynamics of regular insulin and insulin aspart structures obtained from the PDB as a bird's eye view. Accordingly, cross-correlations between residue motions of the aspart structure were analyzed with mean square fluctuations characterized by the flexibility of the residues (Fig. 34). Similarly, the intrachain residues' cross-correlation displayed that the first ten residues and 13-20th residues had highly correlated motions in chain A as well. In addition, chain B was observed with higher fluctuations at the 2-11st, 17-23rd, and 27-30th positions (Fig. 34A). Three modes, theoretical (fluctuation), and experimental (B-factor) results from GNM were investigated closer to further evaluate the intrinsic residue fluctuations of the aspart structure (Figs. 34B and 34C). The theoretical fluctuations calculated from the three modes are aligned to the B factors in Fig. (34C). Accordingly, the residues around position 17th elucidate the regional flexibility of the C-terminus of aspart chain B compared to lispro

dynamics (Fig. 34C). We also performed a docking analysis to compare the interaction of regular insulin vs. aspart with the insulin receptor. Accordingly, Leu13, Glu17 (Fig. 35A, pale-yellow), and Glu13, Phe24, Tyr26 (Fig. 35B, pale-yellow) residues of aspart insulin have interacted with Asn711, Arg717 (Fig. 35A, gray), and His710, Asn711, Arg717 (Fig. 35B, gray) residues of the IR- α CT segment.

26. INSULIN GLULISINE

Insulin glulisine, Apidra (Sanofi-Aventis Company), mimics the function of endogenously produced human insulin and is similar to the lispro and aspart action. Its effect begins within 15 minutes, its peak levels occur 30 to 90 minutes after injection, and the duration of action is approximately 5 hours. It is also known as "bolus insulin" as it provides high insulin levels in a fleeting time. This analog has been produced as a biosynthetic and fast-acting insulin ana-

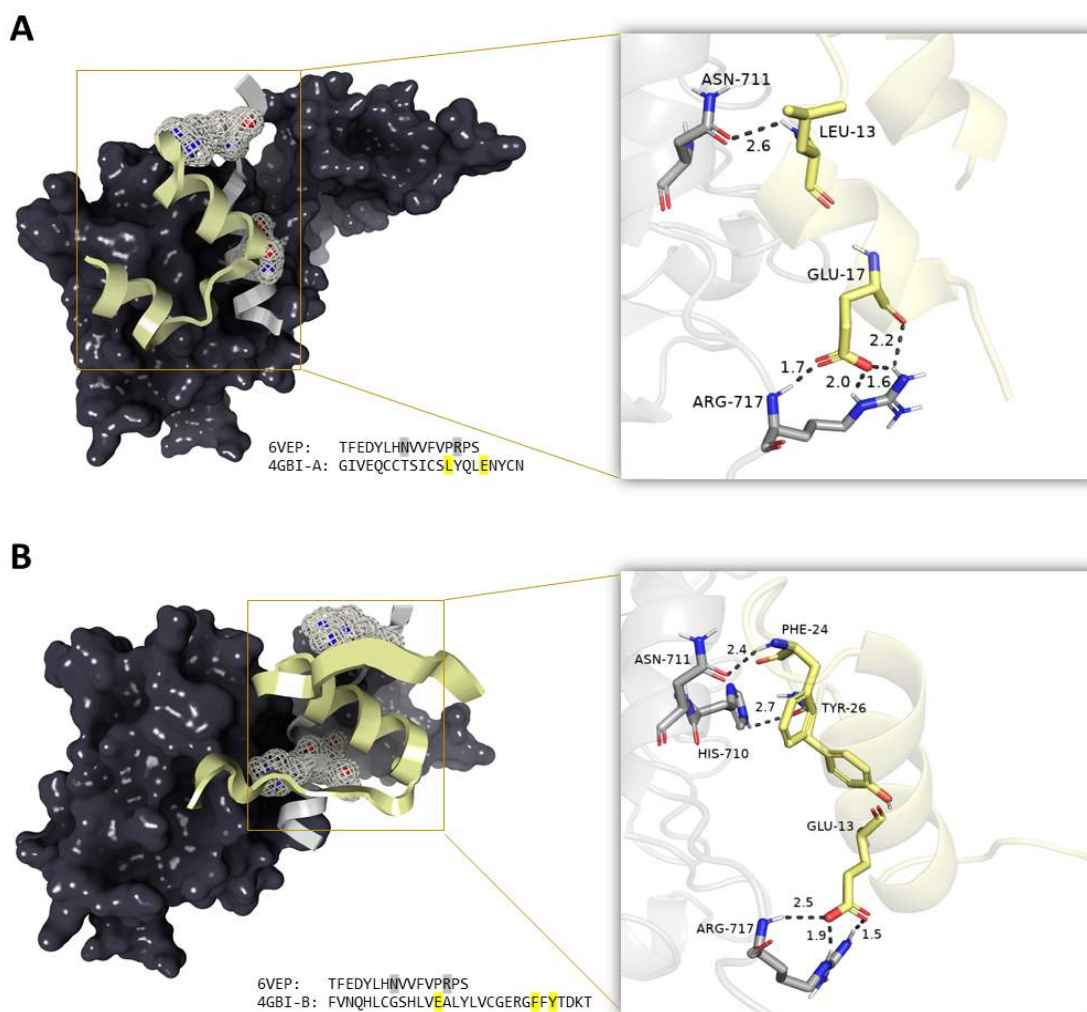


Fig. (35). Insulin aspart and insulin receptor interaction. Docking the aspart (PDB_ID: 4GBI) to the apo-state IR structure (PDB_6VEP) containing the α CT domain (colored in gray) that is critical for insulin binding and L1 domain (colored in black). Interaction with insulin-active residues reported in previous studies (Lukman *et al.*, 2015) has succeeded. The Aspart chain B (A) and/or chain A (B) are excluded for a better view. Interacted residues of α CT domain with the aspart have displayed the mesh mode in the Protein Imager server. (A higher resolution / colour version of this figure is available in the electronic copy of the article).

log using recombinant techniques. This analog works to improve glycemic control in children and adults with diabetes. Compared to native insulin, it has an asparagine residue modification in the position B3 replaced by lysine and B29 replaced by glutamic acid. This structural change causes a higher dissociation effect of glulisine than native insulin and stabilizes its monomer form. The action of insulin glulisine at the beginning is nearly 15 minutes. Its activity peaks occur 60 minutes after the injection and its duration of action is 2-4 hours. The median time to maximum concentration (Tmax) for regular insulin and aspart insulin analog is 60 minutes versus 120 minutes, respectively. As a result, this analogue has a faster rate of absorption than conventional insulin after injection. Typically, 0.15 U/kg body weight dose for type 1 diabetes is characterized by a maximum concentration (Cmax) of 83 mU/L versus 50 mU/L compared to regular insulin. Its absolute bioavailability is approximately 70%;

this change depends on the injection area (thigh 68%, abdomen 73%, deltoid 71%), and its half-life after injection is 42 [409].

We also performed GNM analysis to compare the dynamics of regular insulin and insulin glulisine structures obtained from the PDB as a bird's eye view. Accordingly, cross-correlations between residue motions of the glulisine structure were analyzed with mean square fluctuations characterized by the flexibility of the residues (Fig. 36). Similarly, the intrachain residues' cross-correlation displayed that the first ten residues and 13-20th residues had highly correlated motions in chain A as well. In addition, chain B was observed with higher fluctuations at the 2-7th, 11-13rd, 17-21st, 23-25th, and 27-30th positions (Fig. 36A). Three modes, theoretical (fluctuation), and experimental (B-factor) results from GNM were investigated closer to further evaluate

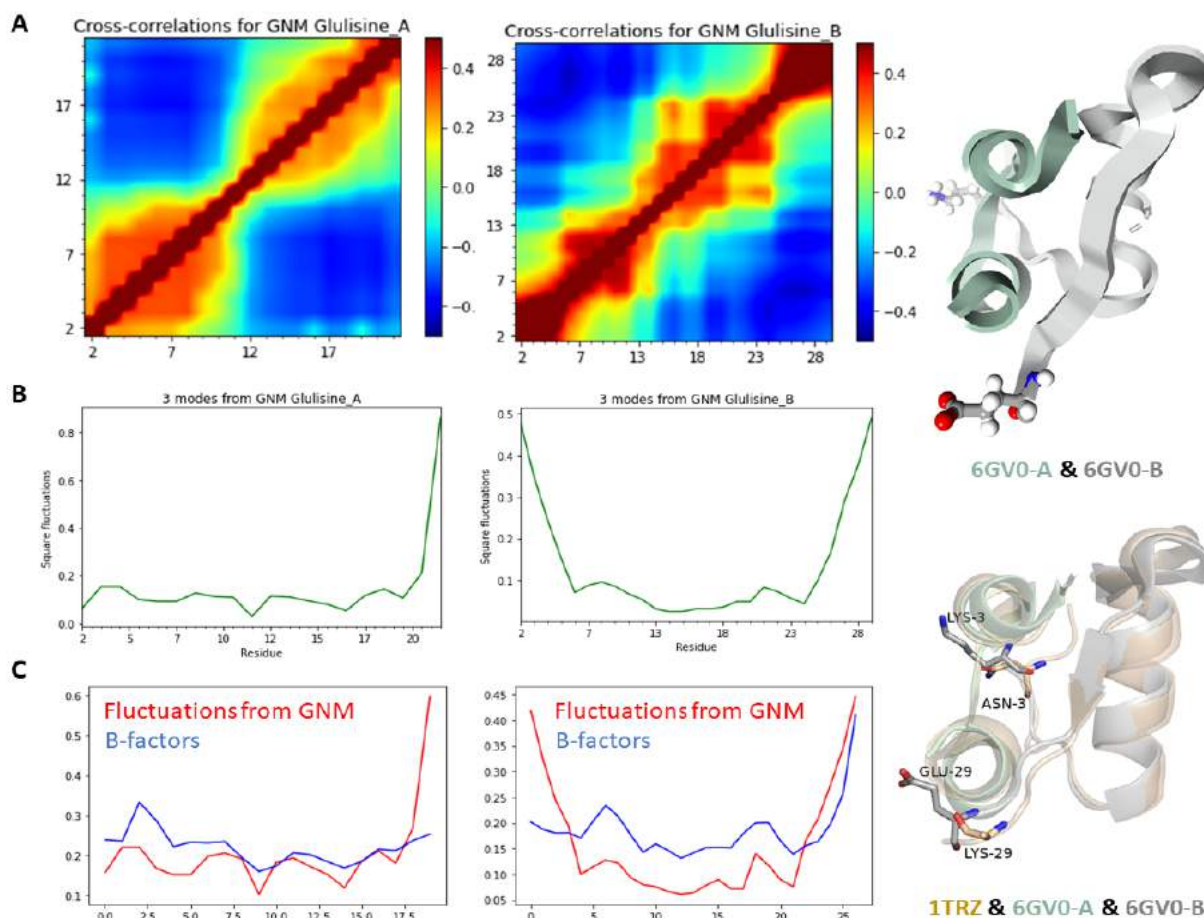


Fig. (36). General analysis of glulisine in terms of cross-correlation and squared fluctuations from Gaussian Network Model (GNM) analysis. Glulisine A and B chains are highly correlated with each other. In the *cross-correlation result from the GNM* analysis, the color range was determined as -0.5 and 0.5 to ensure compatibility between analogs' results (A). According to the squared fluctuations obtained from the weighted 3 *slowest modes*, global motion and residual fluctuations are relatively stable (B). While the figures show the correlation between the theoretical (GNM results; fluctuations from GNM) and the experimental (B-factors), lines show only the residue fluctuations (squared fluctuations even) (C). Glulisine (6GV0) is generated using the Protein Imager server. Superposition of the glulisine (6GV0) and human insulin (1TRZ) was generated by PyMOL software (Root-mean-square deviation (RMSD): 0.42). (A higher resolution / colour version of this figure is available in the electronic copy of the article).

the intrinsic residue fluctuations of the aspart structure (Figs. 36B and 36C). The theoretical fluctuations calculated from the three modes are aligned with the B factors in Fig. 36C. Accordingly, the residues around position 17th elucidate the regional flexibility of the C-terminus of aspart chain B compared to lispro dynamics (Fig. 36C). We also performed a docking analysis to compare the interaction of regular insulin vs. aspart with the insulin receptor. Accordingly, Gly1, Gln5, Ser12, Tyr19 (Fig. 37A, pale-yellow), and His10, Phe24, Tyr26 (Fig. 37B, pale-yellow) residues of glulisine insulin have interacted with Glu706, Asp707, Asn711, Phe714 (Fig. 37A, gray), and Asp707, His710, Pro718 (Fig. 37B, gray) residues of the IR- α CT segment.

27. LONG-ACTING BASAL INSULIN ANALOGS

There are several types of long-acting insulin formulations for commercial use, such as insulin glargine, insulin detemir, and insulin degludec. All analogs are designed to

provide stable, relatively flat, and long-term basal insulin levels compared to the regular insulin formulation [410].

28. INSULIN GLARGINE

Insulin glargine Lantus (Sanofi-Aventis) mimics the function of endogenously produced human insulin (Fig. 38A). This analog works to improve glycemic control in children and adults with diabetes. It has a duration of effect of up to 24 hours and is suitable for dosing once a day before going to bed. Glargine can be considered "basal insulin" in terms of its potency. Therefore, low insulin concentrations are sufficient, as it maintains blood sugar balance at night or between meals. Typically, long-acting analogs are combined with "bolus insulin" as they mimic the endogenous insulin function of the pancreas. This analog has been reformulated by Sanofi under the name Toujeo. It is more concentrated (300IU / mL) than Lantus, which contains 100IU / mL of product. Its effect starts within 6 hours and the duration of

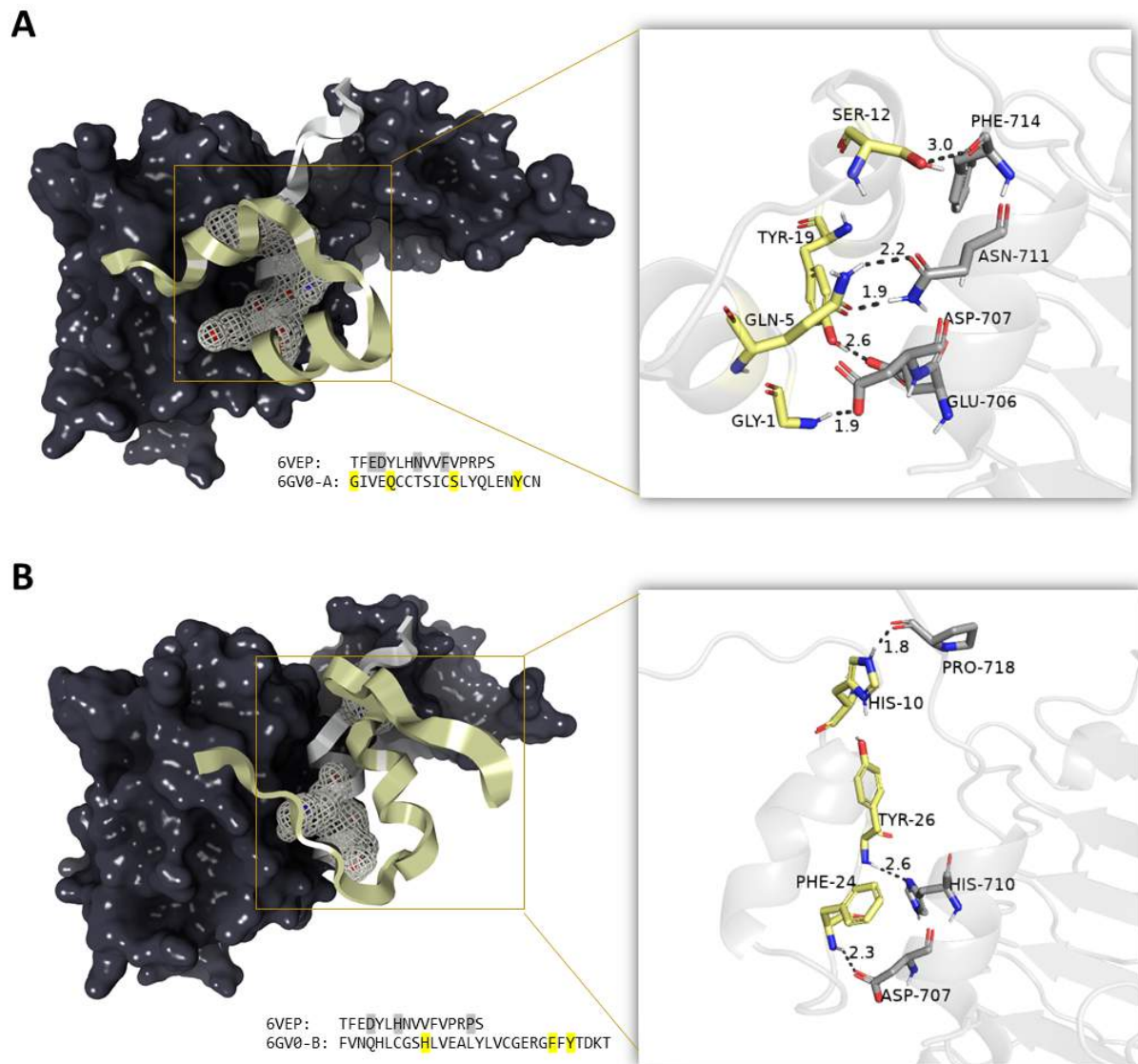


Fig. (37). Insulin glulisine and insulin receptor interaction. Docking the glulisine (PDB_ID: 6GV0) to the Apo-state IR structure (PDB_6VEP) containing the α CT domain (colored in gray) that is critical for insulin binding and L1 domain (colored in black). Interaction with insulin-active residues reported in previous studies (Lukman *et al.*, 2015) has succeeded. The glulisine chain B (A) and/or chain A (B) are excluded for a better view. Interacted residues of α CT domain with the glulisine have displayed the mesh mode in the Protein Imager server. (A higher resolution / colour version of this figure is available in the electronic copy of the article).

the effect is approximately 30 hours. This analog is produced by rDNA techniques. An asparagine characterizes the formulation at the 21st position replaced with glycine as well as the addition of two arginine residues at the 31st and B32nd positions. This product dissolves at pH 4.0, forming micro-precipitates at physiological pH 7.4. It allows small amounts of insulin glargine to be released slowly, giving the product a long duration of action, thus allowing it to mimic basal insulin levels in the body. Its modifications allow the isoelectric point to shift to a neutral pH and stabilize it in acidic conditions relative to normal insulin. After injection, this analog is less soluble due to the body's neutral pH, allowing insulin to be released slowly as micro-precipitates. This provides a relatively constant concentration

over 24 hours compared to native insulin. It also contains small amounts of zinc to further delay absorption. The onset of action is 1.1 hours and its pharmacokinetic profiles for 0.4, 0.6, and 0.9 U/kg Toujeo doses in T1D are characterized by 12- and 16-hour serum insulin concentrations. Finally, this analog is metabolized as two active metabolites: 21a-Gly-des-30b-threonine insulin (M2) and 21a-Gly-human insulin (M1) [410-412].

We performed GNM analysis to compare the dynamics of regular insulin and insulin glargine structures obtained from the PDB as a bird's eye view. Accordingly, chain B of the glargine was observed with higher fluctuations at the 2-7th, 19-23rd, and 27-30th positions (Fig. 38A).

29. INSULIN DETEMIR

Insulin Detemir, Levemir (Novo Nordisk Company), mimics the endogenously produced human insulin (Fig. 38B). This analog works to improve glycemic control in children and adults with diabetes. It has a duration of effect of up to 16-24 hours and is suitable for dosing once a day before going to bed. Because of its potency, detemir can be considered "basal insulin". Like glargine, low detemir concentrations are sufficient for diabetics as it maintains blood sugar balance at night or between meals. This analog is produced by yeast cells using rDNA technology. The formulation has a 14-C fatty acid called myristic acid attached to the lysine residue at the B29 position. The myristoyl moiety enhances albumin binding and self-assembly. Therefore, detemir can dissolve insulin slowly, so it provides a long-acting effect. Its onset is 1 to 2 hours and has a 30% lower receptor binding affinity than native insulin. The Cmax is 6 to 8 hours after subcutaneous injection. The Cmax for 0.5 units/kg of this analog is 4.641 ± 2.299 pmol/L, and the apparent volume of distribution is about 0.1 L/kg. The median time to C max is 12 hours after injection and its absolute bioavailability is approximately 60%. More than 98% is bound to albumin and there is no clinically significant interaction between other protein-bound drugs or fatty acids and insulin detemir. The terminal half-life is 5 to 7 hours, depending on the dose after injection [413].

We also performed GNM analysis to compare the dynamics of regular insulin and insulin detemir structures obtained from the PDB as a bird's eye view. Accordingly, chain B of the detemir was observed with higher fluctuations at the 2-10th, 17-20th, 22-24th, and 27-30th positions (Fig. 38B)

30. INSULIN DEGLUDEC

Insulin Degludec, Tresiba (Novo Nordisk Company), mimics natural human insulin (Fig. 38C). This analog works to improve glycemic control in elderly and 1-year-old patients with DM. It has an effective time of up to 42 hours and is suitable for dosing once a day before going to bed. This analog has an extra hexadecanedioic acid on the lysine residue at position B29, allowing multi-hexamers to form. After injection, this multi-hexamer conformation acts like a drug depot and releases the monomer rather slowly. This phenomenon offers a protracted-time action profile due to its delayed absorption from the tissue into the systemic circulation. Therefore, this analog provides a lower peak than other long-acting insulin analogs. Cmax for 0.4 U/kg of this analog is 4472 pmol/L, and its Tmax is characterized by 9 hours. The average onset of appearance is about an hour and its concentration reaches steady-state levels after 3-4 days. More than 99% of insulin degludec is bound to plasma albumin and there is no clinically significant interaction between other protein-bound drugs and degludec. The terminal half-life is characterized by approximately 25 hours, regardless of the dose [414, 415].

We also performed GNM analysis to compare the dynamics of regular insulin and insulin degludec structures obtained from the PDB as a bird's eye view. Accordingly, chain B of the degludec was observed with higher fluctuations at the 2-10th, 17-20th, 22-24th, and 27-30th positions (Fig. 38C)

31. PREMIXED INSULIN ANALOGS

There are three main types of prefixed insulin analog formulations: 50% insulin lispro with 50% insulin lispro protamine suspension, 25% insulin lispro with 75% insulin lispro protamine suspension, and 30% insulin aspart protamine suspension with 70% insulin aspart protamine. The purpose of these formulations is to minimize the errors of some mixed insulin combinations made by patients. Therefore, the insulin regimen can be simplified and the number of injections per day can be reduced. Typically, the regular premixed insulin effect is approximately 0.5 to 2 hours, and the effect lasts up to 24 hours. However, the effect of premixed insulin analogs is about 15 minutes, and their biological activity is highest at 1 to 4 hours. Similar to regular human insulin premixes, premixed insulin analogs also last up to 24 hours. In addition, the pharmacokinetic profiles of pre-mixed insulin analogs are characterized by less individual variability compared to pre-mixed regular human insulin [416].

32. INSULIN PRODUCTION METHOD

Typically, insulin production is characterized by three main approaches in terms of novel techniques. Two of these techniques involve using the organism *Escherichia coli* (Figs. 39A and 39B) [417-419], while the third method is to use *Saccharomyces cerevisiae* (Fig. 39C) [420] to get the insulin precursor in the medium. When the first two methods are preferred, either the precursor is produced using the large fusion protein in the cytoplasm [418, 419] or the use of a signal peptide to release the product into the periplasmic space is preferred [418-420]. In the two-chain method, insulin is produced in a way that the A and B chains are separate. These strands are produced as a form of the fusion protein in *E. coli* culture containing a vector carrying the interested DNA. After cleavage of the fusion protein using cyanogen bromide (CNBr), the A and B chains are sulfonated by reacting along the sulfonated A chain with the sulfonated B chain. Finally, these products are purified to obtain insulin. Such a method has many disadvantages, such as requiring two fermentation processes and additional steps to prepare the sulfonated B chain and A chain. Hence, this results in low insulin yield [418-420]. In the intracellular proinsulin method, insulin is produced in *E. coli* as a proinsulin precursor in the form of the fusion protein. Similar to the two-chain method, proinsulin is cultured in *E. coli* containing a vector carrying DNA of interest. After cleavage of the fusion protein using the CNBr, proinsulin is obtained. After the precursor is separated in the form of sulfonated proinsulin, it is refolded to form native disulfide bonds using trypsin and carboxypeptidase B. Finally, the resultant product is purified to obtain insulin. However, in this method, the yield of proinsulin decreases sharply during the folding of the disulfide bonds. The causes may be misfolding of the protein or some polymerization problems during the process. Therefore, the additional laborious purification steps resulting from these problems can be cited as disadvantages of such a method [418-420]. The extracellular insulin production method is different from the others in terms of using *Saccharomyces cerevisiae* cells. This approach involves production, purification, reaction with enzymes, hydrolysis with acids, and purification of single-chain insulin. However, this process has an unacceptably low insulin production efficiency [418-420].

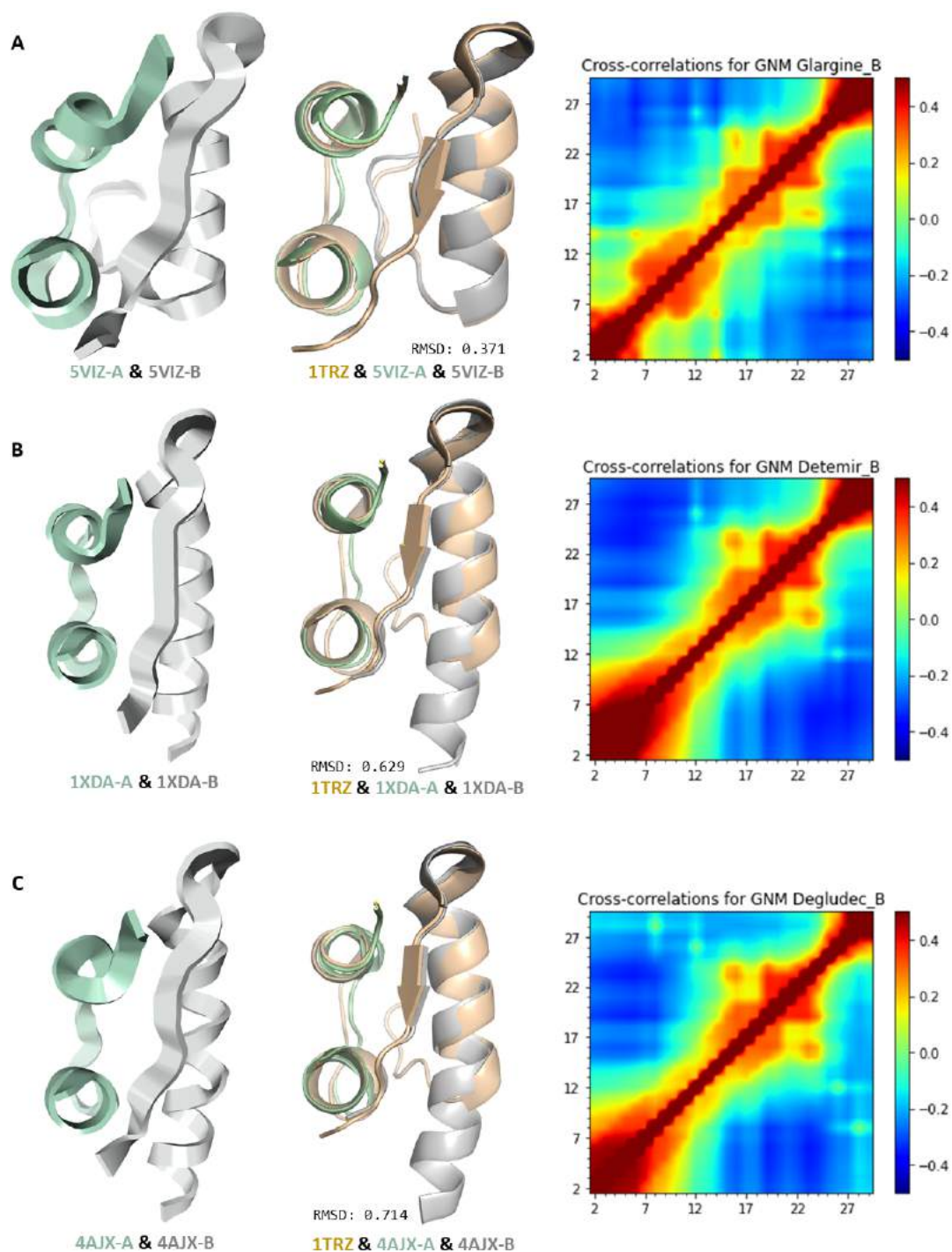


Fig. (38). Detailed comparison of human insulin and long-acting insulin glargine (A) (PDB ID: 5VIZ), insulin detemir (B) (PDB ID: 1XDA), insulin degludec (C) (PDB ID: 4AJX). Long-acting analogs show similar cross-correlation with respect to the correlation between the monomers of glargine (A), detemir (B) and degludec (C). In the cross-correlation result from the GNM analysis, the color range was determined as -0.5 and 0.5 to ensure compatibility between analogs' results. All single structures are generated using the Protein Imager server. Superposition of the long-acting structures was generated by PyMOL software. (A higher resolution / colour version of this figure is available in the electronic copy of the article). (A higher resolution / colour version of this figure is available in the electronic copy of the article).

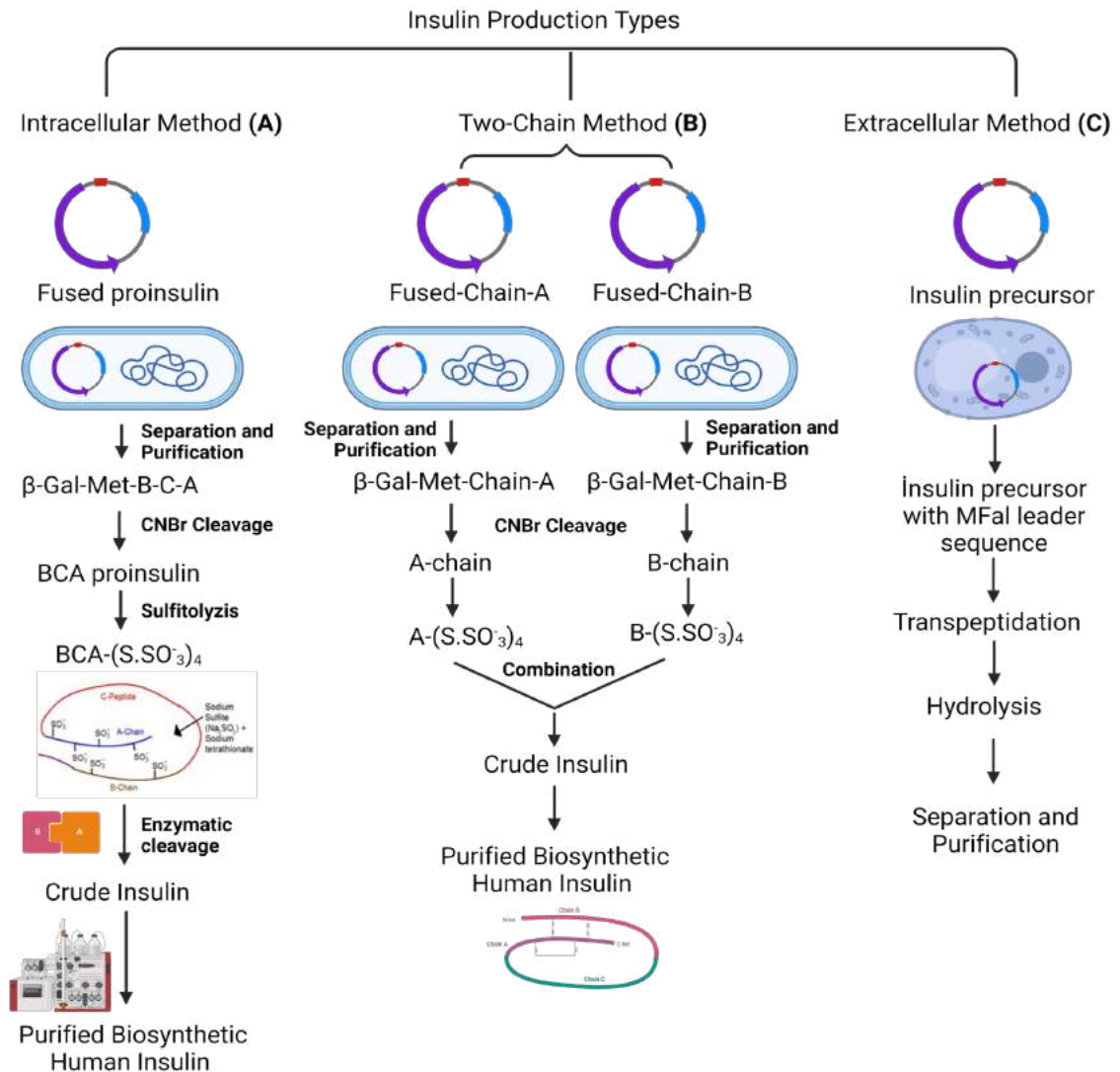


Fig. (39). Comparison of main recombinant insulin production methods. (A higher resolution / colour version of this figure is available in the electronic copy of the article).

Until now, there are many new approaches that have been tried to produce clinically useful insulin. Some are patented and most continue to be patented, while others are presented as research articles. The remaining part of the article will discuss the production of both patented insulin and optimized insulin.

33. OVERVIEW OF PATENTED INSULIN ANALOGS AND PRODUCTION METHODS

In 1992 and 2001, various insulin analog formulations were extensively studied and patented [421-436]. In 2007, an insulin analog in which the asparagine (Asn) at position B3 of the B chain had been substituted to a basic amino acid residue and an amino acid residue at the B29 position of the B chain had been substituted to a neutral/acidic amino acid residue was crystallized by a novel approach. In this crystallization optimization, crystals with $A = 81.5 \text{ \AA}$ and $C = 33.3 \text{ \AA}$ cell units were found in the R3 space group. After the

amorphous powder of this analog was dissolved in a suitable zinc-free liquid, this analog was crystallized for further processing involving their precipitation, isolation, and drying. The validity of this patent is active until 2024 [425]. In 2011, introduced the Aspart modified proinsulin and its production methods. In this approach, the sequence Ri-(Bi-B26)-B27-B28-B29-B30-R2-3-X-R4-R5-(Ai-A20)-A21-R6 has been optimized and described in detail. Furthermore, in the method, *E.coli* was transformed by His Tagged Aspart proinsulin inserted pTrcHis2A(Kan) plasmid. After the inclusion bodies were dissolved in reducing and chaotropic agents at pH 11.8-12, this analog was recovered for other processes through folding, enzymatic cleavage, purification, and elution [426]. In 2012, the same team introduced the Glargine proinsulin and its production methods. In this approach, the sequence R1-(B1-B29)-B30-R2-R3-X-R4-R5-(A1-A20)-A21-R6 has been optimized and described in detail. In addition, in the method, *E.coli* was transformed by a His Tagged Glargine

proinsulin inserted pTrcHis2A(Kan) plasmid. At a similar time, a long-acting insulin glargine analog (1 mg/mL to 20 mg/mL) was developed. This analog involves zinc, magnesium, copper, phenol, m-cresol, and calcium ions at pH from 3.5 to 4.5. After the dissolution of the inclusion bodies in chaotropic agents, this analog was recovered for other processes through folding, purification by metal affinity chromatography, protection of a Lys residue with protective compounds, enzymatic cleavage with an intermediate solution, followed by purification by chromatography column(s) [427]. Likewise, around 2013, a long-acting insulin glargine analogue was patented as well [428]. In the same year, the purification method of detemir was patented. Accordingly, this technique involves equilibrating the column with an acidic solution, adjusting the pH below 5, adding 0.5-1.0 M buffer solution to the column at pH: 2-4, and washing. After collection, the main peak is obtained so that insulin detemir is purified. This technique has some advantages, such as large sample loading, convenience of operation, and high recycling efficiency. Additionally, this method is suitable for industrial production, which is economical, environmentally friendly, and cost-saving [429]. In 2015, the same team introduced the Lis-Pro modified proinsulin and its production methods. In this approach, the R1 -(B1-B27)-B28-B29-B30-R2-R3-X-R4-R5-(A1-A21)-R6 sequence was optimized and described in detail. Furthermore, in the method, *E.coli* was transformed with plasmid pTrcHis2A(Kan). After the inclusion bodies were dissolved in reducing and chaotropic agents at pH 11.8-12, this analog was recovered for other processes by folding, enzymatically cleaving, purification, and elution [430]. In the same year, an aqueous pharmaceutical formulation of glulisine was introduced at concentrations of 200 U/mL to 1000 U/mL in conditions with or without zinc (20 g/mL). Additionally, adjustment of buffer concentrations was formulated with the amount of phosphate, glycerol, trometamol, nonionic surfactant, phenol, and/or m-cresol at pH 3.5 with 9.5 [431]. Moreover, in the same year, insulin and its analogs were purified by high-pressure liquid chromatography and reverse-phase chromatography. This approach was carried out in an acidic cation exchange medium in the presence of an water-miscible organic modifier at elevated temperatures [432]. Likewise, the purification process of insulin and insulin analogs was developed by two tandem microfiltration (MF) methods. Such a method reduces both soluble and insoluble impurities as well as provides a suitable buffer for the downstream purification process of the insulin product [433-434]. In about 2016, a method was developed for dissolving and refolding precursor insulin or its analogs from the inclusion body for use in the production of insulin and its various analogs [434]. In the same year, insulin, insulin derivatives, and hybrid peptide production methods were introduced. After the Xn-B-Arg-Arg-A formula was optimized by some steps, some insulin and its derivatives, such as insulin, lispro, GR, insulin, SR, insulin, SK3R insulin, and a type of proinsulin, were characterized [435].

34. OVERVIEW OF INSULIN ANALOGS AND PRODUCTION METHODS IN THE LITERATURE

In 2014, human proinsulin production in the milk of transgenic animals was optimized using the goat β -casein promoter. The efficiency of this proinsulin production was

about 8.1 g/L. It was observed that there was no problem with the biological activity of insulin after the conversion of proinsulin obtained from milk into mature insulin. Accordingly, it can be suggested that insulin production can be made in dairy milk [436]. In 2015, large-scale refolding of human proinsulin and a new refolding process to produce human insulin were optimized. It has been stated that a high protein concentration is achieved with this approach. This approach paves the way for the large-scale production of similar biologically active proteins [437]. In 2016, plant-based production of proinsulin analogs was optimized using Peanut seeds. Accordingly, it has been observed that some transgenic peanuts express proinsulin successfully. It was also revealed that peanut seeds act like insulin storage areas [438]. In 2018, the molecular chaperone aB-crystalline (aB-Cry) had been preferred as a fusion protein in insulin production. In this way, novel and sensitive insulin production and purification steps were optimized. In this study, in which the two-chain method was preferred, pET28b(+) was preferred as the vector, and *E.coli* was used as the host, providing high yield and proper folding of the enzyme [439]. In 2019, a new bacterial host and a compatible expression vector were optimized. Accordingly, the efficiency of this recombinant human insulin has been observed to be relatively high. In this study, an alternative method for producing recombinant human insulin is introduced [440]. In 2020, PCR-based insulin production was optimized by overexpressing *E.coli* at a lab scale. The yield of the product was 520.92 mg/L. After insulin detection by MALDI-TOF-MS and LC-MS, this product was found to be 100% similar to human insulin. This study eliminated the use of affinity tags, body recovery steps, and enzymatic cleavage of the c-peptide processes [441].

35. CHALLENGES AND FUTURE DIRECTIONS

Insulin has been a molecule characterized by diabetes treatment for nearly a century. However, although therapeutic strategies appear to be evolving, the approaches are the same: diabetes-focused injectable therapies. Perspectives concentrated solely on glucose management remain non-pragmatic conventional modalities, thus suppressing the risk of life-threatening hypoglycemia rather than treating it. These perspectives include insulin alternatives such as microreceptors, aptamers, non-insulin peptides, and antibodies and are found in the literature as approaches whose optimization is not fully established and requires validation. Diabetes is not a disease by itself, but rather a critical phenomenon that paves the way to the development of many insulin-related disorders. Diabetic chronicity only occurs in a variety of scales, from microvascular diseases to macrovascular diseases to the diabetic axis, while current treatments are only designed to minimize these symptoms.

The last point reached in insulin production has progressed to supplying high purity insulin with state-of-the-art injection devices. However, insulin production and insulin therapy alone do not provide sufficient results in diabetes management. Medical advances have focused on advanced therapeutic approaches that take into account intermediate measures such as body weight, lipid and glucose, and disease mortality data from a holistic perspective rather than employing insulin-based improvements. Examples in this con-

text include implantable mini-insulin pumps that control glucose with a closed-loop system that simulates pancreatic function, as well as personalized diabetes management approaches with artificial intelligence integrated sensors. In addition to these groundbreaking studies with ongoing optimization, the continuous intravenous insulin infusion method and basal bolus insulin strategies have already occurred in clinical studies as viable methods that begin to mimic holistic and personalized approaches, and such methods have given successful results so far. In addition, stem cell and tissue engineering technologies that pave the way to a non-technical but biological axis for the same goal are among these approaches, including companies that play an active role in β -cell restoration. Such approaches do not only consist of therapies based on insulin/analogues but also make the treatment healthier by approaching the disease from a holistic and personal perspective.

In many ways, adult-onset diabetes has a more complex system than juvenile-onset diabetes. This is due to the complicated symptoms that adult-onset patients have over a wider age range. The absence of a genetic predisposition in adults in the adult-onset condition indicates that the disease is triggered by environmental factors. The most critical example of this is obesity. Such environmental factors and diseases experienced by diabetic patients are closely related to the development of diabetes. This is the evidence of why the prevalence of insulin-related diseases mentioned earlier is so high. Therefore, when dealing with insulin, considering only diabetes is an inadequate interpretation of the scenario and applying insulin therapy as the treatment alone is not sufficient. An example of this situation is that an obese diabetic patient who suffers from weight loss only with surgical intervention often encounters irreversible complications. Individuals who do not want to experience this situation will only turn to obesity-focused drugs. In both cases, since a holistic modality is not applied to the disease, the result will be to suppress symptoms of the disease with only temporary solutions.

A similar situation is valid for nonclinical studies. Focusing on a particular point in the studies will lead to the evaluation of insulin, which is a complex system in itself, the proteins it is associated with, the pathways it triggers, and the diseases it causes in a narrow window. Science has a cumulative nature and progress must be maintained from the previous step. In this way, even these changes in injection techniques, from subcutaneous injections to oral insulin applications, from diabetes diaries to smart insulin pumps, have been developed by approaching insulin on the basis of holistic and personalized medicine. All holistic information about insulin obtained in structural, biological, omics, and clinical axes facilitate the path to be taken in treatment.

CONCLUSION

Insulin has played a central role in our understanding of the underlying mechanisms of metabolic diseases and in the advancement of peptide chemistry, biochemistry, structural biology, and omics strategies. The diabetes global epidemic has led to a dramatic increase in insulin demand. Over time, insulin-oriented optimizations have progressed in correlation with advances in rDNA biosynthesis and synthetic chemis-

try, and high purity insulin production has been successfully achieved. In this way, analogs that provide advanced basal glucose control have been designed, and robust optimization has been achieved in insulin therapy. Although insulin therapy is an established approach clinically, it has not been able to achieve complete integrity from the metabolic perspective. Therefore, it lacks a personalized strategy. As a result, this deficiency has remained closely related to the development of hypoglycemia with the usage of insulin.

Even though the aim of insulin therapy is to eliminate diabetes, any treatment that lacks the axis of holistic and personalized medicine is destined to suppress symptoms of the disease rather than eliminate it. Therefore, more functional strategies are needed in the diagnosis, preventive treatment, and research studies to eradicate insulin-dependent diseases. In this age, where technology has made significant progress compared to the past, making holistic and personalized medicine-based strategies a part of research and clinical studies will enable us to step into a new era where we can offer solutions from a thousand different perspectives.

LIST OF ABBREVIATIONS

| | | |
|------------------|---|---|
| DM | = | Diabetes Mellitus |
| T1D | = | Type-1 Diabetes |
| T2D | = | Type-2 Diabetes |
| rDNA | = | Recombinant DNA |
| GLUT-2 | = | Glucose Transporter 2 |
| PDX-1 | = | Pancreatic Duodenal Homeobox Factor-1 |
| E47/b42 | = | β -cell E box transactivator 2 |
| SRP | = | Signal Recognition Particles |
| RER | = | Rough Endoplasmic Reticulum |
| ER | = | Endoplasmic Reticulum |
| IAPP | = | islet amyloid polypeptide |
| PTB | = | phosphotyrosine binding |
| IRS | = | Insulin Receptor Substrates |
| SH2 | = | Src Homology 2 |
| PI3K | = | Phosphoinositide 3-Kinase |
| PIP ₂ | = | phosphatidylinositol-(4,5)-bisphosphate |
| PIP ₃ | = | phosphatidylinositol (3,4,5)-triphosphate |
| Akt/PKB | = | Protein Kinase B |
| PH | = | Pleckstrin Homology |
| SGK | = | Serine/threonine protein kinase |
| S6K | = | p70 ribosomal protein S6 Kinase |
| PDK1 | = | Phosphoinositide Dependent Kinase-1 |
| CAP | = | c-Cbl-Associated Protein |
| C3G | = | Rho family guanine nucleotide exchange factor |
| GLUT4 | = | Glucose transporter type 4 |

| | | |
|----------------|---|---|
| GYS | = | glycogen synthase |
| INS | = | Insulin |
| CVD | = | Cardiovascular Disease |
| DR | = | diabetic retinopathy |
| aHCM | = | asymptomatic hypertrophic cardiomyopathy |
| IGF-1 | = | insulin-like growth factor-1 |
| JNK | = | c-Jun N-terminal kinase |
| IKK | = | nuclear factor- κ B (I κ B) kinase |
| TH2 | = | T-helper type 2 |
| Igs | = | immunoglobulins |
| CLS | = | crown-like structures |
| IRS-1 | = | insulin receptor substrate protein-1 |
| NF- κ B | = | Nuclear Factor- κ B |
| FA | = | Fatty Acid |
| GRP120 | = | omega-3 fatty acid receptors |
| PPAR | = | peroxisome proliferator-activated receptor |
| MHC-I | = | Major Histocompatibility Complex I |
| IGFR | = | Insulin-like growth factor receptor |
| CNS | = | central nervous system |
| AD | = | Alzheimer's Disease |
| NPH | = | Neutral Protamine Hagedorn |
| PPARG | = | Peroxisome Proliferator Activated Receptor Gamma |
| CDKAL1 | = | CDK5 Regulatory Subunit Associated Protein 1 Like 1 |
| IGF2BP2 | = | Insulin Like Growth Factor 2 MRNA Binding Protein 2 |
| ZnT8 | = | Zinc transporter 8 |
| INSL3 | = | insulin-like peptide 3 |
| RXFPP2 | = | relaxin family peptide receptor 2 |
| PPARGC1A | = | promoter of PPARG Coactivator 1 Alpha |
| IRS2 | = | Insulin Receptor Substrate 2 |
| AKT2 | = | AKT Serine/Threonine Kinase 2 |
| HNF4a | = | Hepatocyte Nuclear Factor 4 Alpha |
| IGFBP2 | = | Insulin Like Growth Factor Binding Protein 2 |
| NT5E | = | 5'- Nucleotidase Ecto |
| PAK7 | = | p21 protein (Cdc42/Rac)-activated kinase 7 |
| TMED | = | Transmembrane emp24 domain |
| TSPAN33 | = | Tetraspanin-33 |
| FACS | = | fluorescence-activated cell sorting |

| | | |
|--------|---|--|
| FXYD2 | = | FXYD Domain Containing Ion Transport Regulator 2 |
| GPD2 | = | Glycerol-3-Phosphate Dehydrogenase 2 |
| m6A | = | mRNA methylation |
| ALKBH5 | = | AlkB family of proteins |
| LRP1 | = | lipoprotein receptorrelated protein 1 |
| DCD | = | diabetic kidney disease |
| NXT | = | Naoxintong Capsule |
| SERT | = | serotonin transporter |
| TPMT | = | thiopurine methyltransferase |
| ECM | = | extracellular matrix |
| DTRI | = | destriptide (B28-B30) insulin |
| GNM | = | Gaussian Network Model |

AUTHORS' CONTRIBUTIONS

The manuscript was prepared by E.A., H.D. with input from these coauthors.

CONSENT FOR PUBLICATION

Not applicable.

FUNDING

This publication has been supported by the 2232 International Fellowship for Outstanding Researchers Program of TÜBİTAK (Project No: 118C270) and the 2244 Industry Doctorate Program of TÜBİTAK (Project No: 119C132).

CONFLICT OF INTEREST

The authors declare no conflict of interest, financial or otherwise.

ACKNOWLEDGEMENT

EA would like to thank Cihat Altaş and Tuğba Aksoy for their invaluable support and discussions. EA would like to thank Iyshwary Vigneswaran Warren, Meryem Eren, Abdullah Kepceoğlu, Jerome A. Johnson, Cengizhan Büyükdag, Mehmet Gül, Ömür Güven, Zeliş Nergiz, Gökhan Tanısalı, Fatma Betül Ertem, Ebru Destan, Mami Burğaç, and Büşra Yüksel for their support during the writing of the "A Brief Atlas of Insulin" review.

REFERENCES

- [1] Warram J, Krolewski A. Joslin's Diabetes Mellitus. Epidemiology of diabetes mellitus. Philadelphia: Lippincott Williams & Wilkins, 2005.
- [2] Goeddel DV, Kleid DG, Bolivar F, *et al.* Expression in *Escherichia coli* of chemically synthesized genes for human insulin. *Proc Natl Acad Sci USA* 1979; 76(1): 106-10. <http://dx.doi.org/10.1073/pnas.76.1.106> PMID: 85300
- [3] Johnson IS. Human insulin from recombinant DNA technology. *Science* 1983; 219(4585): 632-7. <http://dx.doi.org/10.1126/science.6337396>
- [4] Lipska KJ, Ross JS, Van Houten HK, Beran D, Yudkin JS, Shah ND. Use and out-of-pocket costs of insulin for type 2 diabetes mellitus from 2000 through 2010. *JAMA* 2014; 311(22): 2331-3.

- <http://dx.doi.org/10.1001/jama.2014.6316> PMID: 24915266
- [5] Zaykov AN, Mayer JP, DiMarchi RD. Pursuit of a perfect insulin. *Nat Rev Drug Discov* 2016; 15(6): 425-39. <http://dx.doi.org/10.1038/nrd.2015.36> PMID: 26988411
- [6] Glendorf T, Stidsen CE, Normann M, Nishimura E, Sørensen AR, Kjeldsen T. Engineering of insulin receptor isoform-selective insulin analogues. *PLoS One* 2011; 6(5): e20288. <http://dx.doi.org/10.1371/journal.pone.0020288> PMID: 21625452
- [7] Edgerton DS, Moore MC, Winnick JJ, *et al.* Changes in glucose and fat metabolism in response to the administration of a hepato-preferential insulin analog. *Diabetes* 2014; 63(11): 3946-54. <http://dx.doi.org/10.2337/db14-0266> PMID: 24947349
- [8] Gough SCL, Bode BW, Woo VC, *et al.* One-year efficacy and safety of a fixed combination of insulin degludec and liraglutide in patients with type 2 diabetes: Results of a 26-week extension to a 26-week main trial. *Diabetes Obes Metab* 2015; 17(10): 965-73. <http://dx.doi.org/10.1111/dom.12498> PMID: 25980900
- [9] Mo R, Jiang T, Di J, Tai W, Gu Z. Emerging micro- and nanotechnology based synthetic approaches for insulin delivery. *Chem Soc Rev* 2014; 43(10): 3595-629. <http://dx.doi.org/10.1039/c3cs60436e> PMID: 24626293
- [10] Hovorka R. Closed-loop insulin delivery: From bench to clinical practice. *Nat Rev Endocrinol* 2011; 7(7): 385-95. <http://dx.doi.org/10.1038/nrendo.2011.32> PMID: 21343892
- [11] Banting FG, Best CH, Collip JB, Macleod JJR, Noble EC. The effect of pancreatic extract (insulin) on normal rabbits. *Am J Physiol* 1922; 62(1): 162-76.
- [12] Macleod JJR. Insulin and diabetes: A general statement of the physiological and therapeutic effects of insulin. *BMJ* 1922; 2(3227): 833-5. <http://dx.doi.org/10.1136/bmj.2.3227.833> PMID: 20770902
- [13] Lefever E, Vliebergh J, Mathieu C. Improving the treatment of patients with diabetes using insulin analogues: Current findings and future directions. *Expert Opin Drug Saf* 2021; 20(2): 155-69. <http://dx.doi.org/10.1080/14740338.2021.1856813> PMID: 33249944
- [14] Fralick M, Zinman B. The discovery of insulin in Toronto: Beginning a 100 year journey of research and clinical achievement. *Diabetologia* 2021. <http://dx.doi.org/10.1007/s00125-020-05371-6>
- [15] Bliss M. Banting's, Best's, and Collip's accounts of the discovery of insulin. *Bull Hist Med* 1982; 56(4): 554-68. PMID: 6760943
- [16] Shah SN, Joshi SR, Parmar DV. History of insulin. *J Assoc Physicians India* 1997; (Suppl. 1): 4-9. PMID: 11235634
- [17] Vecchio I, Tornali C, Bragazzi NL, Martini M. The discovery of insulin: An important milestone in the history of medicine. *Front Endocrinol (Lausanne)* 2018; 9: 613. <http://dx.doi.org/10.3389/fendo.2018.00613> PMID: 30405529
- [18] Joshi SR, Parikh RM, Das AK. Insulin-history, biochemistry, physiology and pharmacology. *J Assoc Physicians India* 2007; 55(Suppl.): 19-25. PMID: 17927007
- [19] Tokarz VL, MacDonald PE, Klip A. The cell biology of systemic insulin function. *J Cell Biol* 2018; 217(7): 2273-89. <http://dx.doi.org/10.1083/jcb.201802095> PMID: 29622564
- [20] Bogardus C, Lillioja S, Howard BV, Reaven G, Mott D. Relationships between insulin secretion, insulin action, and fasting plasma glucose concentration in nondiabetic and noninsulin-dependent diabetic subjects. *J Clin Invest* 1984; 74(4): 1238-46. <http://dx.doi.org/10.1172/JCI111533> PMID: 6384267
- [21] Howell SL, Taylor KW. Potassium ions and the secretion of insulin by islets of Langerhans incubated *in vitro*. *Biochem J* 1968; 108(1): 17-24. <http://dx.doi.org/10.1042/bj1080017> PMID: 4297939
- [22] Brissova M, Shiota M, Nicholson WE, *et al.* Reduction in pancreatic transcription factor PDX-1 impairs glucose-stimulated insulin secretion. *J Biol Chem* 2002; 277(13): 11225-32. <http://dx.doi.org/10.1074/jbc.M111272200> PMID: 11781323
- [23] Xia CQ, Zhang P, Li S, *et al.* C-Abl inhibitor imatinib enhances insulin production by β cells: c-Abl negatively regulates insulin production *via* interfering with the expression of NKx2.2 and GLUT-2. *PLoS One* 2014; 9(5): e97694. <http://dx.doi.org/10.1371/journal.pone.0097694> PMID: 24835010
- [24] Koranyi L, James DE, Kraegen EW, Permutt MA. Feedback inhibition of insulin gene expression by insulin. *J Clin Invest* 1992; 89(2): 432-6. <http://dx.doi.org/10.1172/JCI115602> PMID: 1737834
- [25] Harper ME, Ullrich A, Saunders GF. Localization of the human insulin gene to the distal end of the short arm of chromosome 11. *Proc Natl Acad Sci USA* 1981; 78(7): 4458-60. <http://dx.doi.org/10.1073/pnas.78.7.4458> PMID: 7027261
- [26] Lemaire K, Ravier MA, Schraenen A, *et al.* Insulin crystallization depends on zinc transporter ZnT8 expression, but is not required for normal glucose homeostasis in mice. *Proc Natl Acad Sci USA* 2009; 106(35): 14872-7. <http://dx.doi.org/10.1073/pnas.0906587106> PMID: 19706465
- [27] Fu Z, Gilbert ER, Liu D. Regulation of insulin synthesis and secretion and pancreatic Beta-cell dysfunction in diabetes. *Curr Diabetes Rev* 2013; 9(1): 25-53. <http://dx.doi.org/10.2174/157339913804143225> PMID: 22974359
- [28] Frederickson CJ, Koh JY, Bush AI. The neurobiology of zinc in health and disease. *Nat Rev Neurosci* 2005; 6(6): 449-62. <http://dx.doi.org/10.1038/nrn1671> PMID: 15891778
- [29] Carroll RJ, Hammer RE, Chan SJ, Swift HH, Rubenstein AH, Steiner DF. A mutant human proinsulin is secreted from islets of Langerhans in increased amounts *via* an unregulated pathway. *Proc Natl Acad Sci USA* 1988; 85(23): 8943-7. <http://dx.doi.org/10.1073/pnas.85.23.8943> PMID: 3057496
- [30] Emdin SO, Dodson GG, Cutfield JM, Cutfield SM. Role of zinc in insulin biosynthesis. Some possible zinc-insulin interactions in the pancreatic B-cell. *Diabetologia* 1980; 19(3): 174-82. <http://dx.doi.org/10.1007/BF00275265> PMID: 6997118
- [31] Smith LF. Species variation in the amino acid sequence of insulin. *Am J Med* 1966; 40(5): 662-6. [http://dx.doi.org/10.1016/0002-9343\(66\)90145-8](http://dx.doi.org/10.1016/0002-9343(66)90145-8) PMID: 5949593
- [32] Tiran J, Avruch LI, Albisser AM. A circulation and organs model for insulin dynamics. *Am J Physiol Endocrinol Metab Gastrointest Physiol* 1979; 237(4): E331-9. <http://dx.doi.org/10.1152/ajpendo.1979.237.4.E331>
- [33] Meier JJ, Veldhuis JD, Butler PC. Pulsatile insulin secretion dictates systemic insulin delivery by regulating hepatic insulin extraction in humans. *Diabetes* 2005; 54(6): 1649-56. <http://dx.doi.org/10.2337/diabetes.54.6.1649> PMID: 15919785
- [34] Li YV. Zinc and insulin in pancreatic beta-cells. *Endocrine* 2014; 45(2): 178-89. <http://dx.doi.org/10.1007/s12020-013-0032-x> PMID: 23979673
- [35] Lizcano JM, Alessi DR. The insulin signalling pathway. *Curr Biol* 2002; 12(7): R236-8. [http://dx.doi.org/10.1016/S0960-9822\(02\)00777-7](http://dx.doi.org/10.1016/S0960-9822(02)00777-7) PMID: 11937037
- [36] Boura-Halfon S, Zick Y. Phosphorylation of IRS proteins, insulin action, and insulin resistance. *Am J Physiol Endocrinol Metab* 2009; 296(4): E581-91. <http://dx.doi.org/10.1152/ajpendo.90437.2008> PMID: 18728222
- [37] Shisheva A. Phosphoinositides in insulin action on GLUT4 dynamics: Not just PtdIns(3,4,5)P₃. *Am J Physiol Endocrinol Metab* 2008; 295(3): E536-44. <http://dx.doi.org/10.1152/ajpendo.90353.2008> PMID: 18492765
- [38] Mackenzie RWA, Elliott BT. Akt/PKB activation and insulin signaling: A novel insulin signaling pathway in the treatment of type 2 diabetes. *Diabetes Metab Syndr Obes* 2014; 7: 55-64. <http://dx.doi.org/10.2147/DMSO.S48260> PMID: 24611020
- [39] Feng J, Park J, Cron P, Hess D, Hemmings BA. Identification of a PKB/Akt hydrophobic motif Ser-473 kinase as DNA-dependent protein kinase. *J Biol Chem* 2004; 279(39): 41189-96. <http://dx.doi.org/10.1074/jbc.M406731200> PMID: 15262962
- [40] Biondi RM, Kieloch A, Currie RA, Deak M, Alessi DR. The PIF-binding pocket in PDK1 is essential for activation of S6K and SGK, but not PKB. *EMBO J* 2001; 20(16): 4380-90. <http://dx.doi.org/10.1093/emboj/20.16.4380> PMID: 11500365
- [41] Chiang SH, Baumann CA, Kanzaki M, *et al.* Insulin-stimulated GLUT4 translocation requires the CAP-dependent activation of TC10. *Nature* 2001; 410(6831): 944-8. <http://dx.doi.org/10.1038/35073608> PMID: 11309621
- [42] Cohen P, Nimmo HG, Proud CG. How does insulin stimulate glycogen synthesis? *Biochem Soc Symp* 1978; (43): 69-95.

- PMID: 219866
- [43] Shen SW, Reaven GM, Farquhar JW. Comparison of impedance to insulin-mediated glucose uptake in normal subjects and in subjects with latent diabetes. *J Clin Invest* 1970; 49(12): 2151-60. <http://dx.doi.org/10.1172/JCI106433> PMID: 5480843
- [44] Gathercole LL, Morgan SA, Bujalska IJ, Hauton D, Stewart PM, Tomlinson JW. Regulation of lipogenesis by glucocorticoids and insulin in human adipose tissue. *PLoS One* 2011; 6(10): e26223. <http://dx.doi.org/10.1371/journal.pone.0026223> PMID: 22022575
- [45] Beitner R, Kalant N. Stimulation of glycolysis by insulin. *J Biol Chem* 1971; 246(2): 500-3. [http://dx.doi.org/10.1016/S0021-9258\(18\)62516-5](http://dx.doi.org/10.1016/S0021-9258(18)62516-5) PMID: 5542017
- [46] Keku TO, Lund PK, Galanko J, Simmons JG, Woosley JT, Sandler RS. Insulin resistance, apoptosis, and colorectal adenoma risk. *Cancer Epidemiol Biomarkers Prev* 2005; 14(9): 2076-81. <http://dx.doi.org/10.1158/1055-9965.EPI-05-0239> PMID: 16172212
- [47] Proud CG. Regulation of protein synthesis by insulin. *Biochem Soc Trans* 2006; 34(Pt 2): 213-6. <http://dx.doi.org/10.1042/BST0340213> PMID: 16545079
- [48] Saltiel AR, Kahn CR. Insulin signalling and the regulation of glucose and lipid metabolism. *Nature* 2001; 414(6865): 799-806. <http://dx.doi.org/10.1038/414799a> PMID: 11742412
- [49] Goldstein BJ, Ahmad F, Ding W, Li PM, Zhang WR. Regulation of the insulin signalling pathway by cellular protein-tyrosine phosphatases. *Mol Cell Biochem* 1998; 182(1-2): 91-9. <http://dx.doi.org/10.1023/A:1006812218502> PMID: 9609118
- [50] Khan AH, Pessin JE. Insulin regulation of glucose uptake: A complex interplay of intracellular signalling pathways. *Diabetologia* 2002; 45(11): 1475-83. <http://dx.doi.org/10.1007/s00125-002-0974-7> PMID: 12436329
- [51] Di Camillo B, Carlon A, Eduati F, Toffolo GM. A rule-based model of insulin signalling pathway. *BMC Syst Biol* 2016; 10(1): 38. <http://dx.doi.org/10.1186/s12918-016-0281-4> PMID: 27245161
- [52] Diseases associated with INS | Open Targets Platform. Available from: <https://platform.opentargets.org/target/ENSG00000254647/associations?view=t:bubbles>
- [53] EMBL-EBI. Available from: https://www.ebi.ac.uk/ols/ontologies/efo/terms/graph?iri=http://www.ebi.ac.uk/efo/EFO_0009605
- [54] Hanna SJ, Powell WE, Long AE, *et al.* Slow progressors to type 1 diabetes lose islet autoantibodies over time, have few islet antigen-specific CD8⁺ T cells and exhibit a distinct CD95^{hi} B cell phenotype. *Diabetologia* 2020; 63(6): 1174-85. <http://dx.doi.org/10.1007/s00125-020-05114-7> PMID: 32157332
- [55] Ramirez DG, Abenjoar E, Hernandez C, *et al.* Contrast-enhanced ultrasound with sub-micron sized contrast agents detects insulinitis in mouse models of type1 diabetes. *Nat Commun* 2020; 11(1): 2238. <http://dx.doi.org/10.1038/s41467-020-15957-8> PMID: 32382089
- [56] Bao S, Wu YL, Wang X, *et al.* Agriophyllum oligosaccharides ameliorate hepatic injury in type 2 diabetic db/db mice targeting INS-R/IRS-2/PI3K/AKT/PPAR- γ /Glut4 signal pathway. *J Ethnopharmacol* 2020; 257: 112863. <http://dx.doi.org/10.1016/j.jep.2020.112863> PMID: 32302715
- [57] Wei W, Tian H, Fu X, Yao R, Su D. Participates in vertical sleeve gastrectomy for type II diabetes mellitus by regulating TGR5. *Med Sci Monit* 2020; 26: e920628. <http://dx.doi.org/10.12659/MSM.920628> PMID: 32242546
- [58] De Franco E, Saint-Martin C, Brusgaard K, *et al.* Update of variants identified in the pancreatic β -cell K_{ATP} channel genes KCNJ11 and ABCC8 in individuals with congenital hyperinsulinism and diabetes. *Hum Mutat* 2020; 41(5): 884-905. <http://dx.doi.org/10.1002/humu.23995> PMID: 32027066
- [59] Alshaiikh OM, Yoon JY, Chan BA, *et al.* Pancreatic neuroendocrine tumor producing insulin and vasopressin. *Endocr Pathol* 2018; 29(1): 15-20. <http://dx.doi.org/10.1007/s12022-017-9492-5> PMID: 28718084
- [60] Zheng Y, Wu C, Yang J, *et al.* Insulin-like growth factor 1-induced enolase 2 deacetylation by HDAC3 promotes metastasis of pancreatic cancer. *Signal Transduct Target Ther* 2020; 5(1): 53. <http://dx.doi.org/10.1038/s41392-020-0146-6> PMID: 32398667
- [61] Evidence for INS and cardiovascular disease. Open Targets Platform Available from: https://platform.opentargets.org/evidence/ENSG00000254647/EFO_0000319
- [62] Fontbonne AM, Eschwege EM. Insulin and cardiovascular disease: Paris prospective study. *Diabetes Care* 1991; 14(6): 461-9.
- [63] Nabel EG. Cardiovascular disease. *N Engl J Med* 2003; 349(1): 60-72.
- [64] Steinberger J, Moorehead C, Katch V, Rocchini AP. Relationship between insulin resistance and abnormal lipid profile in obese adolescents. *J Pediatr* 1995; 126(5 Pt 1): 690-5. [http://dx.doi.org/10.1016/S0022-3476\(95\)70394-2](http://dx.doi.org/10.1016/S0022-3476(95)70394-2) PMID: 7751990
- [65] Ferreira AP, Oliveira CER, Franca NM. Metabolic syndrome and risk factors for cardiovascular disease in obese children: the relationship with insulin resistance (HOMA-IR). *J Pediatr (Rio J)* 2007; 83(1): 21-6. <http://dx.doi.org/10.2223/JPED.1562> PMID: 17183416
- [66] Ormazabal V, Nair S, Elfeky O, Aguayo C, Salomon C, Zuñiga FA. Association between insulin resistance and the development of cardiovascular disease. *Cardiovasc Diabetol* 2018; 17(1): 122. <http://dx.doi.org/10.1186/s12933-018-0762-4> PMID: 30170598
- [67] Reaven G. Insulin resistance and coronary heart disease in nondiabetic individuals. *Arterioscler Thromb Vasc Biol* 2012; 32(8): 1754-9. <http://dx.doi.org/10.1161/ATVBAHA.111.241885> PMID: 22815340
- [68] Giacco F, Brownlee M. Oxidative stress and diabetic complications. *Circ Res* 2010; 107(9): 1058-70. <http://dx.doi.org/10.1161/CIRCRESAHA.110.223545> PMID: 21030723
- [69] Bornfeldt KE, Tabas I. Insulin resistance, hyperglycemia, and atherosclerosis. *Cell Metab* 2011; 14(5): 575-85. <http://dx.doi.org/10.1016/j.cmet.2011.07.015> PMID: 22055501
- [70] Gast KB, Tjeerdema N, Stijnen T, Smit JWA, Dekkers OM. Insulin resistance and risk of incident cardiovascular events in adults without diabetes: Meta-analysis. *PLoS One* 2012; 7(12): e52036. <http://dx.doi.org/10.1371/journal.pone.0052036> PMID: 23300589
- [71] Sarwar N, Gao P, Seshasai SR, *et al.* Diabetes mellitus, fasting blood glucose concentration, and risk of vascular disease: A collaborative meta-analysis of 102 prospective studies. *Lancet* 2010; 375(9733): 2215-22. [http://dx.doi.org/10.1016/S0140-6736\(10\)60484-9](http://dx.doi.org/10.1016/S0140-6736(10)60484-9) PMID: 20609967
- [72] Sarwar N, Sattar N, Gudnason V, Danesh J. Circulating concentrations of insulin markers and coronary heart disease: A quantitative review of 19 Western prospective studies. *Eur Heart J* 2007; 28(20): 2491-7. <http://dx.doi.org/10.1093/eurheartj/ehm115> PMID: 17513304
- [73] Drinkwater JJ, Davis TME, Davis WA. The relationship between carotid disease and retinopathy in diabetes: A systematic review. *Cardiovasc Diabetol* 2020; 19(1): 54. <http://dx.doi.org/10.1186/s12933-020-01023-6> PMID: 32375803
- [74] Mujaj B, Bos D, Kavousi M, *et al.* Serum insulin levels are associated with vulnerable plaque components in the carotid artery: The Rotterdam Study. *Eur J Endocrinol* 2020; 182(3): 343-50. <http://dx.doi.org/10.1530/EJE-19-0620> PMID: 31958313
- [75] van Hoek I, Hodgkiss-Geere H, Bode EF, *et al.* Associations among echocardiography, cardiac biomarkers, insulin metabolism, morphology, and inflammation in cats with asymptomatic hypertrophic cardiomyopathy. *J Vet Intern Med* 2020; 34(2): 591-9. <http://dx.doi.org/10.1111/jvim.15730> PMID: 32045061
- [76] Chaudhuri A, Janicke D, Wilson MF, *et al.* Anti-inflammatory and profibrinolytic effect of insulin in acute ST-segment-elevation myocardial infarction. *Circulation* 2004; 109(7): 849-54. <http://dx.doi.org/10.1161/01.CIR.0000116762.77804.FC> PMID: 14757687
- [77] Kwon TG, Jang AY, Kim SW, *et al.* Design and rationale of a randomized control trial testing the effectiveness of combined therapy with Statin plus FENO-fibrate and statin alone in non-diabetic, combined dyslipidemia patients with non-intervened intermediate coronary artery disease - STAFENO study. *Trials* 2020; 21(1): 353. <http://dx.doi.org/10.1186/s13063-020-04291-5> PMID: 32321551
- [78] Larsen AH, Jessen N, Nørrelund H, *et al.* A randomised, double-blind, placebo-controlled trial of metformin on myocardial efficiency in insulin-resistant chronic heart failure patients without diabetes. *Eur J Heart Fail* 2020; 22(9): 1628-37.

- <http://dx.doi.org/10.1002/ejhf.1656> PMID: 31863557
- [79] Ohkuma T, Van Gaal L, Shaw W, *et al.* Clinical outcomes with canagliflozin according to baseline body mass index: results from post hoc analyses of the CANVAS Program. *Diabetes Obes Metab* 2020; 22(4): 530-9.
<http://dx.doi.org/10.1111/dom.13920> PMID: 31729107
- [80] Immune system disease profile page. Open Targets Platform. Available from: https://platform.opentargets.org/disease/EFO_0000540
- [81] Medzhitov R, Janeway CA Jr. Innate immunity: impact on the adaptive immune response. *Curr Opin Immunol* 1997; 9(1): 4-9.
[http://dx.doi.org/10.1016/S0952-7915\(97\)80152-5](http://dx.doi.org/10.1016/S0952-7915(97)80152-5) PMID: 9039775
- [82] Eheim A, Medrikova D, Herzig S. Immune cells and metabolic dysfunction. *Semin Immunopathol* 2014; 36(1): 13-25.
<http://dx.doi.org/10.1007/s00281-013-0403-7> PMID: 24212254
- [83] Weisberg SP, McCann D, Desai M, Rosenbaum M, Leibel RL, Ferrante AW Jr. Obesity is associated with macrophage accumulation in adipose tissue. *J Clin Invest* 2003; 112(12): 1796-808.
<http://dx.doi.org/10.1172/JCI200319246> PMID: 14679176
- [84] Morrison MC, Kleemann R. Role of macrophage migration inhibitory factor in obesity, insulin resistance, type 2 diabetes, and associated hepatic co-morbidities: A comprehensive review of human and rodent studies. *Front Immunol* 2015; 6: 308.
<http://dx.doi.org/10.3389/fimmu.2015.00308> PMID: 26124760
- [85] Patel PS, Buras ED, Balasubramanyam A. The role of the immune system in obesity and insulin resistance. *J Obes* 2013; 2013: 616193.
<http://dx.doi.org/10.1155/2013/616193> PMID: 23577240
- [86] Lumeng CN, DelProposto JB, Westcott DJ, Saitiel AR. Phenotypic switching of adipose tissue macrophages with obesity is generated by spatiotemporal differences in macrophage subtypes. *Diabetes* 2008; 57(12): 3239-46.
<http://dx.doi.org/10.2337/db08-0872> PMID: 18829989
- [87] Miyachi Y, Tsuchiya K, Shiba K, *et al.* A reduced M1-like/M2-like ratio of macrophages in healthy adipose tissue expansion during SGLT2 inhibition. *Sci Rep* 2018; 8(1): 16113.
<http://dx.doi.org/10.1038/s41598-018-34305-x> PMID: 30382157
- [88] Shimokawa C, Kato T, Takeuchi T, *et al.* CD8⁺ regulatory T cells are critical in prevention of autoimmune-mediated diabetes. *Nat Commun* 2020; 11(1): 1922.
<http://dx.doi.org/10.1038/s41467-020-15857-x> PMID: 32321922
- [89] Yeo L, Pujol-Autonell I, Baptista R, *et al.* Circulating β cell-specific CD8⁺ T cells restricted by high-risk HLA class I molecules show antigen experience in children with and at risk of type 1 diabetes. *Clin Exp Immunol* 2020; 199(3): 263-77.
<http://dx.doi.org/10.1111/cei.13391> PMID: 31660582
- [90] Kamoda T, Saito T, Kinugasa H, *et al.* A case of Shwachman-Diamond syndrome presenting with diabetes from early infancy. *Diabetes Care* 2005; 28(6): 1508-9.
<http://dx.doi.org/10.2337/diacare.28.6.1508> PMID: 15920082
- [91] Murray BR, Jewell JR, Jackson KJ, Agboola O, Alexander BR, Sharma P. Type III hypersensitivity reaction to subcutaneous insulin preparations in a type 1 diabetic. *J Gen Intern Med* 2017; 32(7): 841-5.
<http://dx.doi.org/10.1007/s11606-017-4037-7> PMID: 28337685
- [92] Li J, Sipple J, Maynard S, *et al.* Fanconi anemia links reactive oxygen species to insulin resistance and obesity. *Antioxid Redox Signal* 2012; 17(8): 1083-98.
<http://dx.doi.org/10.1089/ars.2011.4417> PMID: 22482891
- [93] Cronin CC, Shanahan F. Insulin-dependent diabetes mellitus and coeliac disease. *Lancet* 1997; 349(9058): 1096-7.
[http://dx.doi.org/10.1016/S0140-6736\(96\)09153-2](http://dx.doi.org/10.1016/S0140-6736(96)09153-2) PMID: 9107261
- [94] Vigneri R, Sciacca L, Vigneri P. Rethinking the relationship between insulin and cancer. *Trends Endocrinol Metab* 2020; 31(8): 551-60.
<http://dx.doi.org/10.1016/j.tem.2020.05.004> PMID: 32600959
- [95] Aaronson SA. Growth factors and cancer. *Science* 1991; 254(5035): 1146-53.
<http://dx.doi.org/10.1126/science.1659742>
- [96] Cai W, Sakaguchi M, Kleinridders A, *et al.* Domain-dependent effects of insulin and IGF-1 receptors on signalling and gene expression. *Nat Commun* 2017; 8: 14892.
<http://dx.doi.org/10.1038/ncomms14892> PMID: 28345670
- [97] Malaguamera R, Belfiore A. The insulin receptor: A new target for cancer therapy. *Front Endocrinol (Lausanne)* 2011; 2: 93.
<http://dx.doi.org/10.3389/fendo.2011.00093> PMID: 22654833
- [98] LeRoith D, Roberts CT Jr. The insulin-like growth factor system and cancer. *Cancer Lett* 2003; 195(2): 127-37.
[http://dx.doi.org/10.1016/S0304-3835\(03\)00159-9](http://dx.doi.org/10.1016/S0304-3835(03)00159-9) PMID: 12767520
- [99] Nervous system disease profile page. Open Targets Platform. Available from: https://platform.opentargets.org/disease/EFO_0000618
- [100] Belfiore A, Frasca F, Pandini G, Sciacca L, Vigneri R. Insulin receptor isoforms and insulin receptor/insulin-like growth factor receptor hybrids in physiology and disease. *Endocr Rev* 2009; 30(6): 586-623.
<http://dx.doi.org/10.1210/er.2008-0047> PMID: 19752219
- [101] Ye P, Xing Y, Dai Z, D'Ercole AJ. *In vivo* actions of insulin-like growth factor-I (IGF-I) on cerebellum development in transgenic mice: Evidence that IGF-I increases proliferation of granule cell progenitors. *Brain Res Dev Brain Res* 1996; 95(1): 44-54.
[http://dx.doi.org/10.1016/0165-3806\(96\)00492-0](http://dx.doi.org/10.1016/0165-3806(96)00492-0) PMID: 8873975
- [102] Park CR. Cognitive effects of insulin in the central nervous system. *Neurosci Biobehav Rev* 2001; 25(4): 311-23.
[http://dx.doi.org/10.1016/S0149-7634\(01\)00016-1](http://dx.doi.org/10.1016/S0149-7634(01)00016-1) PMID: 11445137
- [103] Kim B, Feldman EL. Insulin resistance in the nervous system. *Trends Endocrinol Metab* 2012; 23(3): 133-41.
<http://dx.doi.org/10.1016/j.tem.2011.12.004> PMID: 22245457
- [104] O'Kusky JR, Ye P, D'Ercole AJ. Insulin-like growth factor-I promotes neurogenesis and synaptogenesis in the hippocampal dentate gyrus during postnatal development. *J Neurosci* 2000; 20(22): 8435-42.
<http://dx.doi.org/10.1523/JNEUROSCI.20-22-08435.2000> PMID: 11069951
- [105] Poduslo JF, Curran GL, Wengenack TM, Malester B, Duff K. Permeability of proteins at the blood-brain barrier in the normal adult mouse and double transgenic mouse model of Alzheimer's disease. *Neurobiol Dis* 2001; 8(4): 555-67.
<http://dx.doi.org/10.1006/mbdi.2001.0402> PMID: 11493021
- [106] de la Monte SM, Wands JR. Review of insulin and insulin-like growth factor expression, signaling, and malfunction in the central nervous system: Relevance to Alzheimer's disease. *J Alzheimers Dis* 2005; 7(1): 45-61.
<http://dx.doi.org/10.3233/JAD-2005-7106> PMID: 15750214
- [107] de la Monte SM. Insulin resistance and Alzheimer's disease. *BMB Rep* 2009; 42: 475-81.
- [108] Batista AF, Forny-Germano L, Clarke JR, *et al.* The diabetes drug liraglutide reverses cognitive impairment in mice and attenuates insulin receptor and synaptic pathology in a non-human primate model of Alzheimer's disease. *J Pathol* 2018; 245(1): 85-100.
<http://dx.doi.org/10.1002/path.5056> PMID: 29435980
- [109] Ferreira LSS, Fernandes CS, Vieira MNN, De Felice FG. Insulin resistance in Alzheimer's disease. *Front Neurosci* 2018; 12: 830.
<http://dx.doi.org/10.3389/fnins.2018.00830> PMID: 30542257
- [110] De Felice FG, Vieira MN, Bomfim TR, *et al.* Protection of synapses against Alzheimer's-linked toxins: Insulin signaling prevents the pathogenic binding of Abeta oligomers. *Proc Natl Acad Sci USA* 2009; 106(6): 1971-6.
<http://dx.doi.org/10.1073/pnas.0809158106> PMID: 19188609
- [111] Townsend M, Mehta T, Selkoe DJ. Soluble Abeta inhibits specific signal transduction cascades common to the insulin receptor pathway. *J Biol Chem* 2007; 282(46): 33305-12.
<http://dx.doi.org/10.1074/jbc.M610390200> PMID: 17855343
- [112] Bomfim TR, Forny-Germano L, Sathler LB, *et al.* An anti-diabetes agent protects the mouse brain from defective insulin signaling caused by Alzheimer's disease-associated A β oligomers. *J Clin Invest* 2012; 122(4): 1339-53.
<http://dx.doi.org/10.1172/JCI57256> PMID: 22476196
- [113] Sebastião I, Candeias E, Santos MS, de Oliveira CR, Moreira PI, Duarte AI. Insulin as a bridge between type 2 diabetes and Alzheimer disease - how anti-diabetics could be a solution for dementia. *Front Endocrinol (Lausanne)* 2014; 5: 110.
<http://dx.doi.org/10.3389/fendo.2014.00110> PMID: 25071725
- [114] Lourenco MV, Clarke JR, Frozza RL, *et al.* TNF- α mediates PKR-dependent memory impairment and brain IRS-1 inhibition induced

- by Alzheimer's β -amyloid oligomers in mice and monkeys. *Cell Metab* 2013; 18(6): 831-43.
<http://dx.doi.org/10.1016/j.cmet.2013.11.002> PMID: 24315369
- [115] Tai J, Liu W, Li Y, Li L, Hölscher C. Neuroprotective effects of a triple GLP-1/GIP/glucagon receptor agonist in the APP/PS1 transgenic mouse model of Alzheimer's disease. *Brain Res* 2018; 1678: 64-74.
<http://dx.doi.org/10.1016/j.brainres.2017.10.012> PMID: 29050859
- [116] Faheem A, Rehman K, Jabeen K, Akash MSH. Nicotine-mediated upregulation of microRNA-141 expression determines adipokine-intervened insulin resistance. *Environ Toxicol Pharmacol* 2020; 80: 103506.
<http://dx.doi.org/10.1016/j.etap.2020.103506> PMID: 33002592
- [117] Cerecedo-Lopez CD, Cantu-Aldana A, Patel NJ, Aziz-Sultan MA, Frerichs KU, Du R. Insulin in the management of acute ischemic stroke: A systematic review and meta-analysis. *World Neurosurg* 2020; 136: e514-34.
<http://dx.doi.org/10.1016/j.wneu.2020.01.056> PMID: 31954893
- [118] Ryan AS, Hafer-Macko C, Ortmeyer HK. Insulin resistance in skeletal muscle of chronic stroke. *Brain Sci* 2021; 11(1): 20. PMID: 33375333
- [119] Koslow SH, Stokes PE, Mendels J, Ramsey A, Casper R. Insulin tolerance test: human growth hormone response and insulin resistance in primary unipolar depressed, bipolar depressed and control subjects. *Psychol Med* 1982; 12(1): 45-55.
<http://dx.doi.org/10.1017/S0033291700043270> PMID: 7043520
- [120] Corica G, Ceraudo M, Campana C, *et al.* Octreotide-resistant acromegaly: Challenges and solutions. *Ther Clin Risk Manag* 2020; 16: 379-91.
<http://dx.doi.org/10.2147/TCRM.S183360> PMID: 32440136
- [121] Guerreiro V, Bernardes I, Pereira J *et al.* Acromegaly with congenital generalized lipodystrophy - Two rare insulin resistance conditions in one patient: A case report. *J Med Case Rep* 2020; 14: 34.
<http://dx.doi.org/10.1186/s13256-020-2352-9>
- [122] Peng S, Yang J, Wang Y, *et al.* Low-dose intranasal insulin improves cognitive function and suppresses the development of epilepsy. *Brain Res* 2020; 1726: 146474.
<http://dx.doi.org/10.1016/j.brainres.2019.146474> PMID: 31557476
- [123] Ellis B, Arsiwalla D. The moderating role of anxiety in the associations between sleep and insulin resistance. CSBS INSPiRE Student Res Engagem Conf 2020. Available from: <https://scholarworks.uni.edu/csbsresearchconf/2020/all/73>
- [124] Rodríguez-Rabassa M, López P, Sánchez R, *et al.* Inflammatory biomarkers, microbiome, depression, and executive dysfunction in alcohol users. *Int J Environ Res Public Health* 2020; 17(3): E689.
<http://dx.doi.org/10.3390/ijerph17030689> PMID: 31973090
- [125] McDonald TS, Kumar V, Fung JN, Woodruff TM, Lee JD. Glucose clearance and uptake is increased in the SOD1^{G93A} mouse model of amyotrophic lateral sclerosis through an insulin-independent mechanism. *FASEB J* 2021; 35(7): e21707.
<http://dx.doi.org/10.1096/fj.202002450R> PMID: 34118098
- [126] Toth C, Brussee V, Martinez JA, McDonald D, Cunningham FA, Zochodne DW. Rescue and regeneration of injured peripheral nerve axons by intrathecal insulin. *Neuroscience* 2006; 139(2): 429-49.
<http://dx.doi.org/10.1016/j.neuroscience.2005.11.065> PMID: 16529870
- [127] Brener A, Sagi L, Shtamler A, Levy S, Fattal-Valevski A, Leventhal Y. Insulin-like growth factor-1 status is associated with insulin resistance in young patients with spinal muscular atrophy. *Neuromuscul Disord* 2020; 30(11): 888-96.
<http://dx.doi.org/10.1016/j.nmd.2020.09.025> PMID: 33071067
- [128] Genetic, familial or congenital disease profile page. Open Targets Platform Available from: https://platform.opentargets.org/disease/OTAR_0000018
- [129] Zambon AA, Muntoni F. Congenital muscular dystrophies: What is new? *Neuromuscul Disord* 2021; 31(10): 931-42.
<http://dx.doi.org/10.1016/j.nmd.2021.07.009> PMID: 34470717
- [130] Lindhurst MJ, Parker VER, Payne F, *et al.* Mosaic overgrowth with fibroadipose hyperplasia is caused by somatic activating mutations in PIK3CA. *Nat Genet* 2012; 44(8): 928-33.
<http://dx.doi.org/10.1038/ng.2332> PMID: 22729222
- [131] Mori M, Kumada T, Inoue K, *et al.* Ketogenic diet for refractory epilepsy with MEHMO syndrome: Caution for acute necrotizing pancreatitis. *Brain Dev* 2021; 43(6): 724-8.
<http://dx.doi.org/10.1016/j.braindev.2021.02.002> PMID: 33714664
- [132] Auer MK, Birnbaum W, Hartmann MF, *et al.* Metabolic effects of estradiol *versus* testosterone in complete androgen insensitivity syndrome. *Endocrine* 2022.
<http://dx.doi.org/10.1007/s12020-022-03017-8>
- [133] Baker LA, Nef S, Nguyen MT, *et al.* The insulin-3 gene: lack of a genetic basis for human cryptorchidism. *J Urol* 2002; 167(6): 2534-7.
[http://dx.doi.org/10.1016/S0022-5347\(05\)65029-X](http://dx.doi.org/10.1016/S0022-5347(05)65029-X) PMID: 11992081
- [134] Kanaka-Gantenbein C, Kitsiou S, Mavrou A, *et al.* Tall stature, insulin resistance, and disturbed behavior in a girl with the triple X syndrome harboring three SHOX genes: Offspring of a father with mosaic Klinefelter syndrome but with two maternal X chromosomes. *Horm Res* 2004; 61(5): 205-10. PMID: 14752208
- [135] Rasio E, Antaki A, Van Campenhout J. Diabetes mellitus in gonadal dysgenesis: studies of insulin and growth hormone secretion. *Eur J Clin Invest* 1976; 6(1): 59-66.
<http://dx.doi.org/10.1111/j.1365-2362.1976.tb00494.x> PMID: 1253808
- [136] Musculoskeletal or connective tissue disease profile page. Open Targets Platform Available from: https://platform.opentargets.org/disease/OTAR_0000006
- [137] DeFronzo RA, Tripathy D. Skeletal muscle insulin resistance is the primary defect in type 2 diabetes. *Diabetes Care* 2009; 32(Suppl. 2): S157-63.
<http://dx.doi.org/10.2337/dc09-S302> PMID: 19875544
- [138] Garneau L, Aguer C. Role of myokines in the development of skeletal muscle insulin resistance and related metabolic defects in type 2 diabetes. *Diabetes Metab* 2019; 45(6): 505-16.
<http://dx.doi.org/10.1016/j.diabet.2019.02.006> PMID: 30844447
- [139] Jabłońska K, Mołęda P, Safranow K, Majkowska L. Rapid-acting and regular insulin are equal for high fat-protein meal in individuals with type 1 diabetes treated with multiple daily injections. *Diabetes Ther* 2018; 9(1): 339-48.
<http://dx.doi.org/10.1007/s13300-017-0364-2> PMID: 29344829
- [140] Avery H. Insulin fat atrophy a traumatic atrophic panniculitis. *BMJ* 1929; 1(3560): 597-9.
<http://dx.doi.org/10.1136/bmj.1.3560.597-a> PMID: 20774578
- [141] Shigematsu Y, Hamada M, Nagai T, *et al.* Risk for atrial fibrillation in patients with hypertrophic cardiomyopathy: Association with insulin resistance. *J Cardiol* 2011; 58(1): 18-25.
<http://dx.doi.org/10.1016/j.jjcc.2011.03.001> PMID: 21515029
- [142] Cannarella R, Barbagallo F, Condorelli RA, Aversa A, La Vignera S, Calogero AE. Osteoporosis from an endocrine perspective: The role of hormonal changes in the elderly. *J Clin Med* 2019; 8(10): E1564.
<http://dx.doi.org/10.3390/jcm8101564> PMID: 31581477
- [143] Xia J, Zhong Y, Huang G, Chen Y, Shi H, Zhang Z. The relationship between insulin resistance and osteoporosis in elderly male type 2 diabetes mellitus and diabetic nephropathy. *Ann Endocrinol (Paris)* 2012; 73(6): 546-51.
<http://dx.doi.org/10.1016/j.ando.2012.09.009>
- [144] Prill H, Luu A, Yip B, *et al.* Differential uptake of NAGLU-IGF2 and unmodified NAGLU in cellular models of Sanfilippo syndrome type B. *Mol Ther Methods Clin Dev* 2019; 14: 56-63.
<http://dx.doi.org/10.1016/j.omtm.2019.05.008> PMID: 31309128
- [145] Muniyappa R, Warren MA, Zhao X, *et al.* Reduced insulin sensitivity in adults with pseudohypoparathyroidism type 1a. *J Clin Endocrinol Metab* 2013; 98(11): E1796-801.
<http://dx.doi.org/10.1210/jc.2013-1594> PMID: 24030943
- [146] Liu J, Liu W, Li H, *et al.* Identification of key genes and pathways associated with cholangiocarcinoma development based on weighted gene correlation network analysis. *PeerJ* 2019; 7: e7968.
<http://dx.doi.org/10.7717/peerj.7968> PMID: 31687280
- [147] Liu G, Liu S, Xing G, Wang F. IncRNA PVT1/MicroRNA-17-5p/PTEN axis regulates secretion of E2 and P4, proliferation, and apoptosis of ovarian granulosa cells in PCOS. *Mol Ther Nucleic Acids* 2020; 20: 205-16.
<http://dx.doi.org/10.1016/j.omtn.2020.02.007> PMID: 32179451

- [148] Devis-Jauregui L, Eritija N, Davis ML, Matias-Guiu X, Llobet-Navàs D. Autophagy in the physiological endometrium and cancer. *Autophagy* 2021; 17(5): 1077-95. <http://dx.doi.org/10.1080/15548627.2020.1752548> PMID: 32401642
- [149] Pugliese G, Penno G, Natali A, *et al.* Diabetic kidney disease: new clinical and therapeutic issues. Joint position statement of the Italian Diabetes Society and the Italian Society of Nephrology on "The natural history of diabetic kidney disease and treatment of hyperglycemia in patients with type 2 diabetes and impaired renal function". *J Nephrol* 2020; 33(1): 9-35. <http://dx.doi.org/10.1007/s40620-019-00650-x> PMID: 31576500
- [150] Kukla A, Hill J, Merzkani M, *et al.* The use of GLP1R agonists for the treatment of type 2 diabetes in kidney transplant recipients. *Transplant Direct* 2020; 6(2): e524. <http://dx.doi.org/10.1097/TXD.0000000000000971> PMID: 32095510
- [151] Ratnakumar A, Weinhold N, Mar JC, Riaz N. Protein-Protein interactions uncover candidate 'core genes' within omnigenic disease networks. *PLoS Genet* 2020; 16(7): e1008903. <http://dx.doi.org/10.1371/journal.pgen.1008903> PMID: 32678846
- [152] Gao W, Guo N, Zhao S, *et al.* Carboxypeptidase A4 promotes cardiomyocyte hypertrophy through activating PI3K-AKT-mTOR signaling. *Biosci Rep* 2020; 40(5): BSR20200669. <http://dx.doi.org/10.1042/BSR20200669> PMID: 32347291
- [153] Meerson A. Leptin-responsive MiR-4443 is a small regulatory RNA independent of the canonic microRNA biogenesis pathway. *Biomolecules* 2020; 10(2): E293. <http://dx.doi.org/10.3390/biom10020293> PMID: 32069948
- [154] Kern W, Stange EF, Fehm HL, Klein HH. Glucocorticoid-induced diabetes mellitus in gastrointestinal diseases TT - Glucocorticoid-induzierter Diabetes mellitus bei gastroenterologischen Erkrankungen. *Z Gastroenterol* 1999.
- [155] Kaaks R. Nutrition, hormones, and breast cancer: Is insulin the missing link? *Cancer Causes Control* 1996; 7(6): 605-25. <http://dx.doi.org/10.1007/BF00051703> PMID: 8932921
- [156] Pellegrino M, Traversi G, Arena A, *et al.* Effect of p53 activation through targeting MDM2/MDM4 heterodimer on T regulatory and effector cells in the peripheral blood of Type 1 diabetes patients. *PLoS One* 2020; 15(1): e0228296. <http://dx.doi.org/10.1371/journal.pone.0228296> PMID: 31995625
- [157] Rose DP, Komninou D, Stephenson GD. Obesity, adipocytokines, and insulin resistance in breast cancer. *Obes Rev* 2004; 5(3): 153-65. <http://dx.doi.org/10.1111/j.1467-789X.2004.00142.x> PMID: 15245384
- [158] Bruning PF, Bonfrère JMG, van Noord PAH, Hart AAM, de Jong-Bakker M, Nooijen WJ. Insulin resistance and breast-cancer risk. *Int J Cancer* 1992; 52(4): 511-6. <http://dx.doi.org/10.1002/ijc.2910520402> PMID: 1399128
- [159] Papa V, Pezzino V, Costantino A, *et al.* Elevated insulin receptor content in human breast cancer. *J Clin Invest* 1990; 86(5): 1503-10. <http://dx.doi.org/10.1172/JCI114868> PMID: 2243127
- [160] Lee J, Chang Y, Kim Y, Park B, Ryu S. Insulin resistance and the development of breast cancer in premenopausal women: The Kangbuk Samsung Health Study. *Breast Cancer Res Treat* 2022; 192(2): 401-9. <http://dx.doi.org/10.1007/s10549-022-06513-7> PMID: 34997879
- [161] Barbieri M, Ragno E, Benvenuti E, *et al.* New aspects of the insulin resistance syndrome: Impact on haematological parameters. *Diabetologia* 2001; 44(10): 1232-7. <http://dx.doi.org/10.1007/s0012501100634> PMID: 11692171
- [162] Niklasson B, Hörnfeldt B, Lundman B. Could myocarditis, insulin-independent diabetes mellitus, and Guillain-Barré syndrome be caused by one or more infectious agents carried by rodents? *Emerg Infect Dis* 1998; 4(2): 187-93. <http://dx.doi.org/10.3201/eid0402.980206> PMID: 9621189
- [163] Maeno T, Okumura A, Ishikawa T, *et al.* Mechanisms of increased insulin resistance in non-cirrhotic patients with chronic hepatitis C virus infection. *J Gastroenterol Hepatol* 2003; 18(12): 1358-63. <http://dx.doi.org/10.1046/j.1440-1746.2003.03179.x> PMID: 14675263
- [164] Bisschop PH, de Rooij SE, Zwinderman AH, van Oosten HE, van Munster BC. Cortisol, insulin, and glucose and the risk of delirium in older adults with hip fracture. *J Am Geriatr Soc* 2011; 59(9): 1692-6. <http://dx.doi.org/10.1111/j.1532-5415.2011.03575.x> PMID: 21883119
- [165] Amgarth-Duff I, Hosie A, Caplan G, Agar M. A systematic review of the overlap of fluid biomarkers in delirium and advanced cancer-related syndromes. *BMC Psychiatry* 2020; 20(1): 182. <http://dx.doi.org/10.1186/s12888-020-02584-2> PMID: 32321448
- [166] Association AD. Diagnosis and classification of diabetes mellitus. *Diabetes Care* 2010; 33: S62-9.
- [167] Inzucchi SE. Clinical practice. Diagnosis of diabetes. *N Engl J Med* 2012; 367(6): 542-50. <http://dx.doi.org/10.1056/NEJMcpl103643> PMID: 22873534
- [168] Mantzoros C. Insulin resistance: Definition and clinical spectrum. *UpToDate* 2018.
- [169] Banting FG, Best CH, Collip JB, Campbell WR, Fletcher AA. Pancreatic extracts in the treatment of diabetes mellitus. 1922. *Indian. J Med Res* 2007; 125(3): 141-6. PMID: 17580419
- [170] Haeusler RA, McGraw TE, Accili D. Metabolic Signalling: Biochemical and cellular properties of insulin receptor signalling. *Nat Rev Mol Cell Biol* 2018; 19: 31-44.
- [171] Himsworth HP. Diabetes mellitus. Its differentiation into insulin-sensitive and insulin-insensitive types. *Lancet* 1936; 230: 127-30. [http://dx.doi.org/10.1016/S0140-6736\(01\)36134-2](http://dx.doi.org/10.1016/S0140-6736(01)36134-2)
- [172] Hagedorn HC. Protamine Insulinate. *Proc R Soc Med* 1937; 30(6): 805-14. <http://dx.doi.org/10.1177/003591573703000643> PMID: 19991109
- [173] Siddiqui H, Scupola A. User involvement in R&D at novo nordisk diabetes treatment development. Available from: https://rucforsk.ruc.dk/ws/portalfiles/portal/64978123/Master_Thesis_2019_Helmand_Turu.pdf
- [174] Odegard PS, Capoccia KL. Inhaled insulin: Exubera. *Ann Pharmacother* 2005; 39(5): 843-53.
- [175] White S, Bennett DB, Cheu S, *et al.* EXUBERA: pharmaceutical development of a novel product for pulmonary delivery of insulin. *Diabetes Technol Ther* 2005; 7(6): 896-906. <http://dx.doi.org/10.1089/dia.2005.7.896> PMID: 16386095
- [176] Bailey CJ, Barnett AH. Why is Exubera being withdrawn? *BMJ* 2007; 335: 1156. <http://dx.doi.org/10.1136/bmj.39409.507662.94>
- [177] Monami M, Mannucci E. Efficacy and safety of degludec insulin: A meta-analysis of randomised trials. *Curr Med Res Opin* 2013; 29(4): 339-42. <http://dx.doi.org/10.1185/03007995.2013.772507> PMID: 23368895
- [178] De Jesus DF, Kulkarni RN. "Omics" and "epi-omics" underlying the β -cell adaptation to insulin resistance. *Mol Metab* 2019; 27S: S42-8. <http://dx.doi.org/10.1016/j.molmet.2019.06.003> PMID: 31500830
- [179] Grant SFA, Thorleifsson G, Reynisdottir I, *et al.* Variant of transcription factor 7-like 2 (TCF7L2) gene confers risk of type 2 diabetes. *Nat Genet* 2006; 38(3): 320-3. <http://dx.doi.org/10.1038/ng1732> PMID: 16415884
- [180] Altshuler D, Hirschhorn JN, Klannemark M, *et al.* The common PPAR γ Pro12Ala polymorphism is associated with decreased risk of type 2 diabetes. *Nat Genet* 2000; 26(1): 76-80. <http://dx.doi.org/10.1038/79216> PMID: 10973253
- [181] Mitchell RK, Mondragon A, Chen L, *et al.* Selective disruption of Tcf7l2 in the pancreatic β cell impairs secretory function and lowers β cell mass. *Hum Mol Genet* 2015; 24(5): 1390-9. <http://dx.doi.org/10.1093/hmg/ddu553> PMID: 25355422
- [182] Scott LJ, Mohlke KL, Bonnycastle LL, *et al.* A genome-wide association study of type 2 diabetes in finns detects multiple susceptibility variants. *Science* 2007; 316(5829): 1341-5. <http://dx.doi.org/10.1126/science.1142382>
- [183] Consortium WTCC, Burton PR, Donnelly P, *et al.* Genome-wide association study of 14,000 cases of seven common diseases and 3,000 shared controls. *Nature* 2007; 447(7145): 661-78. <http://dx.doi.org/10.1038/nature05911> PMID: 17554300
- [184] Saxena R, Voight BF, Lyssenko V, *et al.* Genome-wide association analysis identifies loci for type 2 diabetes and triglyceride levels. *Science* 2007; 316(5829): 1331-6. <http://dx.doi.org/10.1126/science.1142358>

- [185] Davidson HW, Wenzlau JM, O'Brien RM. Zinc transporter 8 (ZnT8) and β cell function. *Trends Endocrinol Metab* 2014; 25(8): 415-24.
<http://dx.doi.org/10.1016/j.tem.2014.03.008> PMID: 24751356
- [186] Syring KE, Boortz KA, Oeser JK, *et al.* Combined deletion of Slc30a7 and Slc30a8 unmasks a critical role for ZnT8 in glucose-stimulated insulin secretion. *Endocrinology* 2016; 157(12): 4534-41.
<http://dx.doi.org/10.1210/en.2016-1573> PMID: 27754787
- [187] Ayers K, Kumar R, Robevska G, *et al.* Familial bilateral cryptorchidism is caused by recessive variants in *RXFP2*. *J Med Genet* 2019; 56(11): 727-33.
<http://dx.doi.org/10.1136/jmedgenet-2019-106203> PMID: 31167797
- [188] Cannon ME, Currin KW, Young KL, *et al.* Open chromatin profiling in adipose tissue marks genomic regions with functional roles in cardiometabolic traits. *G3 (Bethesda)* 2019; 9(8): 2521-33.
- [189] Tekola-Ayele F, Lee A, Workalemahu T, *et al.* Genetic overlap between birthweight and adult cardiometabolic diseases has implications for genomic medicine. *Sci Rep* 2019; 9(1): 4076.
<http://dx.doi.org/10.1038/s41598-019-40834-w> PMID: 30858448
- [190] Harrison sm, Bush nc, Wang y, *et al.* Insulin-like peptide 3 (insl3) serum concentration during human male fetal life. *Front Endocrinol (Lausanne)* 2019; 10: 596.
<http://dx.doi.org/10.3389/fendo.2019.00596> PMID: 31611843
- [191] Zhu Z, Zhang F, Hu H, *et al.* Integration of summary data from GWAS and eQTL studies predicts complex trait gene targets. *Nat Genet* 2016; 48(5): 481-7.
<http://dx.doi.org/10.1038/ng.3538> PMID: 27019110
- [192] Wu Y, Zeng J, Zhang F, *et al.* Integrative analysis of omics summary data reveals putative mechanisms underlying complex traits. *Nat Commun* 2018; 9(1): 918.
<http://dx.doi.org/10.1038/s41467-018-03371-0> PMID: 29500431
- [193] Xue A, Wu Y, Zhu Z, *et al.* Genome-wide association analyses identify 143 risk variants and putative regulatory mechanisms for type 2 diabetes. *Nat Commun* 2018; 9(1): 2941.
<http://dx.doi.org/10.1038/s41467-018-04951-w> PMID: 30054458
- [194] Jaspers S, Lok S, Lofton-Day CE, *et al.* The genomics of Insulin 5. In: Tregear GW, Ivell R, Bathgate RA, Wade JD, Eds. *Relaxin 2000*. Dordrecht: Springer, 2001; pp. 363-9.
http://dx.doi.org/10.1007/978-94-017-2877-5_61
- [195] Bhandare R, Schug J, Le Lay J, *et al.* Genome-wide analysis of histone modifications in human pancreatic islets. *Genome Res* 2010; 20(4): 428-33.
<http://dx.doi.org/10.1101/gr.102038.109> PMID: 20181961
- [196] Khetan S, Kursawe R, Youn A, *et al.* Type 2 diabetes-associated genetic variants regulate chromatin accessibility in human islets. *Diabetes* 2018; 67(11): 2466-77.
<http://dx.doi.org/10.2337/db18-0393>
- [197] Raurell-Vila H, Ramos-Rodríguez M, Pasquali L. Assay for transposase accessible chromatin (ATAC-Seq) to chart the open chromatin landscape of human Pancreatic Islets. *Methods Mol Biol* 2018; 1766: 197-208.
- [198] Gao T, McKenna B, Li C, *et al.* Pdx1 maintains β cell identity and function by repressing an α cell program. *Cell Metab* 2014; 19(2): 259-71.
<http://dx.doi.org/10.1016/j.cmet.2013.12.002> PMID: 24506867
- [199] Parveen N, Dhawan S. DNA methylation patterning and the regulation of beta cell homeostasis. *Front Endocrinol (Lausanne)* 2021; 12: 651258.
<http://dx.doi.org/10.3389/fendo.2021.651258> PMID: 34025578
- [200] LaPierre MP, Stoffel M. MicroRNAs as stress regulators in pancreatic beta cells and diabetes. *Mol Metab* 2017; 6(9): 1010-23.
<http://dx.doi.org/10.1016/j.molmet.2017.06.020> PMID: 28951825
- [201] Frost RJA, Olson EN. Control of glucose homeostasis and insulin sensitivity by the Let-7 family of microRNAs. *Proc Natl Acad Sci USA* 2011; 108(52): 21075-80.
<http://dx.doi.org/10.1073/pnas.1118922109> PMID: 22160727
- [202] Motterle A, Gattesco S, Peyot ML, *et al.* Identification of islet-enriched long non-coding RNAs contributing to β -cell failure in type 2 diabetes. *Mol Metab* 2017; 6(11): 1407-18.
<http://dx.doi.org/10.1016/j.molmet.2017.08.005> PMID: 29107288
- [203] Singer RA, Sussel L. Islet long noncoding RNAs: A playbook for discovery and characterization. *Diabetes* 2018; 67(8): 1461-70.
<http://dx.doi.org/10.2337/dbi18-0001> PMID: 29937433
- [204] Poy MN, Hausser J, Trajkovski M, *et al.* miR-375 maintains normal pancreatic alpha- and beta-cell mass. *Proc Natl Acad Sci USA* 2009; 106(14): 5813-8.
<http://dx.doi.org/10.1073/pnas.0810550106> PMID: 19289822
- [205] De Jesus DF, Kulkarni RN. Epigenetic modifiers of islet function and mass. *Trends Endocrinol Metab* 2014; 25(12): 628-36.
<http://dx.doi.org/10.1016/j.tem.2014.08.006> PMID: 25246382
- [206] Ling C, Del Guerra S, Lupi R, *et al.* Epigenetic regulation of PPARGC1A in human type 2 diabetic islets and effect on insulin secretion. *Diabetologia* 2008; 51(4): 615-22.
<http://dx.doi.org/10.1007/s00125-007-0916-5> PMID: 18270681
- [207] Sachdeva MM, Claiborn KC, Khoo C, *et al.* Pdx1 (MODY4) regulates pancreatic beta cell susceptibility to ER stress. *Proc Natl Acad Sci USA* 2009; 106(45): 19090-5.
<http://dx.doi.org/10.1073/pnas.0904849106> PMID: 19855005
- [208] Stoffers DA, Zinkin NT, Stanojevic V, Clarke WL, Habener JF. Pancreatic agenesis attributable to a single nucleotide deletion in the human IPF1 gene coding sequence. *Nat Genet* 1997; 15(1): 106-10.
<http://dx.doi.org/10.1038/ng0197-106> PMID: 8988180
- [209] Volkmar M, Dedeurwaerder S, Cunha DA, *et al.* DNA methylation profiling identifies epigenetic dysregulation in pancreatic islets from type 2 diabetic patients. *EMBO J* 2012; 31(6): 1405-26.
<http://dx.doi.org/10.1038/emboj.2011.503> PMID: 22293752
- [210] Yang BT, Dayeh TA, Kirkpatrick CL, *et al.* Insulin promoter DNA methylation correlates negatively with insulin gene expression and positively with HbA1c levels in human pancreatic islets. *Diabetologia* 2011; 54: 360-7.
<http://dx.doi.org/10.1007/s00125-010-1967-6>
- [211] Volkov P, Bacos K, Ofori JK, *et al.* Whole-Genome bisulfite sequencing of human pancreatic islets reveals novel differentially methylated regions in type 2 diabetes pathogenesis. *Diabetes* 2017; 66(4): 1074-85.
<http://dx.doi.org/10.2337/db16-0996> PMID: 28052964
- [212] Willmer T, Johnson R, Louw J, Pfeiffer C. Blood-based DNA methylation biomarkers for type 2 diabetes: Potential for clinical applications. *Front Endocrinol (Lausanne)* 2018; 9: 744.
<http://dx.doi.org/10.3389/fendo.2018.00744> PMID: 30564199
- [213] Gunton JE, Kulkarni RN, Yim S, *et al.* ARNT/HIF1beta mediates altered gene expression and pancreatic-islet dysfunction in human type 2 diabetes. *Cell* 2005; 122(3): 337-49.
<http://dx.doi.org/10.1016/j.cell.2005.05.027> PMID: 16096055
- [214] Marselli L, Thorne J, Dahiya S, *et al.* Gene expression profiles of Beta-cell enriched tissue obtained by laser capture microdissection from subjects with type 2 diabetes. *PLoS One* 2010; 5(7): e11499.
<http://dx.doi.org/10.1371/journal.pone.0011499> PMID: 20644627
- [215] Fadista J, Vikman P, Laakso EO, *et al.* Global genomic and transcriptomic analysis of human pancreatic islets reveals novel genes influencing glucose metabolism. *Proc Natl Acad Sci USA* 2014; 111(38): 13924-9.
<http://dx.doi.org/10.1073/pnas.1402665111> PMID: 25201977
- [216] Bader E, Migliorini A, Gegg M, *et al.* Identification of proliferative and mature β -cells in the islets of Langerhans. *Nature* 2016; 535(7612): 430-4.
<http://dx.doi.org/10.1038/nature18624> PMID: 27398620
- [217] Dorrell C, Schug J, Canaday PS, *et al.* Human islets contain four distinct subtypes of β cells. *Nat Commun* 2016; 7: 11756.
<http://dx.doi.org/10.1038/ncomms11756> PMID: 27399229
- [218] Williams MD, Joglekar MV, Satoor SN, *et al.* Epigenetic and transcriptome profiling identifies a population of visceral adipose-derived progenitor cells with the potential to differentiate into an endocrine pancreatic lineage. *Cell Transplant* 2019; 28(1): 89-104.
<http://dx.doi.org/10.1177/0963689718808472> PMID: 30376726
- [219] Xin Y, Kim J, Okamoto H, *et al.* RNA sequencing of single human islet cells reveals type 2 diabetes genes. *Cell Metab* 2016; 24(4): 608-15.
<http://dx.doi.org/10.1016/j.cmet.2016.08.018> PMID: 27667665
- [220] Segerstolpe Å, Palasantza A, Eliasson P, *et al.* Single-cell transcriptome profiling of human pancreatic islets in health and type 2 diabetes. *Cell Metab* 2016; 24(4): 593-607.
<http://dx.doi.org/10.1016/j.cmet.2016.08.020> PMID: 27667667
- [221] Lawlor N, George J, Bolisetty M, *et al.* Single-cell transcriptomes identify human islet cell signatures and reveal cell-type-specific

- expression changes in type 2 diabetes. *Genome Res* 2017; 27(2): 208-22.
<http://dx.doi.org/10.1101/gr.212720.116> PMID: 27864352
- [222] Arystarkhova E, Liu YB, Salazar C, *et al.* Hyperplasia of pancreatic beta cells and improved glucose tolerance in mice deficient in the FXD2 subunit of Na,K-ATPase. *J Biol Chem* 2013; 288(10): 7077-85.
<http://dx.doi.org/10.1074/jbc.M112.401190> PMID: 23344951
- [223] Nachtergaele S, He C. Chemical modifications in the life of an mRNA transcript. *Annu Rev Genet* 2018; 52: 349-72.
<http://dx.doi.org/10.1146/annurev-genet-120417-031522> PMID: 30230927
- [224] Desrosiers R, Friderici K, Rottman F. Identification of methylated nucleosides in messenger RNA from Novikoff hepatoma cells. *Proc Natl Acad Sci USA* 1974; 71(10): 3971-5.
<http://dx.doi.org/10.1073/pnas.71.10.3971> PMID: 4372599
- [225] Lavi S, Shatkin AJ. Methylated simian virus 40-specific RNA from nuclei and cytoplasm of infected BSC-1 cells. *Proc Natl Acad Sci USA* 1975; 72(6): 2012-6.
<http://dx.doi.org/10.1073/pnas.72.6.2012> PMID: 166375
- [226] Zheng G, Dahl JA, Niu Y, *et al.* ALKBH5 is a mammalian RNA demethylase that impacts RNA metabolism and mouse fertility. *Mol Cell* 2013; 49(1): 18-29.
<http://dx.doi.org/10.1016/j.molcel.2012.10.015> PMID: 23177736
- [227] Jia G, Fu Y, Zhao X, *et al.* N6-methyladenosine in nuclear RNA is a major substrate of the obesity-associated FTO. *Nat Chem Biol* 2011; 7(12): 885-7.
<http://dx.doi.org/10.1038/nchembio.687> PMID: 22002720
- [228] Roignant JY, Soller M. m⁶A in mRNA: An ancient mechanism for fine-tuning gene expression. *Trends Genet* 2017; 33(6): 380-90.
<http://dx.doi.org/10.1016/j.tig.2017.04.003> PMID: 28499622
- [229] Nedelkov D, Niederkofler EE, Oran PE, Peterman S, Nelson RW. Top-down mass spectrometric immunoassay for human insulin and its therapeutic analogs. *J Proteomics* 2018; 175: 27-33.
<http://dx.doi.org/10.1016/j.jprot.2017.08.001> PMID: 28780057
- [230] Marks V, Teale JD. Investigation of hypoglycaemia. *Clin Endocrinol (Oxf)* 1996; 44(2): 133-6.
<http://dx.doi.org/10.1046/j.1365-2265.1996.659478.x> PMID: 8849564
- [231] Brackenridge A, Wallbank H, Lawrenson RA, Russell-Jones D. Emergency management of diabetes and hypoglycaemia. *Emerg Med J* 2006; 23(3): 183-5.
<http://dx.doi.org/10.1136/emj.2005.026252> PMID: 16498153
- [232] Kristensen PL, Hansen LS, Jespersen MJ, *et al.* Insulin analogues and severe hypoglycaemia in type 1 diabetes. *Diabetes Res Clin Pract* 2012; 96(1): 17-23.
<http://dx.doi.org/10.1016/j.diabres.2011.10.046> PMID: 22136722
- [233] Sonksen PH. Insulin, growth hormone and sport. *J Endocrinol* 2001; 170(1): 13-25.
<http://dx.doi.org/10.1677/joe.0.1700013> PMID: 11431133
- [234] Marks V, Wark G. Forensic aspects of insulin. *Diabetes Res Clin Pract* 2013; 101(3): 248-54.
<http://dx.doi.org/10.1016/j.diabres.2013.05.002> PMID: 23751444
- [235] Parfitt C, Church D, Armston A, *et al.* Commercial insulin immunoassays fail to detect commonly prescribed insulin analogues. *Clin Biochem* 2015; 48(18): 1354-7.
<http://dx.doi.org/10.1016/j.clinbiochem.2015.07.017> PMID: 26171976
- [236] Blackburn M. Advances in the quantitation of therapeutic insulin analogues by LC-MS/MS. *Bioanalysis* 2013; 5(23): 2933-46.
<http://dx.doi.org/10.4155/bio.13.257> PMID: 24295119
- [237] Sundsten T, Ortsäter H. Proteomics in diabetes research. *Mol Cell Endocrinol* 2009; 297(1-2): 93-103.
<http://dx.doi.org/10.1016/j.mce.2008.06.018> PMID: 18657591
- [238] Mitok KA, Freiburger EC, Schueler KL, *et al.* Islet proteomics reveals genetic variation in dopamine production resulting in altered insulin secretion. *J Biol Chem* 2018; 293(16): 5860-77.
<http://dx.doi.org/10.1074/jbc.RA117.001102> PMID: 29496998
- [239] Larsson S, Resjö S, Gomez MF, James P, Holm C. Characterization of the lipid droplet proteome of a clonal insulin-producing β -cell line (INS-1 832/13). *J Proteome Res* 2012; 11(2): 1264-73.
<http://dx.doi.org/10.1021/pr200957p> PMID: 22268682
- [240] Elhadad MA, Jonasson C, Huth C, *et al.* Deciphering the plasma proteome of type 2 diabetes. *Diabetes* 2020; 69(12): 2766-78.
<http://dx.doi.org/10.2337/db20-0296> PMID: 32928870
- [241] Carlsson AC, Nowak C, Lind L, *et al.* Growth differentiation factor 15 (GDF-15) is a potential biomarker of both diabetic kidney disease and future cardiovascular events in cohorts of individuals with type 2 diabetes: A proteomics approach. *Ups J Med Sci* 2020; 125(1): 37-43.
<http://dx.doi.org/10.1080/03009734.2019.1696430> PMID: 31805809
- [242] Jedrychowski MP, Gartner CA, Gygi SP, *et al.* Proteomic analysis of GLUT4 storage vesicles reveals LRP1 to be an important vesicle component and target of insulin signaling. *J Biol Chem* 2010; 285(1): 104-14.
<http://dx.doi.org/10.1074/jbc.M109.040428> PMID: 19864425
- [243] Gibney MJ, Walsh M, Brennan L, Roche HM, German B, van Ommen B. Metabolomics in human nutrition: opportunities and challenges. *Am J Clin Nutr* 2005; 82(3): 497-503.
<http://dx.doi.org/10.1093/ajcn/82.3.497> PMID: 16155259
- [244] Lu J, Xie G, Jia W, Jia W. Metabolomics in human type 2 diabetes research. *Front Med* 2013; 7(1): 4-13.
<http://dx.doi.org/10.1007/s11684-013-0248-4> PMID: 23377891
- [245] Gu X, Al Dubayee M, Alshahrani A, *et al.* Distinctive metabolomics patterns associated with insulin resistance and type 2 diabetes mellitus. *Front Mol Biosci* 2020; 7: 609806.
<http://dx.doi.org/10.3389/fmolb.2020.609806> PMID: 33381523
- [246] Bos MM, Noordam R, Bennett K, *et al.* Metabolomics analyses in non-diabetic middle-aged individuals reveal metabolites impacting early glucose disturbances and insulin sensitivity. *Metabolomics* 2020; 16(3): 35.
<http://dx.doi.org/10.1007/s11306-020-01653-7> PMID: 32124065
- [247] Salihovic S, Broeckling CD, Ganna A, *et al.* Non-targeted urine metabolomics and associations with prevalent and incident type 2 diabetes. *Sci Rep* 2020; 10(1): 16474.
<http://dx.doi.org/10.1038/s41598-020-72456-y> PMID: 33020500
- [248] Yan Z, Wu H, Zhou H, *et al.* Integrated metabolomics and gut microbiome to the effects and mechanisms of naoxintong capsule on type 2 diabetes in rats. *Sci Rep* 2020; 10(1): 10829.
<http://dx.doi.org/10.1038/s41598-020-67362-2> PMID: 32616735
- [249] Li L, Krznar P, Erban A, *et al.* Metabolomics identifies a biomarker revealing *in vivo* loss of functional β -cell mass before diabetes onset. *Diabetes* 2019; 68(12): 2272-86.
<http://dx.doi.org/10.2337/db19-0131> PMID: 31537525
- [250] Zhang Y, Zhang S, Wang G. Metabolomic biomarkers in diabetic kidney diseases-A systematic review. *J Diabetes Complications* 2015; 29(8): 1345-51.
<http://dx.doi.org/10.1016/j.jdiacomp.2015.06.016> PMID: 26253264
- [251] Kim OY, Lee JH, Sweeney G. Metabolomic profiling as a useful tool for diagnosis and treatment of chronic disease: Focus on obesity, diabetes and cardiovascular diseases. *Expert Rev Cardiovasc Ther* 2013; 11(1): 61-8.
<http://dx.doi.org/10.1586/erc.12.121> PMID: 23259446
- [252] Lynch CJ, Adams SH. Branched-chain amino acids in metabolic signalling and insulin resistance. *Nat Rev Endocrinol* 2014; 10(12): 723-36.
<http://dx.doi.org/10.1038/nrendo.2014.171> PMID: 25287287
- [253] Zhao X, Gang X, Liu Y, Sun C, Han Q, Wang G. Using metabolomic profiles as biomarkers for insulin resistance in childhood obesity: A systematic review. *J Diabetes Res* 2016; 2016: 8160545.
<http://dx.doi.org/10.1155/2016/8160545> PMID: 27517054
- [254] Huang M, Joseph JW. Metabolomic analysis of pancreatic β -cell insulin release in response to glucose. *Islets* 2012; 4(3): 210-22.
<http://dx.doi.org/10.4161/isl.20141> PMID: 22847496
- [255] Han J, Tan H, Duan Y, *et al.* The cardioprotective properties and the involved mechanisms of NaoXinTong capsule. *Pharmacol Res* 2019; 141: 409-17.
<http://dx.doi.org/10.1016/j.phrs.2019.01.024> PMID: 30660824
- [256] Parry S, Hadaschik D, Blancher C, *et al.* Glycomics investigation into insulin action. *Biochim Biophys Acta* 2006; 1760(4): 652-68.
<http://dx.doi.org/10.1016/j.bbagen.2005.12.013> PMID: 16473469
- [257] Apweiler R, Hermjakob H, Sharon N. On the frequency of protein glycosylation, as deduced from analysis of the SWISS-PROT database. *Biochim Biophys Acta* 1999; 1473(1): 4-8.
[http://dx.doi.org/10.1016/S0304-4165\(99\)00165-8](http://dx.doi.org/10.1016/S0304-4165(99)00165-8) PMID: 10580125
- [258] Wormald MR, Petrescu AJ, Pao YL, Glithero A, Elliott T, Dwek RA. Conformational studies of oligosaccharides and glycopeptides:

- Complementarity of NMR, X-ray crystallography, and molecular modelling. *Chem Rev* 2002; 102(2): 371-86.
<http://dx.doi.org/10.1021/cr990368i> PMID: 11841247
- [259] Crocker PR. Siglecs: sialic-acid-binding immunoglobulin-like lectins in cell-cell interactions and signalling. *Curr Opin Struct Biol* 2002; 12(5): 609-15.
[http://dx.doi.org/10.1016/S0959-440X\(02\)00375-5](http://dx.doi.org/10.1016/S0959-440X(02)00375-5) PMID: 12464312
- [260] Esko JD, Selleck SB. Order out of chaos: Assembly of ligand binding sites in heparan sulfate. *Annu Rev Biochem* 2002; 71: 435-71.
<http://dx.doi.org/10.1146/annurev.biochem.71.110601.135458> PMID: 12045103
- [261] Rabinovich GA, Baum LG, Tinari N, *et al.* Galectins and their ligands: Amplifiers, silencers or tuners of the inflammatory response? *Trends Immunol* 2002; 23(6): 313-20.
[http://dx.doi.org/10.1016/S1471-4906\(02\)02232-9](http://dx.doi.org/10.1016/S1471-4906(02)02232-9) PMID: 12072371
- [262] Dwek RA. Towards understanding the function of sugars. *Biochem Soc Trans* 1995; 23(1): 1-25.
- [263] Helenius A, Aebi M. Roles of N-linked glycans in the endoplasmic reticulum. *Annu Rev Biochem* 2004; 73: 1019-49.
<http://dx.doi.org/10.1146/annurev.biochem.73.011303.073752> PMID: 15189166
- [264] Wang C, Eufemi M, Turano C, Giartosio A. Influence of the carbohydrate moiety on the stability of glycoproteins. *Biochemistry* 1996; 35(23): 7299-307.
<http://dx.doi.org/10.1021/bi9517704> PMID: 8652506
- [265] Dennis JW, Granovsky M, Warren CE. Protein glycosylation in development and disease. *BioEssays* 1999; 21(5): 412-21.
[http://dx.doi.org/10.1002/\(SICI\)1521-1878\(199905\)21:5<412::AID-BIES8>3.0.CO;2-5](http://dx.doi.org/10.1002/(SICI)1521-1878(199905)21:5<412::AID-BIES8>3.0.CO;2-5) PMID: 10376012
- [266] Eckel RH, Alberti KGMM, Grundy SM, Zimmet PZ. The metabolic syndrome. *Lancet* 2010; 375(9710): 181-3.
[http://dx.doi.org/10.1016/S0140-6736\(09\)61794-3](http://dx.doi.org/10.1016/S0140-6736(09)61794-3) PMID: 20109902
- [267] Lim J-M, Wollaston-Hayden EE, Teo CF, Hausman D, Wells L. Quantitative secretome and glycome of primary human adipocytes during insulin resistance. *Clin Proteomics* 2014; 11(1): 20.
<http://dx.doi.org/10.1186/1559-0275-11-20> PMID: 24948903
- [268] Marshall S, Bacote V, Traxinger RR. Discovery of a metabolic pathway mediating glucose-induced desensitization of the glucose transport system. Role of hexosamine biosynthesis in the induction of insulin resistance. *J Biol Chem* 1991; 266(8): 4706-12.
[http://dx.doi.org/10.1016/S0021-9258\(19\)67706-9](http://dx.doi.org/10.1016/S0021-9258(19)67706-9) PMID: 2002019
- [269] Patti ME, Virkamäki A, Landaker EJ, Kahn CR, Yki-Järvinen H. Activation of the hexosamine pathway by glucosamine *in vivo* induces insulin resistance of early postreceptor insulin signaling events in skeletal muscle. *Diabetes* 1999; 48(8): 1562-71.
<http://dx.doi.org/10.2337/diabetes.48.8.1562> PMID: 10426374
- [270] Bosch RR, Pouwels MJJM, Span PN, *et al.* Hexosamines are unlikely to function as a nutrient-sensor in 3T3-L1 adipocytes: A comparison of UDP-hexosamine levels after increased glucose flux and glucosamine treatment. *Endocrine* 2004; 23(1): 17-24.
<http://dx.doi.org/10.1385/ENDO:23:1:17> PMID: 15034192
- [271] Cohen-Forster L, Andre J, Mozere G, Peyroux J, Sternberg M. Kidney sialidase and sialyltransferase activities in spontaneously and experimentally diabetic rats. Influence of insulin and sorbinil treatments. *Biochem Pharmacol* 1990; 40(3): 507-13.
[http://dx.doi.org/10.1016/0006-2952\(90\)90549-Z](http://dx.doi.org/10.1016/0006-2952(90)90549-Z) PMID: 2200408
- [272] Rellier N, Ruggiero-Lopez D, Lecomte M, Lagarde M, Wiernsperger N. *In vitro* and *in vivo* alterations of enzymatic glycosylation in diabetes. *Life Sci* 1999; 64(17): 1571-83.
[http://dx.doi.org/10.1016/S0024-3205\(99\)00094-6](http://dx.doi.org/10.1016/S0024-3205(99)00094-6) PMID: 10353622
- [273] Wiese TJ, Dunlap JA, Yorek MA. Effect of L-fucose and D-glucose concentration on L-fucoprotein metabolism in human Hep G2 cells and changes in fucosyltransferase and α -L-fucosidase activity in liver of diabetic rats. *Biochim Biophys Acta* 1997; 1335(1-2): 61-72.
[http://dx.doi.org/10.1016/S0304-4165\(96\)00123-7](http://dx.doi.org/10.1016/S0304-4165(96)00123-7) PMID: 9133643
- [274] Pickup JC, Day C, Bailey CJ, *et al.* Plasma sialic acid in animal models of diabetes mellitus: evidence for modulation of sialic acid concentrations by insulin deficiency. *Life Sci* 1995; 57(14): 1383-91.
[http://dx.doi.org/10.1016/0024-3205\(95\)02096-2](http://dx.doi.org/10.1016/0024-3205(95)02096-2) PMID: 7564886
- [275] Biol MC, Lenoir D, Greco S, Galvain D, Hugueny I, Louisot P. Role of insulin and nutritional factors in intestinal glycoprotein fucosylation during postnatal development. *Am J Physiol* 1998; 275(5): G936-42.
 PMID: 9815021
- [276] Lenoir D, Gréco S, Louisot P, Biol MC. Implication of insulin and nutritional factors in the regulation of intestinal galactosyltransferase activity during postnatal development. *Metabolism* 2000; 49(4): 526-31.
[http://dx.doi.org/10.1016/S0026-0495\(00\)80020-7](http://dx.doi.org/10.1016/S0026-0495(00)80020-7) PMID: 10778880
- [277] Pak K, Kim K, Seo S, Lee MJ, Kim IJ. Serotonin transporter is negatively associated with body mass index after glucose loading in humans. *Brain Imaging Behav* 2022; 16(3): 1246-51.
- [278] Jia W, He Y-F, Qian X-J, Chen J. TPMT mRNA expression: A novel prognostic biomarker for patients with colon cancer by bioinformatics analysis. *Int J Gen Med* 2022; 15: 151-60.
<http://dx.doi.org/10.2147/IJGM.S338575> PMID: 35023953
- [279] Mooranian A, Ionescu CM, Walker D, *et al.* Single-cellular biological effects of cholesterol-catabolic bile acid-based nano/micro capsules as anti-inflammatory cell protective systems. *Biomolecules* 2022; 12(1): 73.
<http://dx.doi.org/10.3390/biom12010073> PMID: 35053221
- [280] Chan SJ, Cao QP, Steiner DF. Evolution of the insulin superfamily: Cloning of a hybrid insulin/insulin-like growth factor cDNA from amphioxus. *Proc Natl Acad Sci USA* 1990; 87(23): 9319-23.
<http://dx.doi.org/10.1073/pnas.87.23.9319> PMID: 1701257
- [281] Wang S, Wei W, Zheng Y, *et al.* The role of insulin C-peptide in the coevolution analyses of the insulin signaling pathway: A hint for its functions. *PLoS One* 2012; 7(12): e52847.
<http://dx.doi.org/10.1371/journal.pone.0052847> PMID: 23300796
- [282] Wahren J, Ekberg K, Johansson J, *et al.* Role of C-peptide in human physiology. *Am J Physiol Endocrinol Metab* 2000; 278(5): E759-68.
<http://dx.doi.org/10.1152/ajpendo.2000.278.5.E759> PMID: 10780930
- [283] Hills CE, Brunskill NJ. Intracellular signalling by C-peptide. *Exp Diabetes Res* 2008; 2008: 635158.
<http://dx.doi.org/10.1155/2008/635158> PMID: 18382618
- [284] Wahren J, Kallas A, Sima AAF. The clinical potential of C-peptide replacement in type 1 diabetes. *Diabetes* 2012; 61(4): 761-72.
<http://dx.doi.org/10.2337/db11-1423> PMID: 22442295
- [285] Nordquist L, Brown R, Fasching A, Persson P, Palm F. Proinsulin C-peptide reduces diabetes-induced glomerular hyperfiltration *via* efferent arteriole dilation and inhibition of tubular sodium reabsorption. *Am J Physiol - Ren Physiol* 2009; 297(5): F1265.
- [286] Johansson BL, Borg K, Fernqvist-Forbes E, Kernell A, Odergren T, Wahren J. Beneficial effects of C-peptide on incipient nephropathy and neuropathy in patients with type 1 diabetes mellitus. *Diabet Med* 2000; 17(3): 181-9.
<http://dx.doi.org/10.1046/j.1464-5491.2000.00274.x> PMID: 10784221
- [287] Samnegård B, Jacobson SH, Jaremko G, *et al.* C-peptide prevents glomerular hypertrophy and mesangial matrix expansion in diabetic rats. *Nephrol Dial Transplant* 2005; 20(3): 532-8.
<http://dx.doi.org/10.1093/ndt/gfh683> PMID: 15665028
- [288] Johansson J, Ekberg K, Shafqat J, *et al.* Molecular effects of proinsulin C-peptide. *Biochem Biophys Res Commun* 2002; 295(5): 1035-40.
[http://dx.doi.org/10.1016/S0006-291X\(02\)00721-0](http://dx.doi.org/10.1016/S0006-291X(02)00721-0) PMID: 12135597
- [289] Munte CE, Vilela L, Kalbitzer HR, Garratt RC. Solution structure of human proinsulin C-peptide. *FEBS J* 2005; 272(16): 4284-93.
<http://dx.doi.org/10.1111/j.1742-4658.2005.04843.x> PMID: 16098208
- [290] Shafqat J, Juntti-Berggren L, Zhong Z, *et al.* Proinsulin C-peptide and its analogues induce intracellular Ca²⁺ increases in human renal tubular cells. *Cell Mol Life Sci* 2002; 59(7): 1185-9.
<http://dx.doi.org/10.1007/s00018-002-8496-5> PMID: 12222964
- [291] Rhodes CJ. Processing of the insulin molecule. In: LeRoith D, Taylor SI, Olefsky JM, Eds. *Diabetes Mellitus: A Fundamental and Clinical Text*. Philadelphia: Lippincott Williams & Wilkin, 2004.

- [292] Liu M, Wright J, Guo H, Xiong Y, Arvan P. Proinsulin entry and transit through the endoplasmic reticulum in pancreatic beta cells. *Vitam Horm* 2014; 95: 35-62.
<http://dx.doi.org/10.1016/B978-0-12-800174-5.00002-8>
- [293] Sun J, Cui J, He Q, Chen Z, Arvan P, Liu M. Proinsulin misfolding and endoplasmic reticulum stress during the development and progression of diabetes. *Mol Aspects Med* 2015; 42: 105-18.
<http://dx.doi.org/10.1016/j.mam.2015.01.001> PMID: 25579745
- [294] Hills CE, Brunskill NJ. Cellular and physiological effects of C-peptide. *Clin Sci (Lond)* 2009; 116(7): 565-74.
<http://dx.doi.org/10.1042/CS20080441> PMID: 19243312
- [295] Wahren J, Shafiqat J, Johansson J, Chibalin A, Ekberg K, Jörnvall H. Molecular and cellular effects of C-peptide--new perspectives on an old peptide. *Exp Diabetes Res* 2004; 5(1): 15-23.
<http://dx.doi.org/10.1080/15438600490424479> PMID: 15198368
- [296] Wahren J, Ekberg K, Jörnvall H. C-peptide is a bioactive peptide. *Diabetologia* 2007; 50(3): 503-9.
<http://dx.doi.org/10.1007/s00125-006-0559-y> PMID: 17235526
- [297] Chevenne D, Trivin F, Porquet D. Insulin assays and reference values. *Diabetes Metab* 1999; 25(6): 459-76.
PMID: 10633871
- [298] Steiner DF. The biosynthesis of insulin. In: Seino S, Bell GI, Eds. *Pancreatic Beta Cell in Health and Disease*. Springer, Tokyo, 2008; pp. 31-49.
http://dx.doi.org/10.1007/978-4-431-75452-7_3
- [299] Docherty K, Hutton JC. Carboxypeptidase activity in the insulin secretory granule. *FEBS Lett* 1983; 162(1): 137-41.
[http://dx.doi.org/10.1016/0014-5793\(83\)81065-5](http://dx.doi.org/10.1016/0014-5793(83)81065-5) PMID: 6311629
- [300] Orzi L, Ravazzola M, Amherdt M, *et al.* Conversion of proinsulin to insulin occurs coordinately with acidification of maturing secretory vesicles. *J Cell Biol* 1986; 103(6 Pt 1): 2273-81.
<http://dx.doi.org/10.1083/jcb.103.6.2273> PMID: 3536964
- [301] Smith GD, Swenson DC, Dodson EJ, Dodson GG, Reynolds CD. Structural stability in the 4-zinc human insulin hexamer. *Proc Natl Acad Sci USA* 1984; 81(22): 7093-7.
<http://dx.doi.org/10.1073/pnas.81.22.7093> PMID: 6390430
- [302] Mayer JP, Zhang F, DiMarchi RD. Insulin structure and function. *Peptide Sci* 2007; 88(5): 687-713.
- [303] Smith GD, Ciszak E, Magrum LA, Pangborn WA, Blessing RH. R6 hexameric insulin complexed with m-cresol or resorcinol. *Acta Crystallogr Sect D Biol Crystallogr* 2000; 56(Pt 12): 1541-8.
- [304] Ciszak E, Smith GD. Crystallographic evidence for dual coordination around zinc in the T3R3 human insulin hexamer. *Biochemistry* 1994; 33(6): 1512-7.
<http://dx.doi.org/10.1021/bi00172a030> PMID: 8312271
- [305] Schlitter J, Engels M, Krüger P, Jacoby E, Wollmer A. Targeted molecular dynamics simulation of conformational change-application to the T↔ R transition in insulin. *Mol Simul* 1993; 10(2-6): 291-308.
<http://dx.doi.org/10.1080/08927029308022170>
- [306] Hodgkin DC. X rays and the structures of insulin. *BMJ* 1971; 4(5785): 447-51.
<http://dx.doi.org/10.1136/bmj.4.5785.447> PMID: 5166450
- [307] Weiss MA. The structure and function of insulin: Decoding the TR transition. *Vitam Horm* 2009; 80: 33-49.
- [308] Rahuel-Clermont S, French CA, Kaarsholm NC, Dunn MF, Chou CI. Mechanisms of stabilization of the insulin hexamer through allosteric ligand interactions. *Biochemistry* 1997; 36(19): 5837-45.
<http://dx.doi.org/10.1021/bi963038q> PMID: 9153424
- [309] Setter SM, Corbett CF, Campbell RK, White JR. Insulin aspart: A new rapid-acting insulin analog. *Ann Pharmacother* 2000; 34(12): 1423-31.
<http://dx.doi.org/10.1345/aph.19414> PMID: 11144701
- [310] Malaisse WJ, Hutton JC, Kawazu S, Herchuelz A, Valverde I, Sener A. The stimulus-secretion coupling of glucose-induced insulin release. XXXV. The links between metabolic and cationic events. *Diabetologia* 1979; 16(5): 331-41.
<http://dx.doi.org/10.1007/BF01223623> PMID: 37138
- [311] Lacy PE. Structure and function of the endocrine cell types of the islets. *Adv Metab Disord* 1974; 7(0): 171-82.
<http://dx.doi.org/10.1016/B978-0-12-027307-2.50013-X> PMID: 4213400
- [312] Smith GD, Ciszak E. The structure of a complex of hexameric insulin and 4'-hydroxyacetanilide. *Proc Natl Acad Sci USA* 1994; 91(19): 8851-5.
<http://dx.doi.org/10.1073/pnas.91.19.8851> PMID: 8090735
- [313] Ciszak E, Beals JM, Frank BH, Baker JC, Carter ND, Smith GD. Role of C-terminal B-chain residues in insulin assembly: the structure of hexameric LysB28ProB29-human insulin. *Structure* 1995; 3(6): 615-22.
[http://dx.doi.org/10.1016/S0969-2126\(01\)00195-2](http://dx.doi.org/10.1016/S0969-2126(01)00195-2) PMID: 8590022
- [314] Smith GD, Ciszak E, Pangborn W. A novel complex of a phenolic derivative with insulin: structural features related to the T→R transition. *Protein Sci* 1996; 5(8): 1502-11.
<http://dx.doi.org/10.1002/pro.5560050806> PMID: 8844841
- [315] Whittingham JL, Havelund S, Jonassen I. Crystal structure of a prolonged-acting insulin with albumin-binding properties. *Biochemistry* 1997; 36(10): 2826-31.
<http://dx.doi.org/10.1021/bi9625105> PMID: 9062110
- [316] Whittingham JL, Edwards DJ, Antson AA, Clarkson JM, Dodson GG. Interactions of phenol and m-cresol in the insulin hexamer, and their effect on the association properties of B28 pro → Asp insulin analogues. *Biochemistry* 1998; 37(33): 11516-23.
<http://dx.doi.org/10.1021/bi980807s> PMID: 9708987
- [317] Yao ZP, Zeng ZH, Li HM, Zhang Y, Feng YM, Wang DC. Structure of an insulin dimer in an orthorhombic crystal: The structure analysis of a human insulin mutant (B9 Ser→Glu). *Acta Crystallogr Sect D Biol Crystallogr* 1999; 55(Pt 9): 1524-32.
- [318] Tang L, Whittingham JL, Verma CS, Caves LSD, Dodson GG. Structural consequences of the B5 histidine → tyrosine mutation in human insulin characterized by X-ray crystallography and conformational analysis. *Biochemistry* 1999; 38(37): 12041-51.
<http://dx.doi.org/10.1021/bi990700k> PMID: 10508408
- [319] Von Dreele RB, Stephens PW, Smith GD, Blessing RH. The first protein crystal structure determined from high-resolution X-ray powder diffraction data: A variant of T3R3 human insulin-zinc complex produced by grinding. *Acta Crystallogr Sect D Biol Crystallogr* 2000; 56(Pt 12): 1549-53.
- [320] Smith GD, Pangborn WA, Blessing RH. Phase changes in T(3)R(3)(f) human insulin: temperature or pressure induced? *Acta Crystallogr D Biol Crystallogr* 2001; 57(Pt 8): 1091-100.
<http://dx.doi.org/10.1107/S0907444901007685> PMID: 11468392
- [321] Ye J, Chang W, Liang D. Crystal structure of destriptide (B28-B30) insulin: Implications for insulin dissociation. *Biochim Biophys Acta* 2001; 1547(1): 18-25.
[http://dx.doi.org/10.1016/S0167-4838\(01\)00160-1](http://dx.doi.org/10.1016/S0167-4838(01)00160-1) PMID: 11343787
- [322] Lee KH, Wucherpennig KW, Wiley DC. Correction: Structure of a human insulin peptide-HLA-DQ8 complex and susceptibility to type 1 diabetes. *Nat Immunol* 2001; 2(6): 501-7.
- [323] Weiss MA, Wan Z, Zhao M, *et al.* Non-standard insulin design: structure-activity relationships at the periphery of the insulin receptor. *J Mol Biol* 2002; 315(2): 103-11.
<http://dx.doi.org/10.1006/jmbi.2001.5224> PMID: 11779231
- [324] Smith GD, Blessing RH. Lessons from an aged, dried crystal of T(6) human insulin. *Acta Crystallogr D Biol Crystallogr* 2003; 59(Pt 8): 1384-94.
<http://dx.doi.org/10.1107/S090744490301165X> PMID: 12876340
- [325] Wan ZL, Xu B, Chu YC, Katsyannis PG, Weiss MA. Crystal structure of allo-IleA2-insulin, an inactive chiral analogue: Implications for the mechanism of receptor binding. *Biochemistry* 2003; 42(44): 12770-83.
- [326] Smith GD, Pangborn WA, Blessing RH. The structure of T6 human insulin at 1.0 Å resolution. *Acta Crystallogr - Sect D Biol Crystallogr* 2003; 59(Pt 3): 474-82.
- [327] Wan Z, Xu B, Huang K, *et al.* Enhancing the activity of insulin at the receptor interface: Crystal structure and photo-cross-linking of A8 analogues. *Biochemistry* 2004; 43(51): 16119-33.
<http://dx.doi.org/10.1021/bi048223f> PMID: 15610006
- [328] Whittingham JL, Jonassen I, Havelund S, *et al.* Crystallographic and solution studies of N-lithocholyl insulin: A new generation of prolonged-acting human insulins. *Biochemistry* 2004; 43(20): 5987-95.
<http://dx.doi.org/10.1021/bi036163s> PMID: 15147182
- [329] Záková L, Brynda J, Au-Alvarez O, *et al.* Toward the insulin-IGF-I intermediate structures: Functional and structural properties of the

- [TyrB25NMePheB26] insulin mutant. *Biochemistry* 2004; 43(51): 16293-300.
<http://dx.doi.org/10.1021/bi048856u> PMID: 15610023
- [330] Wan ZL, Huang K, Xu B, *et al.* Diabetes-associated mutations in human insulin: Crystal structure and photo-cross-linking studies of a-chain variant insulin Wakayama. *Biochemistry* 2005; 44(13): 5000-16.
<http://dx.doi.org/10.1021/bi047585k> PMID: 15794638
- [331] Vernede X, Lavault B, Ohana J, *et al.* UV laser-excited fluorescence as a tool for the visualization of protein crystals mounted in loops. *Acta Crystallogr Sect D Biol Crystallogr* 2006; 62(Pt 3): 253-61.
<http://dx.doi.org/10.1107/S0907444905041429>
- [332] Whittingham JL, Youshang Z, Žáková L, *et al.* I222 crystal form of despentapeptide (B26-B30) insulin provides new insights into the properties of monomeric insulin. *Acta Crystallogr Sect D Biol Crystallogr* 2006; 62(Pt 5): 505-11.
- [333] Shen Y, Joachimiak A, Rosner MR, Tang WJ. Structures of human insulin-degrading enzyme reveal a new substrate recognition mechanism. *Nature* 2006; 443(7113): 870-4.
<http://dx.doi.org/10.1038/nature05143> PMID: 17051221
- [334] Norrman M, Schluckebier G. Crystallographic characterization of two novel crystal forms of human insulin induced by chaotropic agents and a shift in pH. *BMC Struct Biol* 2007; 7: 83.
<http://dx.doi.org/10.1186/1472-6807-7-83> PMID: 18093308
- [335] Norrman M, Hubálek F, Schluckebier G. Structural characterization of insulin NPH formulations. *Eur J Pharm Sci* 2007; 30(5): 414-23.
<http://dx.doi.org/10.1016/j.ejps.2007.01.003> PMID: 17339105
- [336] Srekanth R, Pattabhi V, Rajan SS. Structural interpretation of reduced insulin activity as seen in the crystal structure of human Arg-insulin. *Biochimie* 2008; 90(3): 467-73.
<http://dx.doi.org/10.1016/j.biochi.2007.09.012> PMID: 18029081
- [337] Srekanth R, Pattabhi V, Rajan SS. Metal induced structural changes observed in hexameric insulin. *Int J Biol Macromol* 2009; 44(1): 29-36.
<http://dx.doi.org/10.1016/j.ijbiomac.2008.09.019> PMID: 18977386
- [338] Hua QX, Nakagawa SH, Jia W, *et al.* Design of an active ultra-stable single-chain insulin analog: synthesis, structure, and therapeutic implications. *J Biol Chem* 2008; 283(21): 14703-16.
<http://dx.doi.org/10.1074/jbc.M800313200> PMID: 18332129
- [339] Wagner A, Diez J, Schulze-Briese C, Schluckebier G. Crystal structure of Ultralente - A microcrystalline insulin suspension. *Proteins Struct Funct Bioinforma* 2009.
<http://dx.doi.org/10.1002/prot.22213>
- [340] Manolopoulou M, Guo Q, Malito E, Schilling AB, Tang WJ. Molecular basis of catalytic chamber-assisted unfolding and cleavage of human insulin by human insulin-degrading enzyme. *J Biol Chem* 2009; 284(21): 14177-88.
<http://dx.doi.org/10.1074/jbc.M900068200> PMID: 19321446
- [341] Zhao M, Wan ZL, Whittaker L, *et al.* Design of an insulin analog with enhanced receptor binding selectivity: Rationale, structure, and therapeutic implications. *J Biol Chem* 2009; 284(46): 32178-87.
<http://dx.doi.org/10.1074/jbc.M109.028399> PMID: 19773552
- [342] Thorsøe KS, Schlein M, Steensgaard DB, Brandt J, Schluckebier G, Naver H. Kinetic evidence for the sequential association of insulin binding sites 1 and 2 to the insulin receptor and the influence of receptor isoform. *Biochemistry* 2010; 49(29): 6234-46.
<http://dx.doi.org/10.1021/bi1000118> PMID: 20568733
- [343] Jiráček J, Žáková L, Antolíková E, *et al.* Implications for the active form of human insulin based on the structural convergence of highly active hormone analogues. *Proc Natl Acad Sci USA* 2010; 107(5): 1966-70.
<http://dx.doi.org/10.1073/pnas.0911785107> PMID: 20133841
- [344] Timofeev VI, Chuprov-Netochin RN, Samigina VR, Bezuglov VV, Miroshnikov KA, Kuranova IP. X-ray investigation of gene-engineered human insulin crystallized from a solution containing polysialic acid. *Acta Crystallogr Sect F Struct Biol Cryst Commun* 2010; 66(Pt 3): 259-263.
- [345] Phillips NB, Wan ZL, Whittaker L, *et al.* Supramolecular protein engineering: design of zinc-stapled insulin hexamers as a long acting depot. *J Biol Chem* 2010; 285(16): 11755-9.
<http://dx.doi.org/10.1074/jbc.C110.105825> PMID: 20181952
- [346] Chinai JM, Taylor AB, Ryno LM, *et al.* Molecular recognition of insulin by a synthetic receptor. *J Am Chem Soc* 2011; 133(23): 8810-3.
<http://dx.doi.org/10.1021/ja201581x> PMID: 21473587
- [347] Antolíková E, Žáková L, Turkenburg JP, *et al.* Non-equivalent role of inter- and intramolecular hydrogen bonds in the insulin dimer interface. *J Biol Chem* 2011; 286(42): 36968-77.
<http://dx.doi.org/10.1074/jbc.M111.265249> PMID: 21880708
- [348] Vinther TN, Norrman M, Strauss HM, *et al.* Novel covalently linked insulin dimer engineered to investigate the function of insulin dimerization. *PLoS One* 2012; 7(2): e30882.
<http://dx.doi.org/10.1371/journal.pone.0030882> PMID: 22363506
- [349] Bulek AM, Cole DK, Skowera A, *et al.* Structural basis for the killing of human beta cells by CD8(+) T cells in type 1 diabetes. *Nat Immunol* 2012; 13(3): 283-9.
<http://dx.doi.org/10.1038/ni.2206> PMID: 22245737
- [350] Prugovečki B, Pulić I, Toth M, Matković-Čalogović D. High resolution structure of the manganese derivative of insulin. *Croat Chem Acta* 2012; 85(4): 435-9.
<http://dx.doi.org/10.5562/cca2108>
- [351] Menting JG, Whittaker J, Margetts MB, *et al.* How insulin engages its primary binding site on the insulin receptor. *Nature* 2013; 493(7431): 241-5.
<http://dx.doi.org/10.1038/nature11781> PMID: 23302862
- [352] Žáková L, Kletvíková E, Veverka V, *et al.* Structural integrity of the B24 site in human insulin is important for hormone functionality. *J Biol Chem* 2013; 288(15): 10230-40.
<http://dx.doi.org/10.1074/jbc.M112.448050> PMID: 23447530
- [353] Steensgaard DB, Schluckebier G, Strauss HM, *et al.* Ligand-controlled assembly of hexamers, dimerhexamers, and linear multihexamers structures by the engineered acylated insulin deglucide. *Biochemistry* 2013; 52(2): 295-309.
<http://dx.doi.org/10.1021/bi3008609> PMID: 23256685
- [354] Vinther TN, Norrman M, Ribbel U, *et al.* Insulin analog with additional disulfide bond has increased stability and preserved activity. *Protein Sci* 2013; 22(3): 296-305.
<http://dx.doi.org/10.1002/pro.2211> PMID: 23281053
- [355] Fávero-Retto MP, Palmieri LC, Souza TACB, Almeida FCL, Lima LMTR. Structural meta-analysis of regular human insulin in pharmaceutical formulations. *Eur J Pharm Biopharm* 2013; 85(3 Pt B): 1112-21.
<http://dx.doi.org/10.1016/j.ejpb.2013.05.005> PMID: 23692694
- [356] Avital-Shmilovici M, Mandal K, Gates ZP, Phillips NB, Weiss MA, Kent SBH. Fully convergent chemical synthesis of ester insulin: determination of the high resolution X-ray structure by racemic protein crystallography. *J Am Chem Soc* 2013; 135(8): 3173-85.
<http://dx.doi.org/10.1021/ja311408y> PMID: 23343390
- [357] Palmieri LC, Fávero-Retto MP, Lourenço D, Lima LMTR. A T3R3 hexamer of the human insulin variant B28Asp. *Biophys Chem* 2013; 173-174: 1-7.
<http://dx.doi.org/10.1016/j.bpc.2013.01.003> PMID: 23428413
- [358] Kosinová L, Veverka V, Novotná P, *et al.* Insight into the structural and biological relevance of the T/R transition of the N-terminus of the B-chain in human insulin. *Biochemistry* 2014; 53(21): 3392-402.
<http://dx.doi.org/10.1021/bi500073z> PMID: 24819248
- [359] Menting JG, Yang Y, Chan SJ, *et al.* Protective hinge in insulin opens to enable its receptor engagement. *Proc Natl Acad Sci USA* 2014; 111(33): E3395-404.
<http://dx.doi.org/10.1073/pnas.1412897111> PMID: 25092300
- [360] Pandeyarajan V, Smith BJ, Phillips NB, *et al.* Aromatic anchor at an invariant hormone-receptor interface: function of insulin residue B24 with application to protein design. *J Biol Chem* 2014; 289(50): 34709-27.
<http://dx.doi.org/10.1074/jbc.M114.608562> PMID: 25305014
- [361] Žáková L, Kletvíková E, Lepšík M, *et al.* Human insulin analogues modified at the B26 site reveal a hormone conformation that is undetected in the receptor complex. *Acta Crystallogr Sect D Biol Crystallogr* 2014.
- [362] Beringer DX, Kleijwegt FS, Wiede F, *et al.* T cell receptor reversed polarity recognition of a self-antigen major histocompatibility complex. *Nat Immunol* 2015; 16(11): 1153-61.
<http://dx.doi.org/10.1038/ni.3271> PMID: 26437244

- [363] Motozono C, Pearson JA, De Leenheer E, *et al.* Distortion of the major histocompatibility complex class I binding groove to accommodate an insulin-derived 10-mer peptide. *J Biol Chem* 2015; 290(31): 18924-33.
<http://dx.doi.org/10.1074/jbc.M114.622522> PMID: 26085090
- [364] Mandal K, Dhayalan B, Avital-Shmilovici M, Tokmakoff A, Kent SBH. Crystallization of enantiomerically pure proteins from quasi-racemic mixtures: Structure determination by x-ray diffraction of isotope-labeled ester insulin and human insulin. *ChemBioChem* 2016; 17(5): 421-5.
<http://dx.doi.org/10.1002/cbic.201500600> PMID: 26707939
- [365] Víková J, Collinsová M, Kletvíková E, *et al.* Rational steering of insulin binding specificity by intra-chain chemical crosslinking. *Sci Rep* 2016; 6: 19431.
<http://dx.doi.org/10.1038/srep19431> PMID: 26792393
- [366] Hjorth CF, Norrman M, Wahlund PO, *et al.* Structure, Aggregation, and Activity of a Covalent Insulin Dimer Formed During Storage of Neutral Formulation of Human Insulin. *J Pharm Sci* 2016; 105(4): 1376-86.
<http://dx.doi.org/10.1016/j.xphs.2016.01.003> PMID: 26921119
- [367] Cole DK, Bulek AM, Dolton G, *et al.* Hotspot autoimmune T cell receptor binding underlies pathogen and insulin peptide cross-reactivity. *J Clin Invest* 2016.
<http://dx.doi.org/10.1172/JCI85679>
- [368] El Hage K, Pandeyarajan V, Phillips NB, *et al.* Extending halogen-based medicinal chemistry to proteins: Iodo-insulin as a case study. *J Biol Chem* 2016; 291(53): 27023-41.
<http://dx.doi.org/10.1074/jbc.M116.761015> PMID: 27875310
- [369] Stadinski BD, Obst R, Huseby ESA. A "hotspot" for autoimmune T cells in type 1 diabetes. *J Clin Invest* 2016; 126(6): 2040-2.
<http://dx.doi.org/10.1172/JCI88165> PMID: 27183386
- [370] Dhayalan B, Mandal K, Rege N, *et al.* Scope and limitations of fmoc chemistry spps-based approaches to the total synthesis of insulin lispro *via* ester insulin. *Chemistry* 2017; 23(7): 1709-16.
<http://dx.doi.org/10.1002/chem.201605578> PMID: 27905149
- [371] Lisgarten DR, Palmer RA, Lobley CMC, *et al.* Ultra-high resolution X-ray structures of two forms of human recombinant insulin at 100 K. *Chem Cent J* 2017; 11(1): 73.
<http://dx.doi.org/10.1186/s13065-017-0296-y> PMID: 29086855
- [372] Lieblich SA, Fang KY, Cahn JKB, *et al.* 4S-hydroxylation of insulin at ProB28 accelerates hexamer dissociation and delays fibrillation. *J Am Chem Soc* 2017; 139(25): 8384-7.
<http://dx.doi.org/10.1021/jacs.7b00794> PMID: 28598606
- [373] Palivec V, Viola CM, Kozak M, *et al.* Computational and structural evidence for neurotransmitter-mediated modulation of the oligomeric states of human insulin in storage granules. *J Biol Chem* 2017; 292(20): 8342-55.
<http://dx.doi.org/10.1074/jbc.M117.775924> PMID: 28348075
- [374] van Lierop B, Ong SC, Belgi A, *et al.* Insulin in motion: The A6-A11 disulfide bond allosterically modulates structural transitions required for insulin activity. *Sci Rep* 2017; 7(1): 17239.
<http://dx.doi.org/10.1038/s41598-017-16876-3> PMID: 29222417
- [375] Glidden MD, Aldabbagh K, Phillips NB, *et al.* An ultra-stable single-chain insulin analog resists thermal inactivation and exhibits biological signaling duration equivalent to the native protein. *J Biol Chem* 2018; 293(1): 47-68.
<http://dx.doi.org/10.1074/jbc.M117.808626> PMID: 29114035
- [376] Zhang Z, Liang WG, Bailey LJ, *et al.* Ensemble cryoEM elucidates the mechanism of insulin capture and degradation by human insulin degrading enzyme. *eLife* 2018; 7: e33572.
<http://dx.doi.org/10.7554/eLife.33572> PMID: 29596046
- [377] Rege NK, Wickramasinghe NP, Tustan AN, *et al.* Structure-based stabilization of insulin as a therapeutic protein assembly *via* enhanced aromatic-aromatic interactions. *J Biol Chem* 2018; 293(28): 10895-910.
<http://dx.doi.org/10.1074/jbc.RA118.003650> PMID: 29880646
- [378] Taylor SK, Tran TH, Liu MZ, *et al.* Insulin hexamer-caged gadolinium ion as MRI contrast-agent. *Chemistry* 2018; 24(42): 10646-52.
<http://dx.doi.org/10.1002/chem.201801388> PMID: 29873848
- [379] Weil-Ktorza O, Rege N, Lansky S, *et al.* Substitution of an internal disulfide bridge with a diselenide enhances both foldability and stability of human insulin. *Chemistry* 2019; 25(36): 8513-21.
<http://dx.doi.org/10.1002/chem.201900892> PMID: 31012517
- [380] Hubálek F, Refsgaard HHF, Gram-Nielsen S, Madsen P, Nishimura E, Münzel M, *et al.* Molecular engineering of safe and efficacious oral basal insulin. *Nat Commun* 2020; 11: 3746.
<http://dx.doi.org/10.1038/s41467-020-17487-9>
- [381] Xiong X, Blakely A, Karra P, *et al.* Novel four-disulfide insulin analog with high aggregation stability and potency. *Chem Sci (Camb)* 2019; 11(1): 195-200.
<http://dx.doi.org/10.1039/C9SC04555D> PMID: 32110371
- [382] Xiong X, Menting JG, Disotuar MM, *et al.* A structurally minimized yet fully active insulin based on cone-snail venom insulin principles. *Nat Struct Mol Biol* 2020; 27(7): 683.
- [383] Gillis RB, Solomon HV, Govada L, *et al.* Analysis of insulin glulisine at the molecular level by X-ray crystallography and biophysical techniques. *Sci Rep* 2021; 11(1): 1737.
<http://dx.doi.org/10.1038/s41598-021-81251-2> PMID: 33462295
- [384] Freeman JS. Insulin analog therapy: Improving the match with physiologic insulin secretion. *J Am Osteopath Assoc* 2009; 109(1): 26-36.
PMID: 19193822
- [385] Donner T, Sarkar S. Insulin-pharmacology, therapeutic regimens, and principles of intensive insulin therapy. 2019 Feb 23. In: Feingold KR, Anawalt B, Boyce A, *et al.* Eds. *Endotext* [Internet]. South Dartmouth (MA): MDText.com, Inc.; 2000.
- [386] Fullerton B, Siebenhofer A, Jeitler K, *et al.* Short-acting insulin analogues *versus* regular human insulin for adult, non-pregnant persons with type 2 diabetes mellitus. *Cochrane Database Syst Rev* 2018; 12: CD013228.
<http://dx.doi.org/10.1002/14651858.CD013228> PMID: 30556900
- [387] Atkin S, Javed Z, Fulcher G. Insulin degludec and insulin aspart: Novel insulins for the management of diabetes mellitus. *Ther Adv Chronic Dis* 2015; 6(6): 375-88.
<http://dx.doi.org/10.1177/2040622315608646> PMID: 26568812
- [388] Hirsch IB, Juneja R, Beals JM, Antalis CJ, Wright EE. The evolution of insulin and how it informs therapy and treatment choices. *Endocr Rev* 2020; 41(5): 733-55.
PMID: 32396624
- [389] Mannucci E, Monami M, Marchionni N. Short-acting insulin analogues *vs.* regular human insulin in type 2 diabetes: A meta-analysis. *Diabetes Obes Metab* 2009; 11(1): 53-9.
<http://dx.doi.org/10.1111/j.1463-1326.2008.00934.x> PMID: 18671795
- [390] Fullerton B, Siebenhofer A, Jeitler K, *et al.* Short-acting insulin analogues *versus* regular human insulin for adults with type 1 diabetes mellitus. *Cochrane Database Syst Rev* 2016; (6): CD012161.
<http://dx.doi.org/10.1002/14651858.CD012161> PMID: 27362975
- [391] Daugherty KK. Review of insulin therapy. *J Pharm Pract* 2004; 17(1): 10-9.
<http://dx.doi.org/10.1177/0897190003261304>
- [392] Goldman J, Kapitzka C, Pettus J, Heise T. Understanding how pharmacokinetic and pharmacodynamic differences of basal analog insulins influence clinical practice. *Curr Med Res Opin* 2017; 33(10): 1821-31.
<http://dx.doi.org/10.1080/03007995.2017.1335192> PMID: 28537449
- [393] Liebl A, Davidson J, Mersebach H, Dykiel P, Tack CJ, Heise T. A novel insulin combination of insulin degludec and insulin aspart achieves a more stable overnight glucose profile than insulin glargine: Results from continuous glucose monitoring in a proof-of-concept trial. *J Diabetes Sci Technol* 2013; 7(5): 1328-36.
<http://dx.doi.org/10.1177/193229681300700524> PMID: 24124961
- [394] Oleck J, Kassam S, Goldman JD. Commentary: Why was inhaled insulin a failure in the market? *Diabetes Spectr* 2016; 29(3): 180-4.
<http://dx.doi.org/10.2337/diaspect.29.3.180> PMID: 27574374
- [395] Gast K, Schüler A, Wolff M, *et al.* Rapid-acting and human insulins: Hexamer dissociation kinetics upon dilution of the pharmaceutical formulation. *Pharm Res* 2017; 34(11): 2270-86.
<http://dx.doi.org/10.1007/s11095-017-2233-0> PMID: 28762200
- [396] Nettleton EJ, Tito P, Sunde M, Bouchard M, Dobson CM, Robinson CV. Characterization of the oligomeric states of insulin in self-assembly and amyloid fibril formation by mass spectrometry. *Biophys J* 2000; 79(2): 1053-65.
[http://dx.doi.org/10.1016/S0006-3495\(00\)76359-4](http://dx.doi.org/10.1016/S0006-3495(00)76359-4) PMID: 10920035

- [397] Maikawa CL, Smith AAA, Zou L, *et al.* Stable Monomeric Insulin Formulations Enabled by Supramolecular PEGylation of Insulin Analogues. *Adv Ther (Weinh)* 2020; 3(1): 1900094. <http://dx.doi.org/10.1002/adtp.201900094> PMID: 32190729
- [398] Birnbaum DT, Kilcomons MA, DeFelippis MR, Beals JM. Assembly and dissociation of human insulin and LysB28ProB29-insulin hexamers: A comparison study. *Pharm Res* 1997; 14(1): 25-36. <http://dx.doi.org/10.1023/A:1012095115151> PMID: 9034217
- [399] Yang LW, Rader AJ, Liu X, *et al.* oGNM: online computation of structural dynamics using the Gaussian Network Model. *Nucleic Acids Res* 2006; 34: W24-31. PMID: 16845002
- [400] Bahar I, Rader AJ. Coarse-grained normal mode analysis in structural biology. *Curr Opin Struct Biol* 2005; 15(5): 586-92. <http://dx.doi.org/10.1016/j.sbi.2005.08.007> PMID: 16143512
- [401] Mirmira RG, Nakagawa SH, Tager HS. Importance of the character and configuration of residues B24, B25, and B26 in insulin-receptor interactions. *J Biol Chem* 1991; 266(3): 1428-36. [http://dx.doi.org/10.1016/S0021-9258\(18\)52312-7](http://dx.doi.org/10.1016/S0021-9258(18)52312-7) PMID: 1988428
- [402] Derewenda U, Derewenda Z, Dodson EJ, Dodson GG, Bing X, Markussen J. X-ray analysis of the single chain B29-A1 peptide-linked insulin molecule. A completely inactive analogue. *J Mol Biol* 1991; 220(2): 425-33. [http://dx.doi.org/10.1016/0022-2836\(91\)90022-X](http://dx.doi.org/10.1016/0022-2836(91)90022-X) PMID: 1856866
- [403] Leyer S, Gattner H-G, Leithäuser M, Brandenburg D, Wollmer A, Höcker H. The role of the C-terminus of the insulin B-chain in modulating structural and functional properties of the hormone. *Int J Pept Protein Res* 1995; 46(5): 397-407.
- [404] Hartman I. Insulin analogs: impact on treatment success, satisfaction, quality of life, and adherence. *Clin Med Res* 2008; 6(2): 54-67. <http://dx.doi.org/10.3121/cmr.2008.793> PMID: 18801953
- [405] Holleman F. Insulin lispro (revision number 20). *Diapedia* 2015. <http://dx.doi.org/10.14496/dia.8104096170.20>
- [406] Garnock-Jones KP, Plosker GL. Insulin glulisine: A review of its use in the management of diabetes mellitus. *Drugs* 2009; 69(8): 1035-57. <http://dx.doi.org/10.2165/00003495-200969080-00006> PMID: 19496630
- [407] Haahr H, Heise T. Fast-acting insulin aspart: A review of its pharmacokinetic and pharmacodynamic properties and the clinical consequences. *Clin Pharmacokinet* 2020; 59(2): 155-72. <http://dx.doi.org/10.1007/s40262-019-00834-5> PMID: 31667789
- [408] Simpson KL, Spencer CM. Insulin aspart. *Drugs* 1999; 57(5): 759-65. <http://dx.doi.org/10.2165/00003495-199957050-00013> PMID: 10353301
- [409] Becker RHA, Frick AD. Clinical pharmacokinetics and pharmacodynamics of insulin glulisine. *Clin Pharmacokinet* 2008; 47(1): 7-20. <http://dx.doi.org/10.2165/00003088-200847010-00002> PMID: 18076215
- [410] Bolli GB, Owens DR. Insulin glargine. *Lancet* 2000; 356(9228): 443-5. [http://dx.doi.org/10.1016/S0140-6736\(00\)02546-0](http://dx.doi.org/10.1016/S0140-6736(00)02546-0) PMID: 10981882
- [411] Dunn CJ, Plosker GL, Keating GM, McKeage K, Scott LJ. Insulin glargine: An updated review of its use in the management of diabetes mellitus. *Drugs* 2003; 63(16): 1743-78. <http://dx.doi.org/10.2165/00003495-200363160-00007> PMID: 12904090
- [412] McKeage K, Goa KL. Insulin glargine: A review of its therapeutic use as a long-acting agent for the management of type 1 and 2 diabetes mellitus. *Drugs* 2001; 61(11): 1599-624. <http://dx.doi.org/10.2165/00003495-200161110-00007> PMID: 11577797
- [413] Chapman TM, Perry CM. Insulin detemir: A review of its use in the management of type 1 and 2 diabetes mellitus. *Drugs* 2004; 64(22): 2577-95. <http://dx.doi.org/10.2165/00003495-200464220-00008> PMID: 15516157
- [414] Jonassen I, Havelund S, Hoeg-Jensen T, Steensgaard DB, Wahlund PO, Ribøl U. Design of the novel protraction mechanism of insulin degludec, an ultra-long-acting basal insulin. *Pharm Res* 2012; 29(8): 2104-14. <http://dx.doi.org/10.1007/s11095-012-0739-z> PMID: 22485010
- [415] Vora J, Cariou B, Evans M, *et al.* Clinical use of insulin degludec. *Diabetes Res Clin Pract* 2015; 109(1): 19-31. <http://dx.doi.org/10.1016/j.diabres.2015.04.002> PMID: 25963320
- [416] Wu T, Betty B, Downie M, *et al.* Practical guidance on the use of premix insulin analogs in initiating, intensifying, or switching insulin regimens in type 2 diabetes. *Diabetes Ther* 2015; 6(3): 273-87. <http://dx.doi.org/10.1007/s13300-015-0116-0> PMID: 26104878
- [417] Chance RE, Kroeff EP, Hoffmann JA, Frank BH. Chemical, physical, and biologic properties of biosynthetic human insulin. *Diabetes Care* 1981; 4(2): 147-54. <http://dx.doi.org/10.2337/diacare.4.2.147> PMID: 7011716
- [418] Zimmerman RE, Stokell DJ. Insulin production methods and proinsulin constructs. US Patent 7790677B2, 2010.
- [419] Thim L, Hansen MT, Norris K, *et al.* Secretion and processing of insulin precursors in yeast. *Proc Natl Acad Sci USA* 1986; 83(18): 6766-70. <http://dx.doi.org/10.1073/pnas.83.18.6766> PMID: 3529091
- [420] Chan SJ, Weiss J, Konrad M, *et al.* Biosynthesis and periplasmic segregation of human proinsulin in *Escherichia coli*. *Proc Natl Acad Sci USA* 1981; 78(9): 5401-5. <http://dx.doi.org/10.1073/pnas.78.9.5401> PMID: 7029534
- [421] Chance RE, Dimarci RD, Fank BH, Shields JE. Insulin analogs. AU Patent 630912B2, 1992.
- [422] Brange JJV, Havelund S. Insulin analogues. WO Patent 1989010937A1, 1989.
- [423] Chance RE, DiMarchi RD, Frank BH, Shields JE. Process for preparing insulin analogs. US Patent 5700662A, 1997.
- [424] Ertl J, Haberman P, Geisen K, Seipke G. Insulin derivatives having a rapid onset of action. US Patent 6221633B1, 2001.
- [425] Berchtold H. Crystals of insulin analogs and processes for their preparation. US Patent 7193035B2, 2007.
- [426] Zimmerman RE, Stokell DJ, Akers MP. Compositions de proinsuline aspart et procédés de production d'analogues de l'insuline aspart. WO Patent 2012115637A1, 2012.
- [427] Zimmerman RE, Stokell DJ, Akers MP. Glargine proinsulin and methods of producing glargine insulin analogs therefrom US Patent 20120214965A1, 2012.
- [428] Chan Y-P, Vialas C, Blas M. Long-acting insulin glargine analogue. WO Patent 2015071368A1, 2015.
- [429] Li Y, Du J, Si J, Chu Y, Sun M. Purification method of insulin detemir. CN Patent 103145829B, 2015.
- [430] Zimmerman RE, Stokell DJ, Akers MP. Lis-pro proinsulin compositions and methods of producing lis-pro insulin analogs therefrom. US Patent 20120214199A1, 2012.
- [431] Loos P, Gehrman T, Berchtold H, Werner U, Ganz M. Stable formulation of insulin glulisine. WO Patent 2015059302A1, 2015.
- [432] Ortigosa AD, Coleman MP, George ST, Rauscher MA, Sleevi MC, Chow K. Purifying insulin using cation exchange and reverse phase chromatography in the presence of an organic modifier and elevated temperature. WO Patent 2015138548A1, 2015.
- [433] Grant SS, Iammarino MJ, Kerchner K, *et al.* Process for preparing recombinant insulin using microfiltration. WO Patent 2016144658A1, 2016.
- [434] Ortigosa AD, Chmielowski RA, Sleevi MC. A process for obtaining insulin with correctly formed disulfide bonds. WO Patent 2017040363A1, 2017.
- [435] Borowicz P, Plucienniczak A, Plucienniczak G, *et al.* A method for producing insulin and insulin derivatives, and hybrid peptide used in this method. WO Patent 2017126984A1, 2017.
- [436] Qian X, Kraft J, Ni Y, Zhao FQ. Production of recombinant human proinsulin in the milk of transgenic mice. *Sci Rep* 2014; 4: 6465. <http://dx.doi.org/10.1038/srep06465> PMID: 25267062
- [437] Kim CK, Lee SB, Son YJ. Large-scale refolding and enzyme reaction of human proinsulin for production of human insulin. *J Microbiol Biotechnol* 2015; 25(10): 1742-50. <http://dx.doi.org/10.4014/jmb.1504.04062> PMID: 26139616
- [438] Ling Z, Qi-Qing J, Yu W, *et al.* Transgenic expression and identification of recombinant human proinsulin in peanut. *Braz Arch Biol Technol* 2016; 59: e16150131. <http://dx.doi.org/10.1590/1678-4324-2016150131>

- [439] Akbarian M, Yousefi R. Human α B-crystallin as fusion protein and molecular chaperone increases the expression and folding efficiency of recombinant insulin. *PLoS One* 2018; 13(10): e0206169. <http://dx.doi.org/10.1371/journal.pone.0206169> PMID: 30339677
- [440] Zieliński M, Romanik-Chruścielewska A, Mikiewicz D, *et al.* Expression and purification of recombinant human insulin from *E. coli* 20 strain. *Protein Expr Purif* 2019; 157: 63-9. <http://dx.doi.org/10.1016/j.pep.2019.02.002> PMID: 30735706
- [441] Govender K, Naicker T, Lin J, *et al.* A novel and more efficient biosynthesis approach for human insulin production in *Escherichia coli* (*E. coli*). *AMB Express* 2020; 10(1): 43. <http://dx.doi.org/10.1186/s13568-020-00969-w> PMID: 32152803

DISCLAIMER: The above article has been published, as is, ahead-of-print, to provide early visibility but is not the final version. Major publication processes like copyediting, proofing, typesetting and further review are still to be done and may lead to changes in the final published version, if it is eventually published. All legal disclaimers that apply to the final published article also apply to this ahead-of-print version.